THE UNIVERSITY OF HULL

Predictive Control Approaches to Fault Tolerant Control of Wind Turbines

Being a Thesis submitted for the Degree of Philosophy

in the University of Hull

by

Xiaoran Feng

MSc (Xidian University, China)

BSc (Xidian University, China)

August 2014

Acknowledgement

I would like to express my sincere gratitude to both of my supervisors, Professor Ron Patton and Dr. Ming Hou, who have guided me in every step of my research during the past three years. Professor Ron J Patton has inspired me with many helpful ideas for my PhD research. He is also the one encouraging me whenever I meet difficulties in my research. I also want to thank Dr. Ming Hou for giving me many useful advices during the seminars and thesis advisory panel meetings.

I would like to thank all of my colleagues in the Control and Intelligent Systems Engineering Group in University of Hull, Dr. Lejun Chen, Dr. Chenglei Nie, Dr. Zheng Huang, Dr. Xiaoyu Sun, Dr. Yimeng Tang, Dr. Montadher Sami Shaker, Dr. Eshag Yousef Larbah, Dr. Fengmin Shi, Zhihuo Wang and Bingyong Guo, who have helped my research with many useful discussions. They also created pleasant memories for me in the past three years.

I appreciate the Chinese Scholarship Council and the University of Hull. Both of the institutions offered me a joint scholarship to support my PhD study financially.

Finally, I am grateful to both of my parents, Qiyun Xu and Qi Feng. Their understanding, emotional support and love are with me during the three years of PhD research life.

Abstract

This thesis focuses on active fault tolerant control (AFTC) of wind turbine systems. Faults in wind turbine systems can be in the form of sensor faults, actuator faults, or component faults. These faults can occur in different locations, such as the wind speed sensor, the generator system, drive train system or pitch system. In this thesis, some AFTC schemes are proposed for wind turbine faults in the above locations. Model predictive control (MPC) is used in these schemes to design the wind turbine controller such that system constraints and dual control goals of the wind turbine are considered. In order to deal with the nonlinearity in the turbine model, MPC is combined with Takagi-Sugeno (T-S) fuzzy modelling. Different fault diagnosis methods are also proposed in different AFTC schemes to isolate or estimate wind turbine faults.

The main contributions of the thesis are summarized as follows:

A new effective wind speed (EWS) estimation method via least-squares support vector machines (LSSVM) is proposed. Measurements from the wind turbine rotor speed sensor and the generator speed sensor are utilized by LSSVM to estimate the EWS. Following the EWS estimation, a wind speed sensor fault isolation scheme via LSSVM is proposed.

A robust predictive controller is designed to consider the EWS estimation error. This predictive controller serves as the baseline controller for the wind turbine system operating in the region below rated wind speed.

T-S fuzzy MPC combining MPC and T-S fuzzy modelling is proposed to design the wind turbine controller. MPC can deal with wind turbine system constraints externally. On the other hand, T-S fuzzy modelling can approximate the nonlinear wind turbine system with a linear time varying (LTV) model such that controller design can be based on this LTV model. Therefore, the advantages of MPC and T-S fuzzy modelling are both preserved in the proposed T-S fuzzy MPC.

A T-S fuzzy observer, based on online eigenvalue assignment, is proposed as the sensor fault isolation scheme for the wind turbine system. In this approach, the fuzzy observer is proposed to deal with the nonlinearity in the wind turbine system and estimate system

states. Furthermore, the residual signal generated from this fuzzy observer is used to isolate the faulty sensor.

A sensor fault diagnosis strategy utilizing both analytical and hardware redundancies is proposed for wind turbine systems. This approach is proposed due to the fact that in the real application scenario, both analytical and hardware redundancies of wind turbines are available for designing AFTC systems.

An actuator fault estimation method based on moving horizon estimation (MHE) is proposed for wind turbine systems. The estimated fault by MHE is then compensated by a T-S fuzzy predictive controller. The fault estimation unit and the T-S fuzzy predictive controller are combined to form an AFTC scheme for wind turbine actuator faults.

List of Publications

1. Xiaoran, F. & Patton, R. A model-based predictive control for FTC for wind turbine wind speed sensor fault. *Control and Fault-Tolerant Systems (SysTol), 2013 Conference on*, 9-11 Oct. 2013, Nice, France.
2. Xiaoran, F. & Patton, R. Sensor fault tolerant control of a wind turbine via Takagi-Sugeno fuzzy observer and model predictive control. *UKACC 10th International Conference on Control*, 9-11 July, 2014, Loughborough, United Kingdom.
3. Xiaoran, F. & Patton, R. Active fault tolerant control of a wind turbine via fuzzy MPC and moving horizon estimation. *IFAC World Congress*, 24-29 Aug. 2014, Cape Town, South Africa.
4. Xiaoran, F. & Patton, R. Active fault tolerant control of a wind turbine via T-S fuzzy model predictive control. *22nd Mediterranean Conference on Control and Automation*, 16-19 June, 2014.

Contents

Symbols

0	Zero matrix with compatible dimensions
$\mathbb{R}$	Set of real numbers
$\mathbb{R}^n$	Set of n dimensional real vectors
$\mathbb{R}^{n\times m}$	Set of n by m matrices with elements in $\mathcal{R}$
M^T	The transpose of the matrix M
M^{-1}	The inverse of the invertible matrix M
$M > 0 (M \geq 0)$	M is positive definite (positive semidefinite)
$M < 0 (M \leq 0)$	M is negative definite(negative semidefinite)
λ	An eigenvalue
$\|x\|_1$	L_1 norm of vector $x \in \mathbb{R}^n$, and $\|x\|_1 = \sum_{i=1}^{n} \|x_i\|$
$\|x\|_Q$	$\|x\|_Q = x^T Q x$ with $x \in \mathbb{R}^n$and $Q \in \mathbb{R}^{n\times n}$

Abbreviations

AFTC	Active Fault Tolerant Control
PFTC	Passive Fault Tolerant Control
FD	Fault Diagnosis
FDI	Fault Detection and Identification
FE	Fault Estimation
FTC	Fault Tolerant Control
LMI	Linear Matrix Inequality
MPC	Model Predictive Control
MHE	Moving Horizon Estimation
LTV	Linear Time Varying
EWS	Effective Wind Speed
LPV	Linear Parameter Varying

List of Figures

List of Tables

Chapter 1: Introduction

1.1 Motivation of FTC

Modern technical systems are becoming more complex due to the increased demand on their performance and functions. These systems are inevitably subjected to an ever increasing range of fault types caused by sophisticated hardware structures, system embedding and complex system dynamics. Some technical systems are also safety-critical which means that the occurrence of faults during operation can be catastrophic in terms of danger to human life and mission criticality. However, conventional feedback controllers in these systems are seldom designed to tolerate faults, enhance safety of operation and sustain reliable operation. Unsatisfactory control performance or even instability may occur if technical systems are controlled by these conventional feedback controllers in the presence of faults (Patton, 1997; Isermann, 2011).

On the other hand, during the last 20 years fault tolerant control (FTC) systems have been proposed to take into account faults occurring in sensors, actuators and even internal system components, some or all of which may affect closed-loop performance, stability and ultimately functional reliability (Patton, Frank and Clarke, 1989)

In the early days, FTC systems were designed to maintain system stability with acceptable control performance degradation in the presence of faults so that system failure or breakdown could be avoided. In recent years, FTC systems have advanced greatly and many new FTC methods can achieve desired control performance with little performance degradation in the presence of faults. Besides, FTC systems are also able to maintain desired control performance as conventional feedback controllers do in the absence of faults. The important principles used in FTC are system redundancy (in hardware or analytical form), from which faults can be either estimated or identified and isolated.

Most of the FTC methods are based on either fault estimation (FE) or fault detection and isolation (FDI) as these two approaches are powerful and direct (Blanke and Schröder, 2003) (Zhang and Jiang, 2008). The idea behind FTC is to use the information about the location and time-variant behaviour of a fault to either

reconfigure the control system based on redundant components or directly compensate for the fault by means of FE techniques.

The history of research into FTC dates back to the 1970s. At that time FTC was mainly motivated by control problems in real world safety-critical applications, such as chemical plants, spacecraft, nuclear power plant and aircraft flight control. However, most of the research effort has been made on the development of FTC schemes for aircraft flight control problems. The challenge is to add fault tolerant ability to the aircraft flight control system so that the aircraft can land safely in the presence of a serious fault. The research interest into FTC has increased greatly since the late 1970s due to several commercial aircraft accidents. Delta Flight 1080 on April 12, 1977 (McMahan, 1978; Montoya et al., 1983) and American Airlines DC-10 on May 25, 1979 (Montoya et al., 1983). Following this, many studies on FTC of aircraft systems appeared (Chandler, 1984; Looze, Weiss, Eterno and Barrett, 1985; Ostroff, 1985; Caglayan, Allen and Wehmuller, 1988; Ochi and Kanai, 1991; Maciejowski and Jones, 2003; Ye and Yang, 2006; Edwards, Lombaerts and Smaili, 2010; Yu and Jiang, 2012).

Other historical application research of FTC also helped to stimulate the research interests into FTC. These application examples are mostly safety-critical systems including chemical plants, nuclear power plants and spacecraft (Himmelblau, 1978; Gelderloos and Young, 1982; Garcia, Ray and Edwards, 1991; Bukley, 1995; Blanke, Izadi-Zamanabadi, Bøgh and Lunau, 1997; Cai, Liao and Song, 2008).

Nowadays, FTC research is not limited to safety-critical and high-end technical systems. It has extended to a broader range of areas with various applications examples. In the past decade, some new application studies of FTC appeared, including ship propulsion systems (Izadi-Zamanabadi and Blanke, 1999; Bonivento, Paoli and Marconi, 2003), vehicle systems (Jeong, Sul, Schulz and Patel, 2005; Oudghiri, Chadli and El Hajjaji, 2008), wind turbine systems (Pourmohammad and Fekih, 2011; Badihi, Zhang and Hong, 2013), temperature control systems (Gopinathan, Mehra and Runkle, 1999; Jin and Du, 2006) and robot systems (Lin and Chen, 2007; Koh, Norton and Khoo, 2012). As mentioned above, the main cause of this situation is the growing complexity of modern technical systems, which makes systems prone to faults in sensor, actuators and system components.

A new and growing research area of FTC is the design and development of decentralised/distributed FTC systems. The fault tolerance of decentralised/distributed systems becomes a challenge as the complexity of these systems increases. Therefore, this research area has drawn significant attention since early 2000s. Some studies in this area can be found in (Bao, Zhang and Lee, 2003; El-Farra, 2006; Patton, Kambhampati, Casavola and Franze, 2006; Zhihong and Huajing, 2007; Patton et al., 2007; Panagi and Polycarpou, 2011).

A special motivation for the growing interest into FTC is the demand for guaranteeing productivity of some technical systems for economic reasons. The major concern for these systems is the system operation reliability such that extra economic cost can be avoided. Examples of these systems are wind turbines and power plants, in which reliable and sustainable operation is important. Faults in these systems can result in power efficiency reduction, decreased electrical power generation, giving rise to loss of revenue. Moreover, shutdown of these systems due to faults means a great cost to system owners.

Throughout the history of FTC research, many theoretical methods have been proposed to meet the FTC challenges in various application domains. These methods originated from the following research areas: robust control, fault detection and identification, parameter estimation and reconfigurable control. Some methods are developed with the theory from one of the above research areas while some other methods are developed with theories from several of the above research areas. Detailed classification of various FTC methods can be found in (Patton, 1997; Zhang and Jiang, 2008; Mahmoud and Xia, 2013).

1.2 Terminology

In the early days, the terminology in the FTC community has been quite inconsistent due to the scattered many technical areas in which FTC was studied. Sometimes this situation resulted in confusion and made it difficult to understand the concepts in these technical areas. Therefore, several efforts have been made to achieve commonly acknowledged definition of FTC terminology among all these technical areas (IFIP., 1983; Omdahl, 1988). Some of the terminology used in this thesis is given below and are consistent with the definition given by (Isermann and Ballé, 1997) and (Patton, 1997).

Fault: unpermitted deviation of at least one characteristic property or parameter of the system from the acceptable, usual standard condition.

Failure: permanent interruption of a system's ability to perform a required function under specified operating conditions.

Fault Detection: determination of faults present in a system and time of detection

Fault Isolation: determination of the kind, location and time of detection of a fault.

Fault identification: determination of the size-variant and time-variant behaviour of a fault.

Fault Diagnosis: determination of the kind, size, location and time of detection of a fault by evaluating symptoms. Includes fault detection, isolation and identification

Residual: fault indicator, based on deviations between measurements and model-equation-based calculations.

In the literature, FDI is used as the abbreviation for either fault detection and identification or fault detection and isolation. In this thesis, the term FDI refers to fault detection and isolation. Meanwhile, some researchers (principally in aerospace engineering) use the term FDD to denote fault detection and diagnosis. However, the definition of fault diagnosis already includes the concept of fault detection as shown in the above terminology. Therefore, the term FDD is not used in this thesis to avoid confusion.

From the above terminology it can be seen that the meaning of FDI is twofold in this thesis: (1) determination of the occurrence of faults in the controlled system (fault detection) and (2) determination of the faulty part of the system (fault isolation). In this thesis another term called fault estimation (FE) is also used if the fault signal in the time domain can be estimated. Later for simplicity the term FD is used to denote fault diagnosis, signifying the use of either FDI or FE.

1.3 Fault tolerant control methods

Generally, FTC methods are classified into passive fault tolerant control (PFTC) and active fault tolerant control (AFTC) methods (Patton, 1997). The difference between

these two classes of method is described in this Section. The design of FTC methods has been widely studied and a large number of AFTC and PFTC methods have been proposed in the literature. Each method has its own advantages and limitations and there is always an on-going trend to improve these methods by relaxing the limitations and assumptions in each method. Figure 1-1 illustrates the classification of FTC methods.

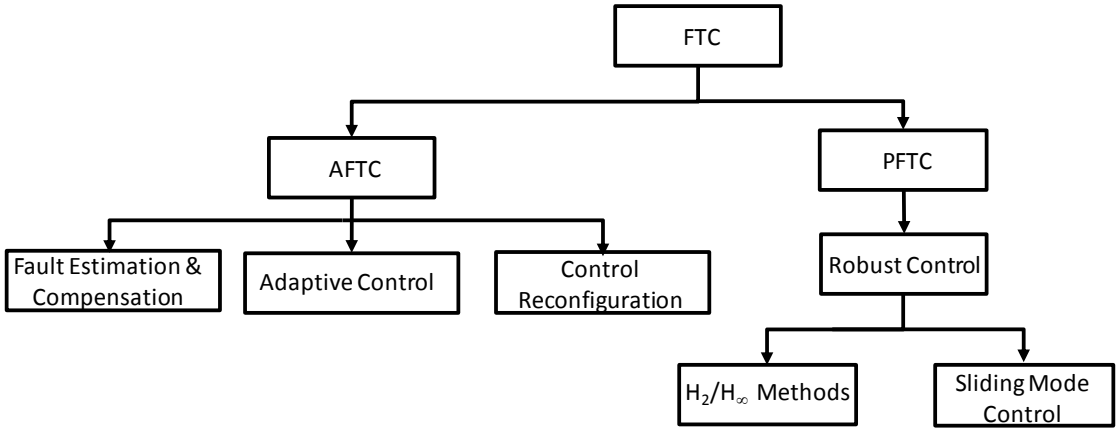

Figure 1-1 Classification of FTC methods

1.3.1 Active fault tolerant control

AFTC systems respond to faults actively through one of the following three actions: (1) compensating for the effects of the faults, (2) adapting to the faulty system dynamics, (3) switch to redundant hardware. Due to these AFTC actions, that controller can still operate normally, albeit at the cost of some degradation in control performance. In the literature, there are some other terminologies used to refer to AFTC, including self-repairing control (Chandler, 1984; Eterno, Weiss, Looze and Willsky, 1985), reconfigurable control (Moerder, Halyo, Broussard and Caglayan, 1989; Gao and Antsaklis, 1991; Qi, Zhu and Jiang, 2013; Nieto-Wire and Sobel, 2014), self-designing control (Monaco, Ward, Barron and Bird, 1997) or adaptive control based on identified or estimated faults (Boskovic and Mehra, 1999).

An FE unit can be integrated into an AFTC scheme to achieve control reconfiguration which is realized through changing to another pre-design control law or to a new control law online (Rauch, 1995; Zhang and Jiang, 2002; Zhang and Jiang, 2008; Qi, Zhu and Jiang, 2013). An FDI unit can also be integrated into an AFTC scheme. Its role is two-fold: (1) to monitor and update the status of the process online in case of potential faults and (2) to inform the control system to react to the faults when they are detected and

isolated. A basic requirement for AFTC schemes is that the presence of an FE or FDI unit should hardly influence the control performance when no fault is present. A typical architecture of AFTC using FE or FDI is shown in Figure 1-2.

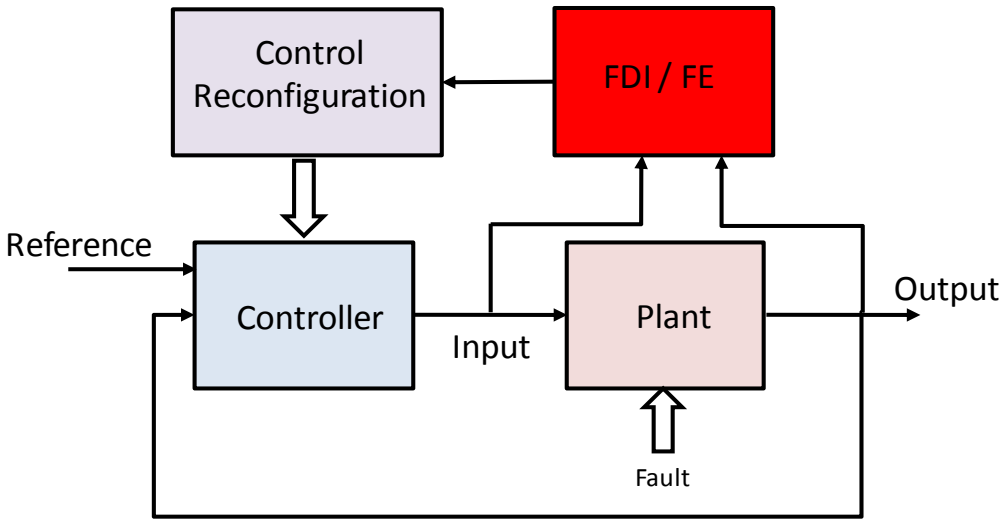

Figure 1-2 AFTC scheme using FDI/FE

Many AFTC approaches are designed through combining an FDI or FE unit with various control methods. These AFTC approaches include: predictive control or moving horizon estimation based approaches (Huzmezan and Maciejowski, 1998; Ichtev, Hellendoom, Babuska and Mollov, 2002; Prakash, Narasimhan and Patwardhan, 2005; Sun, Dong, Li and Gu, 2008; Casavola and Garone, 2010; Izadi, Zhang and Gordon, 2011; Lao, Ellis and Christofides, 2013; Zhang, Lu, Xue and Gao, 2014), sliding mode control based approaches (Huzmezan and Maciejowski, 1998; Edwards and Tan, 2006; Alwi and Edwards, 2008; Hu and Xiao, 2013; Zhao, Jiang, Shi and He, 2014), LPV control based approaches (Khong and Shin, 2007; De Oca, Puig, Theillio and Tornil-Sin, 2009; Varrier, Koenig and Martinez Molina, 2013; Vanek, Péni, Szabó and Bokor, 2014), multiple model-based approaches (Rago, Prasanth, Mehra and Fortenbaugh, 1998; Mirzaee and Salahshoor, 2012; Sami and Patton, 2012c), Eigenstructure assignment-based approaches (Zhang and Jiang, 1999; Zhang and Jiang, 2002; Nieto-Wire and Sobel, 2014).

AFTC can also be realized without using FE or FDI unit. This is achieved by adapting to parameters changes in the model without knowing the information of faults (Tao, Joshi and Ma, 2001; Boskovic and Mehra, 2002; Ye and Yang, 2006; Jiang, Gao, Shi and Xu, 2010; Li, Song, Huang and Chen, 2013). These methods are mostly derived from adaptive control methods and are generally used to deal with component faults or

actuator faults. The schematic diagram of AFTC using parameter adaption is shown in Figure 1-3.

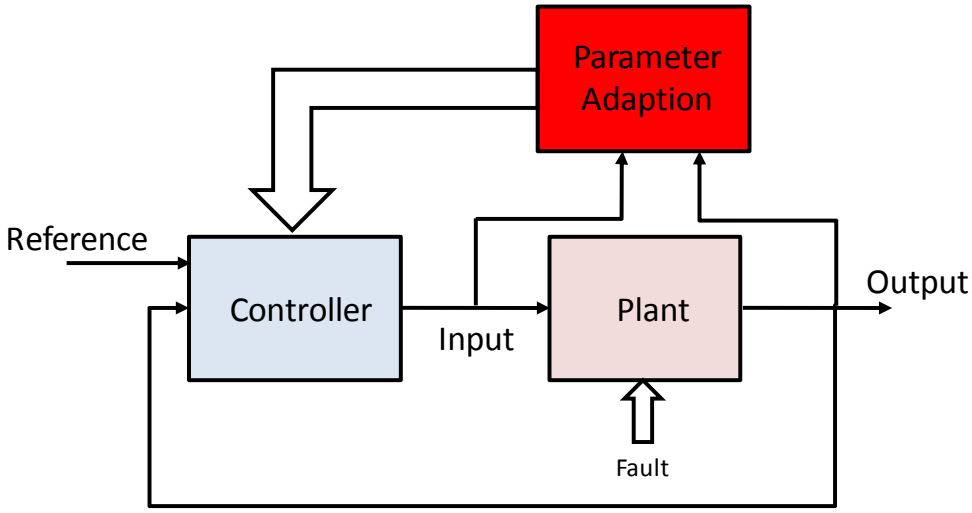

Figure 1-3 AFTC scheme using parameter adaption

1.3.2 Passive fault tolerant control

In PFTC approaches, the controller is designed to tolerate a class of expected faults without using FD unit (Eterno, Weiss, Looze and Willsky, 1985; Stengel, 1991; Jiang and Yu, 2012; Shen, Song and Wang, 2013). When faults occur, the PFTC control law does not react or adapt to fault information. Compared with AFTC, the principle of fault tolerance in PFTC is conservative, rather like the conservative nature of classical robust control methods. The fault effects in PFTC are considered alongside system uncertainty as a more complex form of robustness problem in which the robustness is defined in terms of insensitivity to both uncertainty and fault effects. The effectiveness of PFTC is thus rather limited, although many investigators continue to use this approach. In the literature, PFTC systems are also sometimes known as reliable control systems or control systems with integrity (Veillette, Medanic and Perkins, 1992; Zhang and Jiang, 2008).

Many PFTC methods are proposed using various approaches, including the use of linear optimization and linear matrix inequalities (LMI) (Liao, Wang and Yang, 2002; Hu, 2013), Quantitative feedback theory (Wu, Grimble and Wei, 1999), H_∞ theory (Niemann and Stoustrup, 2002; Niemann and Stoustrup, 2005; Yin, Zheng, Chang and

Lun, 2013; Oubellil and Boukhnifer, 2014), passivity theory (Benosman and Lum, 2010; Wang and Shen, 2014), nonlinear regulation theory (Bonivento, Gentili and Paoli, 2004; Bonivento, Isidori, Marconi and Paoli, 2004) and methods based on absolute stability (Benosman and Lum, 2009).

1.4 Fault Diagnosis methods

Fault diagnosis methods are used to provide the information of faults. The following information about faults can be provided using FD methods: the kind, size, location and time of fault occurrence. FD methods can be used as the approach to monitor the condition of technical systems. Moreover, an FD unit can be integrated into an FTC design to form an AFTC system. FD methods have already attracted a significant amount of research effort and now represent a mature research area with a lot of substantial results (Frank and Ding, 1997; Isermann and Ballé, 1997; Gertler, 1998; Chen and Patton, 1999; Patton, Clark and Frank, 2000; Isermann, 2006; Ding, 2008; Wang, Chai, Ding and Brown, 2009; Isermann, 2011; Zhang, Jiang and Shi, 2013; Haghani Abandan Sari, 2014).

1.4.1 Classification of faults

Faults can be classified from two man perspectives as follows: (1) the location and (2) the characteristics of a fault. A fault can be classified as a sensor fault, an actuator fault or a component fault in terms of the fault location (Chen and Patton, 1999). Figure 1-4 shows the typical locations in which faults can act in controlled systems.

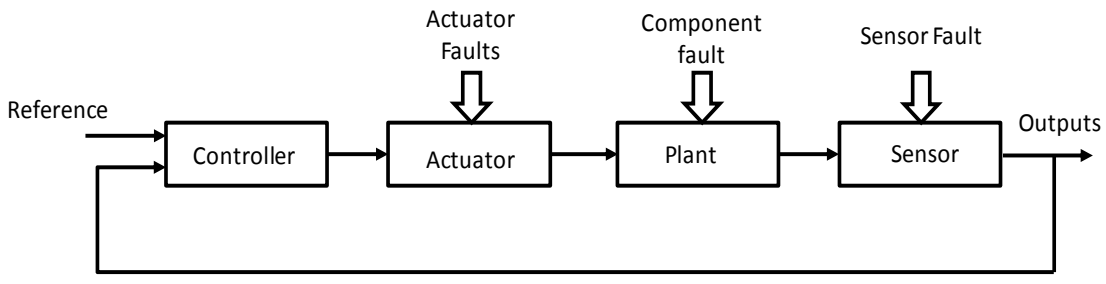

Figure 1-4 Fault classification in terms of location

Sensor Faults: A technical system is always monitored by sensors. Different sensors are used depending on the physical quantity to be measured, e.g. anemometers, accelerometers, thermometers, pressure gauge, etc. Sensor faults will result in incorrect measurements from the sensors. These incorrect measurements can be in the form of

gain factor errors, offsets, or constant values. There are various causes of sensor faults, including aging, corrosion and physical damage. Sensor faults are just erroneous measurements of the plant status and do not affect the plant dynamics. However, the output of the controller will be affected if the measurements of the faulty sensors are used as feedback to the controller.

Actuator Faults: Actuators are used to exert control effort (i.e. the input of the controlled system) on the system to be controlled. They can be in the form of motor drives, hydraulic pistons, valves, etc. Actuator faults represent partial loss of actuator function (i.e. either under or over-actuation) whereas an actuator failure means that the actuator has no effectiveness (i.e. represent a loss of control action). There are various causes of actuator faults, including breakage, jamming, friction and wear out.

Component Faults: This type of fault is sometimes referred to as a process fault. It represents the variation of the system structure or variation of a system parameter. Some forms of component faults include change in mass, torsion coefficient, aerodynamic coefficient and damping constant, changes in friction effects, etc. They generally result from component fatigue or damage. Component faults will affect system dynamics, system input/output characteristics and regions of system operation.

Faults can also be classified as the following three types according to their characteristic in time-domain : (1) abrupt faults, (2) incipient faults and (3) intermittent (Blanke and Schröder, 2003). The characteristics of these faults are shown in Figure 1-5.

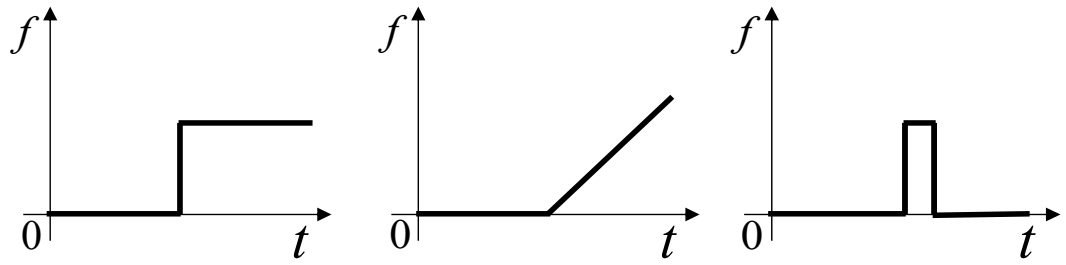

Abrupt fault Incipient fault Intermittent fault

Figure 1-5 Fault classification in terms of time dependency

Abrupt Faults: Abrupt faults are represented by stepwise signals in the time domain. They represent sudden changes of a quantity in the system and are often caused by hardware damage. This kind of fault often exerts a strong influence on control system

performance or stability. Therefore, abrupt faults need to be detected and dealt with quickly.

Incipient Faults: Incipient faults are generally ramp signals in the time domain. They represent a slow change of a quantity in the system and are often caused by slow and consistent effects like aging or wearing. This kind of fault exerts weaker influence than abrupt faults do in the short term. However, incipient faults can have stronger influence than abrupt faults do if they keep on increasing with time. Therefore, this kind of fault should be dealt with at an early stage of development.

Intermittent Fault: Intermittent faults are signals appearing and disappearing repeatedly. One cause of this type of fault is intermittent electrical contact in the electrical components of the system.

1.4.2 Fault diagnosis methods

There are a large quantity of well developed methods in the research area of fault diagnosis (Zhang and Jiang, 2008; Isermann, 2011; Zhang, Jiang and Shi, 2013; Haghani Abandan Sari, 2014). Generally, these methods can be classified into two categories: (1) model-based methods and (2) data-based methods, as shown in Figure 1-6.

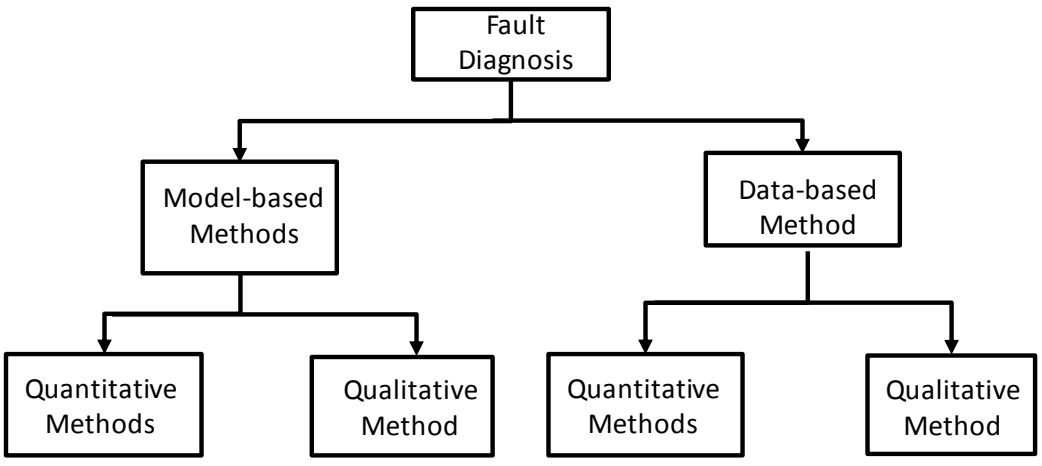

Figure 1-6 Classification of fault diagnosis methods

Model-based FD methods can be further classified into quantitative model-based approaches and qualitative model-based approaches. In the quantitative model-based approaches, the mathematical model of the process is needed to analyze the condition of the plant. This model is built according to knowledge of the physical characteristics of

the process. The relation between inputs and outputs of the process are also presented in this model. Therefore, the characteristic of faults in the process can be obtained from mathematical analysis of the inputs, outputs and the model. The majority of FD methods are in the community of quantitative model-based approach (Patton, Frank and Clarke, 1989; Frank, 1996; Isermann, 2005; Ding, 2008). The classification of the quantitative model-based FD approach is show in Figure 1-7.

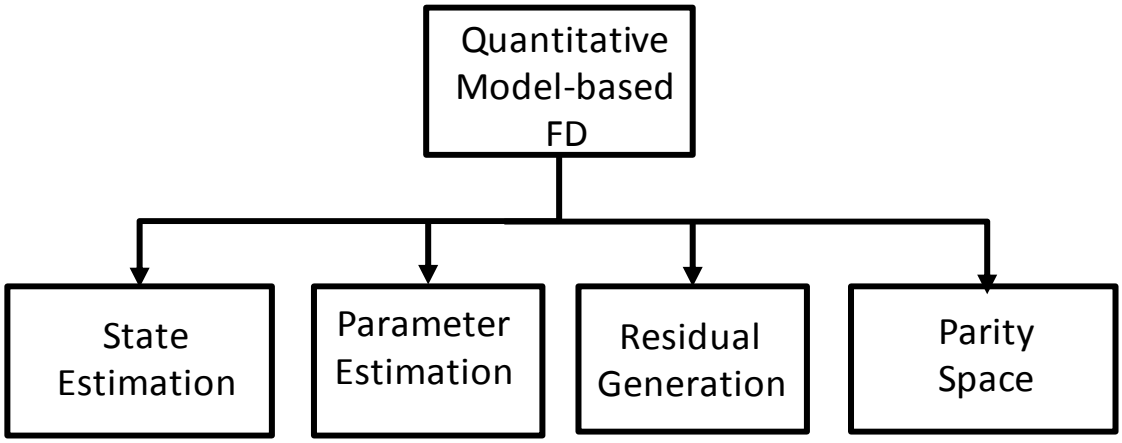

Figure 1-7 Classification of quantitative model-based fault diagnosis methods

In the qualitative model approach, different qualitative functions are used. FD based on qualitative models is beyond the scope of this thesis and will not be discussed in details. Readers are referred to (Venkatasubramanian, Rengaswamy and Kavuri, 2003) for an introduction to this approach.

Data-based FD methods do not use the physical model obtained from the principles of the monitored process. Generally, the raw input/output data and the knowledge of the process are directly used to analyze the condition of the process. Data-based FD approaches can be classified according to whether quantitative methods or qualitative methods are used as shown in Figure 1-6. These approaches include statistical approaches, neural network approaches, fuzzy logic approaches, frequency domain analysis approaches and expert system approaches (Zhang and Jiang, 2008; Li et al., 2011; Jayaswal, Verma and Wadhwani, 2011; Godwin, Matthews and Watson, 2013; Tayarani-Bathaie, Vanini and Khorasani, 2014).

Most FD methods are quantitative model-based methods because of the following advantages of using a mathematical model. First of all, the physical dynamics of the process are transformed into a mathematical model that can be clearly understood in terms of physical and dynamical principles. Hence, the analysis and synthesis of FD

methods for a dynamical process are transformed into mathematical procedures based on the assumed mathematical model of the system. On the other hand, the principle and dynamics of the process are difficult to understand using data-based FD methods due to the "model-free" feature of these methods.

In recent years, the advantages of data-based FD methods are widely noticed due to the growing complexity of modern technical systems (Wang, Chai, Ding and Brown, 2009; Simani, Castaldi and Tilli, 2011; Yin, Wang and Karimi, 2013; Haghani Abandan Sari, 2014). Precise mathematical models of technical systems become more difficult or even impossible to acquire when these systems become more complex. Therefore, quantitative model-based approaches may be difficult to design for these complex systems. Alternatively, precise models are not required for data-based FD methods and these methods can deal with high dimensional systems. Thus the challenge due to modelling of complex system is naturally avoided.

1.5 Outline of the thesis

This thesis focuses on AFTC of wind turbine systems and consists of 8 Chapters. The main contributions are presented in Chapters 4, 5, 6 and 7. The AFTC methods proposed in this thesis are demonstrated through simulation using a model of a realistic modern large wind turbine. The remainder of the thesis is organized as follows:

Chapter 2 shows the state of the art of FTC for wind turbine systems. First of all, the motivation of FTC for wind turbines is explained. Different types of faults in wind turbines are then presented and discussed in order to show the detailed research challenges that can be addressed by the control systems community. Finally, an overview of the recent studies on FTC for wind turbines is given. In this overview, the existing wind turbine FTC approaches are classified according to various control methods used in these FTC schemes.

Chapter 3 describes the modelling and basic control principle of wind turbines. First of all, the modelling of a realistic variable speed wind turbine is presented. Each subsystem of the wind turbine is described in detail. Following the wind turbine modelling, the modelling of various types of wind turbine faults is described. The two wind turbine operation regions are then explained in detail. Finally, the principles of the wind turbine control system are presented. The dual control goal problem of a wind turbine is also explained.

Chapter 4 focuses on the AFTC for wind speed sensor faults. The wind speed sensor is a special kind of sensor to provide the reference signal rather than the feedback to the control system. In this Chapter, a wind speed estimation method is proposed together with an FDI strategy for detecting and isolating wind speed sensor faults. Both the estimation method and the FDI are based on the least squares support vector machine (LSSVM). Thus, the theory of LSSVM is also presented in this Chapter. Meanwhile, robust model predictive control (MPC) using 1-norm cost function is used to design a *baseline controller* (i.e. a basic controller designed without considering the fault tolerant ability and thus has to be combined with an FE or FDI unit to realize FTC), which is to be robust against the wind speed estimation error. Finally, simulation results are given to demonstrate the performance of the proposed AFTC scheme.

The contributions of this Chapter are: (1) a wind speed estimation method using LSSVM, (2) a method using LSSVM for FDI of wind speed sensor fault, and (3) an AFTC scheme using a robust MPC to consider the wind speed estimation error.

Chapter 5 is concerned with AFTC for wind turbine sensor faults. The sensors considered in this Chapter are the pitch angle sensor, generator speed sensor and generator torque sensor. In this approach, the nonlinear wind turbine system model is approximated by a T-S fuzzy model. Therefore, a case study is given to show the steps of developing a T-S fuzzy wind turbine model. In order to detect and isolate sensor faults, a T-S fuzzy observer based on online eigenvalue assignment is then proposed and the residual generated from this fuzzy observer is used for FDI. A baseline controller based on T-S fuzzy MPC is designed to take into account the nonlinearity and the constraints in the wind turbine system. Simulation results are given to demonstrate the performance of the proposed AFTC scheme.

The contributions of this Chapter are: (1) design of a T-S fuzzy observer using online eigenvalue assignment, (2) an FDI method for wind turbine sensor faults by analyzing the characteristic of residual signals, and (3) a T-S fuzzy MPC approach for wind turbine control.

Chapter 6 focuses on another approach of AFTC for wind turbine sensor faults. A special application scenario with insufficient hardware redundancy is considered in this approach. Both analytical and hardware redundancies in the turbine system are utilized to design this AFTC scheme. The overall wind turbine is divided into two subsystems:

(1) a driver train subsystem and (2) a combined generator and pitch subsystem. An FDI unit is designed for the drive train subsystem and an FE unit is designed for the combined generator and pitch subsystem. Finally, simulation results are given to show the performance of the proposed AFTC scheme.

The contributions of this Chapter are: (1) design of a descriptor observer for generator torque sensor fault estimation, (2) an AFTC scheme for wind turbine sensor faults utilizing analytical redundancy and limited hardware redundancy.

Chapter 7 focuses on the design of an AFTC scheme for wind turbine actuator faults. A novel FE unit based on T-S fuzzy moving horizon estimation (MHE) is proposed in this approach. This Chapter commences by presenting the concept and basic principle of MHE. Following this, the T-S fuzzy MHE combining MHE and T-S fuzzy modelling is proposed to estimate actuator faults. The estimated faults are then compensated by a T-S fuzzy MPC. Simulation results are then given to demonstrate the performance of the proposed AFTC scheme.

The contributions of this Chapter are: (1) a method for wind turbine actuator fault estimation using T-S fuzzy MHE, and (2) an AFTC approach for actuator fault tolerant control of wind turbines based on combined fuzzy MPC and MHE.

Chapter 8 summarises the content of this thesis. The summary and conclusions of the contents in the previous seven Chapters are given. The relation between different Chapters is also described. Finally, possible future research directions arising from this thesis are discussed.

Chapter 2: Fault tolerant control of wind turbines

This Chapter reviews the recent development of FTC for wind turbines. First of all, the motivation of research into FTC of wind turbines is explained and discussed in Section 2.1. Secondly, the faults in wind turbines are classified and explained in Section 2.2. Thirdly, various wind turbine FTC approaches are reviewed in Section 2.3. Fourthly, the motivation of the thesis is presented in Section 2.4. Finally, the conclusions are drawn in Section 2.5.

2.1 Introduction

Since 2000, the power capacity of wind turbines has been growing quickly from a few hundred kilowatts to several megawatts due to increasing global demand for more renewable power. The size of wind turbine structure and the complexity of wind turbine hardware are also increasing greatly to meet the need of high power production. A significant number of offshore wind turbines are still being constructed in wind farms throughout Europe, Asia, north American and elsewhere (Global-Wind-Energy-Council, 2014).

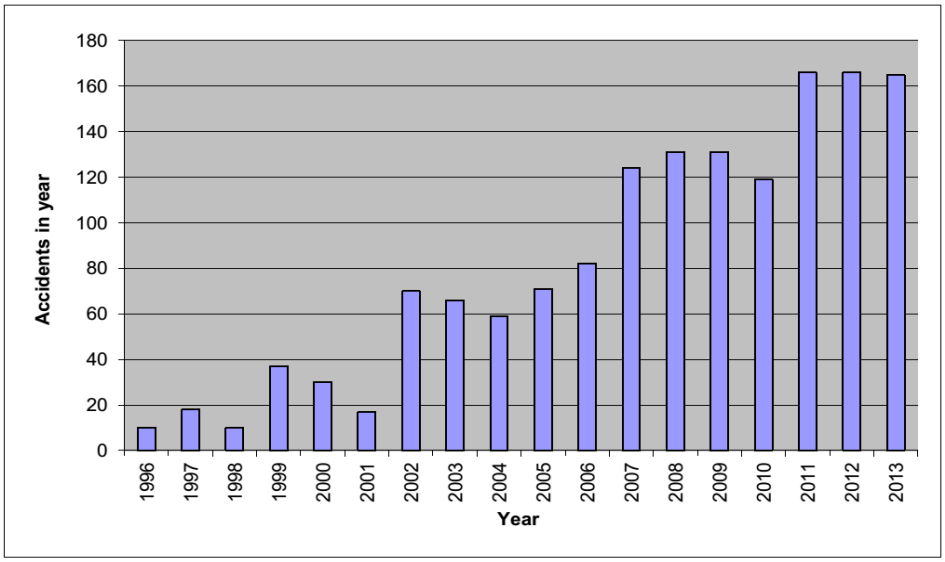

Figure 2-1 Wind turbine accidents to 2013 (Anonymous, 2013a)

However, the growing wind turbine size and complexity poses a challenge for wind turbine reliability. The number of hardware components in a wind turbine increases when the turbine complexity is growing. Thus faults can occur in more wind turbine components and consequently the number of wind turbine accidents due to faults in the components is also increasing. As Figure 2-1 shows, the number of turbine accidents in recent years has increased steadily due to the increasing turbine complexity and growing number of installed turbines. Hence the operation reliability of wind turbines has become a major topic of interest in recent years. FTC of wind turbines is one of the practical techniques to improve wind turbine operation reliability (Pourmohammad and Fekih, 2011). This situation has stimulated research into FTC of wind turbines.

Another motivation of research into FTC of wind turbines is to enhance wind turbine operating efficiency in order to limit additional cost of wind turbines operation. The amount of power produced by a wind turbine can decrease due to faults. Furthermore, a failure in the wind turbine system can result in several months of turbine downtime. However, from an economic viewpoint, the loss of income due to a power decrease or wind turbine downtime is not acceptable by wind farm owners. Therefore, FTC techniques can serve as a precaution to avoid loss of income due to faults or failures.

Difficulty in wind turbine maintenance is also a motivation for developing wind turbine FD/FTC systems. The structure of modern megawatt level wind turbines is very large and high and thus the mechanical and electrical components in the turbine nacelle are not easily approached by maintenance personnel, as shown in Figure 2-2.

Figure 2-2 Wind turbine maintenance (Anonymous, 2013b)

Maintenance work is hard to conduct and is also expensive for these very large wind turbines. This is because ships or helicopters may be needed to support the maintenance operations as illustrated in Figure 2-2. Furthermore, the maintenance staff may not be able to access wind turbines due to severe sea weather conditions in the case of offshore wind turbine maintenance. This harsh operating scenario offers an important opportunity for the development and implementation of FTC systems for wind turbines. These FTC systems can increase turbine reliability and sustainability by reacting to turbine malfunctions and thus decrease the probability of required maintenance. Furthermore, the FDI or FE unit within these FTC systems can be used to remotely monitor the turbine status and limit the need of human operator intervention.

The reliability of wind turbine components is impacted by environmental factors like the temperature variation and the humidity change. Meanwhile, wind turbines are exposed to all kinds of weather conditions, such as snow, icing, lighting, hail, storm and salty corrosion (for offshore wind turbines). These weather conditions will decrease turbine reliability and shorten the lifetime of turbine components. Therefore, the occurrence of faults in turbine systems is inevitable due to the above environmental factors and weather conditions. This situation is a strong motivation for research into FTC of wind turbines.

2.2 Faults in wind turbine systems

The impact of different faults on wind turbines is different (Lu, Li, Wu and Yang, 2009). Some faults result in wind turbine system shut down or even turbine destruction. Some other faults are less severe and result in malfunction of the turbine systems, decreasing power conversion performance. Faults in a wind turbine system can be classified into actuator faults, sensor faults and component faults as described in Section 1.4.1. These three types of faults are described and discussed as follows.

2.2.1 Wind turbine actuator faults

Actuators are crucial for wind turbine operation since they directly influence wind turbine power production. Actuator faults of wind turbines can occur in turbine actuators such as the pitch system, the yaw system and the power convertor in the generator system. In this thesis, the pitch system and the power converter in the

generator system are considered. There are various causes for wind turbine actuator faults in these two locations. These causes can be classified into two categories: (1) internal causes due to the components in the wind turbine (2) external causes due to environmental factors. Generally, actuator faults result in an offset or change in actuator dynamics (Odgaard, Stoustrup and Kinnaert, 2013).

Environmental factors can be the external causes for actuator faults. Accumulated dirt and ice on turbine blades can result in an offset in the turbine pitch actuation signal. An illustration of icing on turbine blades is shown in Figure 2-3. The pitch actuator system is frequently affected by these factors during its lifetime. Meanwhile, rotor imbalance and asymmetry of the turbine blades caused by inaccurate manufacturing considerably affect the pitch actuator system (Lu, Li, Wu and Yang, 2009).

Figure 2-3 Icing on wind turbine blades (Anonymous, 2011b)

The internal source of pitch actuator faults is the hydraulic system or the electrical motor in charge of turbine blade movement. The hydraulic system in the wind turbine is prone to failure. From the year 2000 to 2004, 13.3% of the wind turbine failures in Sweden were due to the hydraulic system according to a study on Swedish wind farm (Ribrant and Bertling, 2007). Faults in the hydraulic system can be due to pressure drop or air content in the oil. The pressure drop is generally due to a blocked pump or leakage in a hose (Odgaard, Stoustrup and Kinnaert, 2013). Air content in the oil is inevitable since there will always be some air in the hydraulic oil. Both the pressure drop and air contamination will change the dynamics of the pitch system.

Generally, actuator faults in the power convertor of the generator system are due to internal causes. Defects in semiconductor devices are major internal causes of the power

converter fault (Lu, Li, Wu and Yang, 2009). Another cause of converter faults is the imprecise estimation of the converter torque, which can result in an offset torque (Odgaard, Stoustrup and Kinnaert, 2013).

2.2.2 Wind turbine sensor faults

There are various sensors to monitor the wind turbine and provide feedback for the turbine controller. These sensors are used to measure blade pitch angle, blade rotating speed, wind speed, generator speed, generator torque, etc. There are both electrical and mechanical causes for sensor faults. Environmental factors can also be possible causes of sensor faults. These faults can result in decreased control performance since the feedback signals in the wind turbine control loop are provided by these sensors.

Environmental factors can influence some sensors mounted on the surface of a wind turbine. Severe weather like lighting, hail and icing are all possible causes of sensor faults. Meanwhile, some sensors are sensitive to environment parameters such as temperature and humidity. Changes of these parameters can result in offsets of sensor outputs.

Mechanical or electrical failures can also result in sensor faults. Some measurements in the wind turbine are obtained with encoders. These encoders can be faulty due to electrical or mechanical failures. A faulty encoder will result in gain factor errors or fixed (unchanged) measurement values. For example, the occurrence of gain factor error fault in a rotor speed sensor can be due to encoders reading more marks on the rotating part , which can happen due to accumulated dirt on the rotating part (Odgaard, Stoustrup and Kinnaert, 2013).

2.2.3 Wind turbine component faults

The component faults are generally located in the turbine drive train system. Most component faults in the drive train system are due to mechanical reasons. These faults are from the gear box, shaft and bearing. Generally, faults in the drive train system require time-consuming and costly maintenance. Drive train faults occur frequently and many fault diagnosis or condition monitoring techniques are proposed to reduce the impact of these faults (Hyers et al., 2006; Wilkinson, Spinato and Tavner, 2007; Amirat

et al., 2009; Hameed et al., 2009). The main challenge is to detect and isolate faults that are beginning to develop before they become more serious.

Gear box faults caused by gear tooth damage are common in the drive train system, as shown in Figure 2-4. Gear tooth damage can be due to offset and eccentricity of tooth wheels (Lu, Li, Wu and Yang, 2009). Furthermore, tooth wear always exists due to the heavy stress on tooth wheels. Gear box faults inevitably result in gear ratio changes.

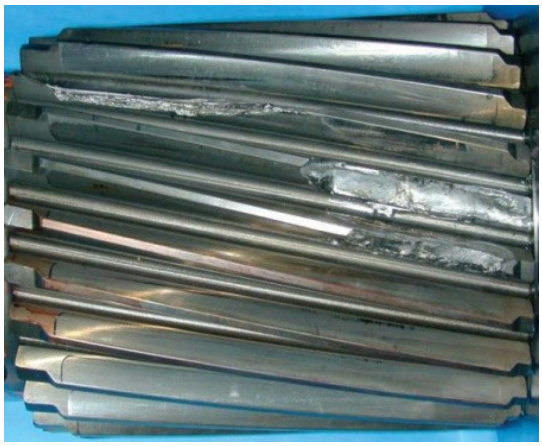

Figure 2-4 Gear tooth damage (Anonymous, 2011a)

The drive train system bearings are also likely to be faulty (Hameed et al., 2009). Fatigue and wear due to heavy loads are inevitable. Moreover, pitting and impending cracks are also causes of faults. These faults will result in changes in dynamics of the drive train system.

The friction coefficient in the drive train changes slowly with time and can evolve over months or years. This change can also result in changes in dynamics of the drive train system.

2.3 FTC approaches for wind turbine systems

Research on FTC for wind turbines has been stimulated since the introduction of a wind turbine benchmark model proposed to provide a common platform for wind turbine research, i.e. a 4.8MW wind turbine benchmark model developed by KK-electronics and Aalborg university (Odgaard, Stoustrup and Kinnaert, 2009). A second wind turbine benchmark model has also been introduced (Odgaard and Johnson, 2012), which is based on a 5MW wind turbine system model made by the US National Renewable

Energy Laboratory (Jonkman and Buhl Jr, 2005). The two benchmark systems outlined here are widely accepted in the community of wind turbine FTC research. In recent years, several reviews of FTC and FDI for wind turbine systems appeared to summarize the methods proposed so far (Amirat et al., 2009; Hameed et al., 2009; Pourmohammad and Fekih, 2011; Badihi, Zhang and Hong, 2013).

Before the proposal of the above two wind turbine benchmark models, most research effort were made in the area of FD/condition monitoring methods for wind turbine systems rather than FTC methods. These FD/condition monitoring methods involve signal processing, model-based or data-driven techniques (Donders, Verdult and Verhaegen, 2002; Changzheng, Changcheng, Yu and Nan, 2005; Guérin, Druaux and Lefebvre, 2005; Ding et al., 2007; Liu, Xu and Yang, 2008).

So far, only a limited number of studies on FTC of wind turbines have appeared. Different approaches are used in these studies, including: T-S fuzzy modelling based approaches (Kamal, Aitouche, Ghorbani and Bayart, 2012; Sami and Patton, 2012b; Badihi, Zhang and Hong, 2014), LPV control based approaches (Sloth, Esbensen and Stoustrup, 2010; Chen, Shi and Patton, 2013), predictive control based approaches (Yang and Maciejowski, 2012; Soliman, Malik and Westwick, 2012) and sliding model-based approaches (Sami and Patton, 2012d; Schulte, 2014). Generally, these FTC methods are either based on residual-based FDI methods or FE methods. Using an FDI unit, the faulty actuators or sensors can be identified and the control system can reconfigure by switching to redundant healthy sensors or actuators if hardware redundancy is available. Alternatively, fault compensation can be achieved using an FE unit and the estimated faults are effectively “hidden” or compensated in the control system. Both the residual-based FDI methods and FE based methods are proven to be effective approaches for AFTC of wind turbines.

There are only a limited number of studies on wind turbine FTC methods and they all have appeared quite recently as mentioned above. Therefore, these studies are not rich enough to be reviewed in a systematic way. However, they can still be reviewed as below according to different theoretical methods used in these wind turbine FTC approaches.

2.3.1 T-S fuzzy modelling based approach

Several approaches based on fuzzy modelling have been used in the AFTC of wind turbine systems. Fuzzy modelling in these approaches is generally utilized to deal with the nonlinearity in the turbine model.

In (Badihi, Zhang and Hong, 2014), a T-S fuzzy model-based approach is proposed for FDI and AFTC for wind turbine actuator faults. First of all, a gain scheduling proportional integral (PI) controller based on a fuzzy gain scheduling technique is designed for the nonlinear wind turbine system. This controller has an extra input of change in tracking error in order to improve control performance for the wind turbine. This extra input achieves a better description of the dynamics of the wind turbine system and provides some level of prediction of system behaviour to facilitate control. Then, a remedy strategy to prevent the propagation of faults and system failure is proposed, which is based on a signal correction algorithm. Based on this remedial strategy, a residual-based FDI is designed for wind turbine sensor faults.

Another approach based on fuzzy modelling is proposed in (Kamal, Aitouche, Ghorbani and Bayart, 2012), in which sensor fault tolerant control of wind turbines subject to model parameter uncertainty is considered. In this approach, a set of local linear models with parameter uncertainty are derived by analyzing the wind turbine operating region. A T-S fuzzy model of the wind turbine is then built based on the local linear models. The parameter uncertainty in the turbine system is considered in this T-S fuzzy model. Based on this fuzzy model, a bank of T-S fuzzy observers is designed as the FDI unit. Each fuzzy observer is driven by a single sensor output to generate the estimated outputs. The difference between the real outputs and estimated outputs is used as the residual signal to identify and isolate sensor faults. When one sensor becomes faulty, the residual generated using the faulty sensor will increase while the residuals generated using the healthy sensors will remain unchanged. Therefore, FDI is achieved by comparing the residual amplitude generated from different observes (i.e. the sensor generating largest residual is the faulty sensor). FTC is realized by switching to the observer generating the smallest residual (i.e. the observer based on healthy sensors). Furthermore, a robust fuzzy controller is proposed in this approach as the FTC unit. Stability analysis of the fuzzy controller considering parameter uncertainty and wind

disturbance is also given. Meanwhile, linear matrix inequities (LMI) are used to acquire the feedback gain of the fuzzy controller.

In (Sami and Patton, 2012b), an AFTC approach combining FE with T-S fuzzy modelling for a wind turbine is presented for wind turbine sensor faults. A T-S fuzzy model of the wind turbine system is derived from a set of local linear models in this approach in order to deal with the nonlinear dynamics in the turbine system. Then, an adaptive fuzzy observer is designed to estimate the system states and sensor faults simultaneously. An LMI method to assign the eigenvalues of the fuzzy observer gain into a disc region in the complex plane is also proposed. FTC is achieved through deducting the estimated fault from the output of the faulty sensor. Finally, a dynamic output feedback fuzzy controller is proposed as the baseline controller for the wind turbine. The LMI method is used again to prove the stability of the fuzzy controller. Both the controller and observer designs in this AFTC scheme are robust against errors in the wind speed measurement.

2.3.2 LPV control based approach

In (Sloth, Esbensen and Stoustrup, 2010), an LPV approach to wind turbine FTC for pitch actuator faults is presented. Both AFTC and PFTC schemes based on LPV control are proposed. First of all, the LPV model of the wind turbine system is built through linearizing the nonlinear wind turbine model and choosing some parameters as the scheduling parameter. For the PFTC LPV control, the fault is treated as the unknown scheduling parameter and results in unknown disturbance. Therefore, the wind turbine controller is designed to be robust against this disturbance through LMI methods. For the AFTC LPV control, an FD unit is used to estimate the faults. This FD unit is designed from a multiple-model estimation approach using an extended Kalman filter. The estimated fault is then used as the scheduling parameter. Again, LMI methods are used to design the controller. This LPV approach is further developed in (Sloth, Esbensen and Stoustrup, 2011) to design a robust LPV controller, which is robust against parameter uncertainty in the LPV model. This uncertainty is due to the mismatch between the LPV model and the original nonlinear turbine model.

In (Chen, Shi and Patton, 2013), an LPV fault tolerant control approach for hydraulic pitch actuation fault of a wind turbine system with independent pitch actuators is proposed. Two actuator fault scenarios are considered. The first scenario considers the pitch actuator stuck at a fixed value and the second scenarios considers the component fault in the pitch actuation system. For the first fault scenario, An FE unit based on H_∞ / H_- robust theory is proposed to estimate the actuator fault of fixed value. FE is achieved using a H_- fault sensitivity index and the robustness is achieved through maximizing the H_∞ performance of a transfer matrix between the estimated fault and the combination of modelling uncertainty and sensor noise. For the second fault scenario, an adaptive observer is proposed as the FE unit to deal with the component fault in the actuation system. Based on the above FE units, fault compensation is achieved using a 'fault hiding' approach. The control strategy in this AFTC approach is a combination of an on-line redesign LPV feedback and feedforward.

An LPV approach using the idea of virtual sensors is proposed for FTC of wind turbine sensor faults in (Rotondo, Puig, Acevedo Valle and Nejjari, 2013). In this approach, the nonlinear wind turbine model is approximated with a LPV model. A bank of virtual sensors is then designed to expand the set of physical sensors. A state observer is designed for the wind turbine LPV model using LMI technique. Meanwhile, a parameter is introduced to select from the physical and virtual sensors to be used by the observer. Fault tolerance is achieved through estimating and compensating the fault.

2.3.3 Predictive control based approach

A hierarchical control scheme via predictive control for wind turbine sensor and actuator faults is presented in (Yang and Maciejowski, 2012). This hierarchical scheme comprises a model predictive pre-compensator, an FDI unit, a global model predictive controller and a supervisory controller. The pre-compensator is a predictive controller, which is used to compensate and hide the effect of faults such that the global controller can be used as a baseline controller without the need to consider faults. Fault estimation and model reference technique are used in the pre-compensator design in order to ensure the compensated system has dynamic behaviour close to a reference model. Constraints on the wind turbine system are also considered in this approach. The global

controller is a nonlinear model predictive controller and serves as the baseline controller for the wind turbine. Meanwhile, a supervisor control is proposed and used to supervise the low level controllers to adjust the system constraints and cost functions of the low level predictive controllers. An FDI unit is used in this scheme to provide information on faults to the supervisor controller.

In (Soliman, Malik and Westwick, 2012), a subspace predictive control approach is proposed for wind turbine actuator FTC. In this approach, a subspace identification method is used to identify the wind turbine model. Moreover, only input and output data are used for model identification and thus the knowledge of the state space model of the wind turbine is not needed. Integral action is considered in the subspace identification to achieve offset-free tracking in the presence of piecewise constant disturbance. The identified model is online updated such that the model is adaptive to system dynamic changes resulting from actuator faults. This updated model is used as the prediction model and a predictive control algorithm is used to solve an optimization problem in order to calculate the control input.

2.3.4 Sliding mode based approach

In (Sami and Patton, 2012d), a sliding mode control scheme is proposed for sensor FTC of wind turbines. A robust linear descriptor observer is proposed in this scheme to simultaneously estimate system states and sensor faults. The estimated aerodynamic torque is used as the input to the observer. However, this estimation is inaccurate. Therefore, the observer is designed to be robust against the uncertainty due to inaccurate estimation. A sliding mode controller is then proposed as the baseline controller to deal with model uncertainty.

A sliding mode observer based FTC system for actuator and sensor faults of wind turbines is presented in (Schulte, 2014). In this approach, a Takagi-Sugeno sliding mode observer is used as the FDI unit to estimate faults of the nonlinear wind turbine system. Disturbances, actuator faults and sensor faults are all considered in the observer. FTC for actuator faults is realized by subtracting the estimated actuator faults from the required control input. FTC for sensor faults is also realized by subtracting the estimated sensor faults from faulty sensor outputs. Stability of the fault tolerant control system is

proved with a Lyapunov function derived from the T-S fuzzy model of the wind turbine system.

2.4 Motivation of the thesis

As discussed in Section 2.3, research into FTC of wind turbines has only been stimulated quite recently with limited numbers of research results. Thus this research area is in an early stage which needs more research effort. Therefore, this thesis proposes some new approaches for FTC of wind turbines in order to make more academic contribution in this new research area.

Research into FTC for wind turbines has been conducted in the university of Hull for two years with some research results (Sami and Patton, 2012d; Sami and Patton, 2012a; Sami and Patton, 2012b; Shaker and Patton, 2014). However, these FTC approaches are all designed for wind turbine operating in the region below rated wind speed. Therefore, this thesis aims to develop further research into FTC of wind turbines based on the previous research results, in order to design new FTC approaches for wind turbine operating in the both regions below and above rated wind speed.

Furthermore, there are some unsolved problems or challenges in this research area. For example, FTC for wind speed sensor faults is seldom considered in this research area although these sensors are important for wind turbine operation, which is explained in Chapter 4. Therefore, this research problem is addressed in this thesis and a FTC scheme for wind speed sensor faults is proposed as a potential strategy for safe operation of wind turbines in the presence of sensor faults.

A motivation for using wind turbine control strategies based on MPC in this thesis is that the wind turbine system constraints can be considered in the framework of MPC. It should be noted that the constraints in a wind turbine system is a practical issue that should be considered. However, this issue is not considered in most of the wind turbine FTC approaches reviewed in the previous Section, except for the predictive control based approaches in Section 2.3.3. Therefore, the FTC schemes proposed in this thesis incorporate controller design based on MPC since this thesis focuses on the application of FTC to wind turbines and thus the practical issues of constraints encountered in the real application scenario should be considered.

2.5 Conclusions

In this Chapter, the motivation for research into FTC of wind turbines is introduced. It is shown that research in this area is motivated by practical concerns including reliability, maintenance and operation cost. These concerns are raised due to the fast development of wind turbine industry in recent years.

After the introduction of the research motivation, the potential faults in different locations of the wind turbine system and the causes for these faults are then presented in order to show the practical research challenge of FTC for wind turbines.

Finally, various FTC methods are reviewed. It can be seen from these methods that approximating the nonlinear wind turbine system with simpler forms of model (i.e. T-S fuzzy model or LPV model) is an effective approach for FD/FTC design. FDI based on residual generation is used in some methods to identify and isolate faults. On the other hand, fault estimation based methods are also used to directly estimate the fault without referring to the residual such that FTC can be realized by compensating the estimated faults.

Chapter 3: Wind turbine modelling and control

3.1 Introduction

In this Chapter, The nonlinear model of a realistic 4.8 MW variable speed wind turbine is described. This model is based on a wind turbine benchmark model proposed in (Odgaard, Stoustrup and Kinnaert, 2009), which is proposed for comparisons between different wind turbine FD/FTC approaches. The model in this Chapter is used in this thesis to design the FD/FTC methods for wind turbine systems. Following the description of this model, the principles of wind turbine system operation are presented. Meanwhile, the wind turbine dual control goals problem involving operation in the regions below and above rated wind speed is also explained.

The remainder of this Chapter is organized as follows: The modelling of the wind turbine is described in Section 3.2. The system constraints that should be satisfied to operate the wind turbine are presented in Section 3.3. Modelling aspects of various wind turbine faults are described in Section 3.4. The operation principles of the wind turbine, together with the control goals in the two wind turbine operating regions, are explained in Section 3.5 in order to outline the challenges to be met by the wind turbine controller design. Conclusions are drawn in Section 3.6.

3.2 Wind turbine modelling

The wind turbine system considered in this thesis comprises three subsystems, i.e. the generator subsystem, the drive train subsystem and the pitch subsystem. The modelling of these three subsystems presented in this Section is based on a benchmark wind turbine model described in (Odgaard, Stoustrup and Kinnaert, 2009; Odgaard, Stoustrup and Kinnaert, 2013). The modelling of the aerodynamic characteristic of the wind acting on the turbine blades is also shown in this Section. The FTC schemes presented in Chapters 4, 5, 6 & 7 are designed based on the overall wind turbine model comprising the models of the three subsystems and the aerodynamic model. The different subsystems within a wind turbine are illustrated in Figure 3-1.

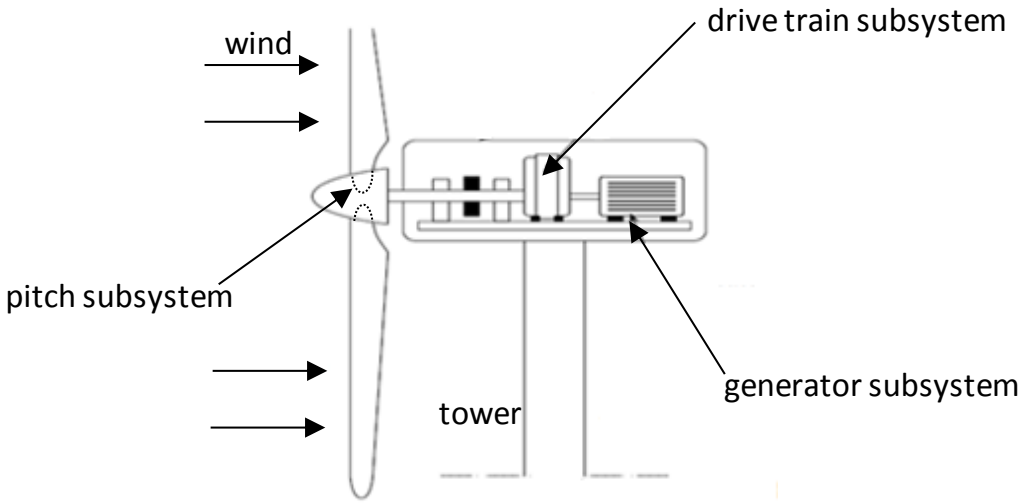

Figure 3-1 Wind turbine subsystems

Besides the control system for the overall wind turbine, there is another control system for the electrical power converter in the generator subsystem. Since this electrical system has faster dynamics than the overall wind turbine, it is not considered here. Hence, this thesis is able to focus on the control problem at the wind turbine system level without ignoring important factors. There is also a yaw pointing control system that is excluded from the overall wind turbine control system design and it is assumed to be functioning correctly and independently.

3.2.1 Pitch model

The hydraulic pitch system is used for changing the wind turbine blade pitch angle. It can be modelled as a second order transfer function as follows (Merritt, 1967):

$$\frac{\beta(s)}{\beta_r(s)} = \frac{\omega_n^2}{s^2 + 2\zeta\omega_n s + \omega_n^2} \tag{3-1}$$

where ζ is the damping factor and ω_n is the natural frequency. β is the turbine blade pitch angle in degrees and β_r is the corresponding reference pitch angle.

3.2.2 Generator model

The generator subsystem produces generator torque to influence the rotation speed of turbine blades. Its dynamics are modelled with a first order transfer function given as:

$$\frac{T_g(s)}{T_{gr}(s)} = \frac{\alpha}{s+\alpha} \tag{3-2}$$

in which T_g is the generator torque and T_{gr} is the reference torque.

The generated electrical power is given as

$$P_g = \eta_g \omega_g T_g \tag{3-3}$$

where ω_g is the generator rotating speed， η_g is the generator efficiency and P_g is the power produced by the generator.

3.2.3 Drive train model

The wind turbine drive train subsystem represents the turbine rotor shaft and the generator shaft coupled with a gear box. Therefore, drive train subsystem can be modelled by means of a two-mass inertia model given as:

$$\begin{bmatrix} \dot{\omega}_r \\ \dot{\omega}_g \\ \dot{\theta}_\Delta \end{bmatrix} = A_{dt} \begin{bmatrix} \omega_r \\ \omega_g \\ \theta_\Delta \end{bmatrix} + B_{dt} \begin{bmatrix} T_a \\ T_g \end{bmatrix} \tag{3-4}$$

in which T_a is the aerodynamic torque resulting from wind acting on the turbine blades. A_{dt} and B_{dt} are the state space matrices given as:

$$A_{dt} = \begin{bmatrix} \frac{-S_{dt} - B_r}{J_r} & \frac{S_{dt}}{N_g J_r} & -\frac{K_{dt}}{J_r} \\ \frac{\eta_{dt} S_{dt}}{N_g J_g} & \frac{-\eta_{dt} S_{dt} - B_g N_g^2}{N_g^2 J_g} & \frac{\eta_{dt} K_{dt}}{N_g J_g} \\ 1 & -\frac{1}{N_g} & 0 \end{bmatrix}$$

$$B_{dt} = \begin{bmatrix} \frac{1}{J_r} & 0 \\ 0 & -\frac{1}{J_g} \\ 0 & 0 \end{bmatrix}$$

where J_r and J_g are the rotor and generator moments of inertia. B_r and B_g are the rotor and generator external damping coefficients, S_{dt} is the torsion damping coefficient, N_g and η_{dt} are the gear ratio and drive train efficiency and K_{dt} is the torsion stiffness. ω_r is the turbine rotor speed and θ_Δ is the torsion angle of the drive train.

3.2.4 Aerodynamic model

The aerodynamic model represents the aerodynamic torque resulting from the wind acting on the turbine blades. It is given as (Burton, Jenkins, Sharpe and Bossanyi, 2011):

$$T_a = \sum_{i=1}^{3} \frac{1}{6} \rho \pi R^3 C_q(\lambda, \beta_i) v^2 \tag{3-5}$$

where ρ and R are the air density and radius of the turbine blades which are given constants. v is the effective wind speed (EWS) and C_q is the nonlinear torque coefficient as a function of β_i and the tip-speed-ratio λ, computed by:

$$\lambda = \frac{\omega_r R}{v} \tag{3-6}$$

As shown in (3-5), the overall aerodynamic torque is the sum of the aerodynamic torque acting on each of the three blades.

A simpler aerodynamic model which is widely used in the literature is given as:

$$T_a = \frac{1}{2} \rho \pi R^3 C_q(\lambda, \beta) v^2 \tag{3-7}$$

The model in (3-7) is based on two assumptions. First of all, the aerodynamic torque acting on each blade is equal to one third of the overall aerodynamic torque. Secondly, collective pitch control is used in the wind turbine control system (i.e. the pitch angle of all the blades is always controlled to be equal).

The overall wind turbine system model is a nonlinear model and can be acquired by combining all the subsystem models described above. As shown in (3-6) and (3-7), the nonlinearity of the wind turbine model comes from the aerodynamic torque, which is a highly nonlinear function of β, v and ω_r.

A nonlinear dynamic model of the overall wind turbine system can be used to design model-based control systems. This nonlinear model is obtained by reformulating (3-1) and (3-2) into state space form and combining them with (3-4) and (3-7):

$$\begin{aligned} \dot{x} &= f(x,u,v) \\ y &= Cx \end{aligned} \tag{3-8}$$

in which $x=[\omega_r \quad \omega_g \quad \theta_\Delta \quad \dot{\beta} \quad \beta \quad T_g]^{\mathrm{T}}$, $y=[\omega_g \quad \beta \quad T_g]^{\mathrm{T}}$, $u=[T_{gr} \quad \beta_r]^{\mathrm{T}}$ and v is the EWS . C is a constant output matrix, which is determined by the sensors used in the FTC/FD system. When the generator speed sensor, pitch angle sensor and generator torque sensor are used, C becomes:

$$C=\begin{bmatrix} 0 & 1 & 0 & 0 & 0 & 0 \\ 0 & 0 & 0 & 0 & 1 & 0 \\ 0 & 0 & 0 & 0 & 0 & 1 \end{bmatrix}$$

All the parameters of the turbine model described in this Section are obtained from the benchmark model (Odgaard, Stoustrup and Kinnaert, 2009) and shown in Table 3-1.

Table 3-1 Parameters of wind turbine model

Pitch model	
ζ	0.6
ω_n	11.11 rad/s
Generator and convertor model	
α	50 rad/s

η_g	0.98
Drive train model	
S_{dt}	9.45 N·m·s/rad
B_r	0 N·m·s/rad
B_g	0 N·m·s/rad
N_g	95
K_{dt}	2.7×10^9 N·m/rad
η_{dt}	0.97
J_q	390 kg·m^2
J_r	5.5×10^7 kg·m^2

Remark 3-1: The EWS in (3-7) is a theoretical value, which is the averaged wind speed over the rotor disc. It is therefore an immeasurable variable. In practice, EWS is approximated by the measurement from wind speed sensor located at top of the turbine nacelle. Alternatively, EWS can also be estimated using various approaches (Østergaard, Brath and Stoustrup, 2007; Xu, Hu and Ehsani, 2012; Sami and Patton, 2012a)

3.3 Wind turbine system constraints

Real wind turbine systems have constraints due to the hardware limitations in wind turbines. For example, the pitching angle of a rotor blade can only be changed within a limited range due to the physical limitations of the pitch hydraulic actuation system. Furthermore, the rate of change of pitch angle is also limited due to the hardware specification of the hydraulic system Some other constraints are applied for safety reasons, such as the turbine generator speed which is not allowed to exceed the maximum generator speed for safe operation.

Constraints in the generator subsystem affect the allowed range of the generator torque. This torque is produced by the power convertor and thus the hardware specification of the power converter determines the range of the generator torque. The generated electrical power is also limited to the rated generator power for safety reasons.

However, some of the wind turbine control approaches in the literature do not consider these practical constraints in the wind turbine system.

The following constraints are used in the wind turbine model presented in this Section.

Table 3-2 Constraints of wind turbine model

Parameters	Constraints
β_r	[-2 degree ， 90 degree]
$\Delta\beta_r$	[-9 degree/s ， 9 degree/s]
T_{gr}	[0 N·m ， 36000 N·m]
ΔT_{gr}	[-12500 N·m/s ， 12500 N·m/s]

3.4 Modelling of faults

A model-based control system can be designed based on the standard wind turbine model (3-8). However, this control system is only suitable for wind turbine control in the fault-free case since faults are not considered. If an AFTC system is designed for wind turbines, the modelling of faults should be taken into account.

Therefore, model-based AFTC approaches for wind turbines are always based on a more complex model combining both the standard wind turbine model (3-8) and the model of faults. There are three types of fault model corresponding to (1) a sensor fault, (2) an actuator fault and (3) a component fault. Either one of the three types of fault model can be combined with (3-8) to design an AFTC system for wind turbines. For example, the actuator fault model should be combined with (3-8) in order to design an AFTC system against actuator faults. Moreover, more than one type of fault model can be used to combine with (3-8) if the AFTC system is designed to deal with more than one type of fault, e.g. both actuator and sensor fault models can be combined with (3-8) to design an AFTC system in order to deal with both actuator and sensor faults simultaneously in wind turbines.

3.4.1 Sensor fault

A wind turbine model making use of a sensor fault model is used in AFTC for wind turbine sensor faults. This reformulated model is shown in the following form:

$$\begin{aligned} \dot{x} &= f(x,u,v) \\ y &= Cx + f_s \end{aligned} \tag{3-9}$$

in which f_s is a vector representing the sensor faults.

As shown in (3-9), modelling of sensor faults show up in the form of an added quantity to the outputs, which is often referred to as additive faults. There is another type of sensor fault known as multiplicative faults representing gain factor errors in sensor outputs. However, it is shown in (Chen and Patton, 1999) that the multiplicative sensor fault can be simply transformed into an additive sensor fault and thus only additive sensor faults need be considered in this thesis.

3.4.2 Actuator fault

A turbine model making use of an actuator fault model is used in AFTC for wind turbine actuator faults. This reformulated model is shown in the following form:

$$\begin{aligned} \dot{x} &= f(x, u + f_a, v) \\ y &= Cx \end{aligned} \tag{3-10}$$

where f_a represents the actuator fault.

The actuator fault shows up in the form of an added quantity to the wind turbine inputs. In the literature, there is also multiplicative actuator fault representing gain factor errors in the actuator (Isermann, 2006), which is given as:

$$\begin{aligned} \dot{x} &= f(x, (1 + \Delta)u, v) \\ y &= Cx \end{aligned} \tag{3-11}$$

Where Δ is the fault parameter representing the multiplicative actuator fault. (3-10) and (3-11) are equivalent in the sense of fault compensation, i.e. both additive and multiplicative actuator faults can be estimated by an FE unit and compensated by the FTC system.

If the turbine AFTC system is dealing with both actuator and sensor faults, the following model combining both the modelling of sensor faults and actuator faults can be used:

$$\begin{aligned} \dot{x} &= f(x, u + f_a, v) \\ y &= Cx + f_s \end{aligned} \tag{3-12}$$

3.4.3 Component fault

Component faults are generally functions of states or inputs and thus will affect system stability (Ding, 2008). A general form of wind turbine model considering component faults is given as:

$$\begin{aligned} \dot{x} &= f(x,u,v) + f_c(x,u,v) \\ y &= Cx \end{aligned} \tag{3-13}$$

where $f_c(x,u,v)$ represents the component faults.

3.5 Wind turbine operation and control

3.5.1 Power characteristic of wind turbine

A wind turbine transforms the wind power into mechanical power. This mechanical power is further transformed into electrical power. However, only a portion of the wind power can be captured by the wind turbine. The captured wind power is given as:

$$P_c = \frac{1}{2}\rho\pi R^2 v^3 C_p(\lambda,\ \beta) \tag{3-14}$$

in which P_c is the captured wind power and $C_p(\lambda,\ \beta)$ is the power coefficient, which is a nonlinear function of the tip speed ratio λ and blade pitch angle β. Furthermore, there is a theoretical maximum value of $C_p(\lambda,\ \beta)$ given as (Abad, 2011):

$$C_{p\_\max}(\lambda_{opt}, 0) = 59.3\% \tag{3-15}$$

where $C_{p\_\max}$ is the maximum power coefficient, representing the maximum percentage of wind power that can be captured by the wind turbine. λ_{opt} is the optimal tip speed ratio, which is a given constant. For the wind turbine model considered in this Chapter, $\lambda_{opt} = 6.5$. (3-15) means that the maximum conversion efficiency from wind power to

the turbine mechanical power is achieved when the tip speed ratio is set to the optimal value $\lambda = \lambda_{opt}$ and pitch angle is set to $\beta = 0$.

The wind turbine operation regions are decided by the power characteristic of the turbine and the wind speed acting on the turbine. The power characteristic of the wind turbine when $\beta = 0$ is shown in Figure 3-2.

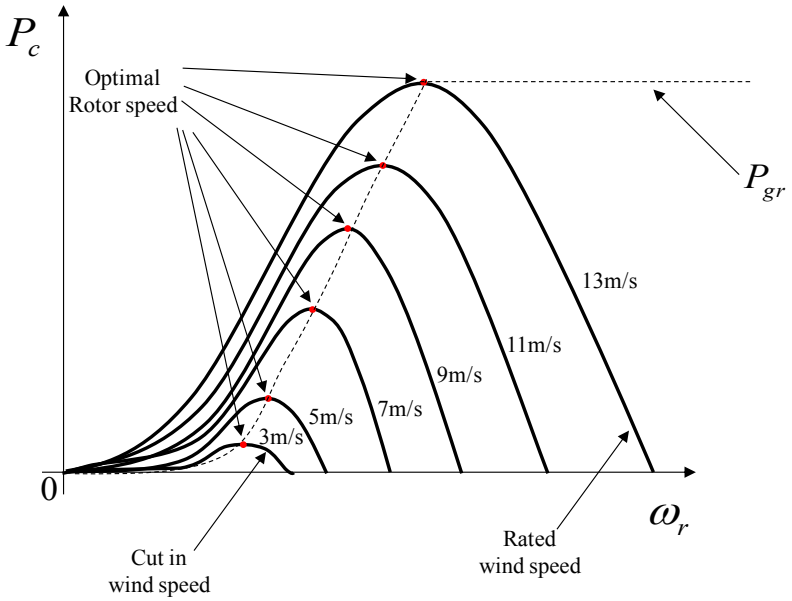

Figure 3-2 power characteristic of the wind turbine when $\beta = 0$

It is shown in Figure 3-2 that there is an optimal rotor speed $\omega_{r\_opt}(t)$ at which the maximum power coefficient is achieved and thus maximum power can be captured from the wind. This optimal rotor speed varies according to the variation of wind speed.

Figure 3-2 also implies that the higher the wind speed is, the more power the turbine can absorb from the wind. However, to ensure safe operation of the wind turbine, the captured wind power cannot exceed the rated generator power P_{gr} greatly. Therefore, the captured wind power should be regulated around the rated power P_{gr} in high wind speed operation. This is achieved by varying the pitch angle β to decrease the power coefficient $C_p(\lambda, \beta)$ in (3-14) such that the captured wind power P_c is below P_{gr}.

3.5.2 Wind turbine operation regions

A variable speed wind turbine operates in two operation regions (Wu, Lang, Zargari and Kouro, 2011; Odgaard, Stoustrup and Kinnaert, 2013), determined by the two speed thresholds as shown in Figure 3-2, i.e. cut in wind speed and the rated wind speed. The cut in wind speed is the threshold at which the wind turbine starts to operate and can capture enough power from the wind to compensate for the power loss in the turbine. The rated wind speed is the threshold at which the wind turbine starts to operate in full capacity and produce power at the level of rated generator power. When the wind speed is between the cut in wind speed and the rated wind speed, the wind turbine operates in the region called *region below rated wind speed*. On the other hand, when the wind speed is high and exceeds the rated wind speed, the wind turbine operates in the region called *region above rated wind speed*. If the wind speed becomes much higher than the rated wind speed, the turbine will pitch out of the wind and stop capturing power to prevent the turbine mechanical and electrical systems from overloading.

In the region below rated wind speed, the wind speed is low and the maximum power that can be captured from the wind is below the rated power of the generator. Therefore, the operation goal in this region is to make the turbine rotate at the speed of the optimal rotor speed $\omega_{r\_opt}(t)$ in order to produce as much power as possible, which is explained in Figure 3-2.

In the region above rated wind speed, the wind speed is high such that the absorbed wind power can exceed the rated generator power. Therefore, the goal of operation in this region is twofold: (1) regulating the captured wind power below the rated generator power for safety reasons and (2) regulating the generator rotating speed below the rated generator speed to prevent the generator from overspeed.

3.5.3 Wind turbine control

The wind turbine control goals in the two operation regions are different due to the two different operating principles described in Section 3.5.2. Therefore, the wind turbine control problem can be viewed as a *dual control goal* problem.

The relation between wind speed, rotor speed and tip speed ratio is shown as follows by reformulating (3-6) as:

$$\omega_r(t) = \lambda \frac{v(t)}{R} \tag{3-16}$$

In the region below rated wind speed, the wind turbine control system tries to track the λ_{opt} such that $C_{p\_\max}$ is achieved and thus maximum energy from the wind can be transformed into mechanical power, which is explained in (3-15). Tracking λ_{opt} is achieved if the turbine rotor speed $\omega_r(t)$ tracks the optimal rotor speed $\omega_{r\_opt}(t)$ derived from (3-16):

$$\omega_{r\_opt}(t) = \lambda_{opt} \frac{v(t)}{R} \tag{3-17}$$

Therefore, the wind turbine control problem in the region below rated wind speed is a tracking problem. The controller manipulates the generator torque reference signal T_{gr} to drive the rotating speed of the wind turbine blades to follow the optimal rotating speed $\omega_{r\_opt}(t)$ for maximum power generation. Meanwhile, the pitch angle should be kept at zero degrees for maximum power conversion efficiency, which is explained in (3-15). Therefore, the pitch angle is regulated at $\beta_{opt} = 0$ by manipulating another control input β_r. Hence, the overall control goal in this region is achieved by manipulating the two control inputs β_r and T_{gr} to control β and ω_r such that β is regulated around $\beta_{opt} = 0$ and ω_r is tracking $\omega_{r\_opt}(t)$.

In the region above rated wind speed, the controller manipulates the generator torque reference signal T_{gr} and the pitch angle reference signal β_r to reduce the captured wind power and keep it around the rated generator power P_{gr}. Meanwhile, the generator speed should be regulated around the rated generator speed ω_{gr}. Therefore, the control goal in this region can be achieved by manipulating the two control inputs to control

two of the outputs ω_g and T_g such that ω_g is regulated around the value of ω_{gr} and T_g is tracking the optimal generator torque $T_{g\_opt}(t)$ given as:

$$T_{g\_opt}(t) = \frac{P_{gr}}{\omega_g(t)\eta_g} \tag{3-18}$$

(3-18) is derived from the torque and power relation in (3-3). (3-18) implies that controlling T_g to track $T_{g\_opt}(t)$ is an indirect way to regulate generated power around P_{gr}.

Multiple controller approaches may be used to deal with the above wind turbine dual control goal problem. Therefore, one controller can be designed for region below rated wind speed and another can be designed for region above rated wind speed. The wind turbine switches between the two controllers during operation. The rated wind speed can serve as the criterion for switching. The controller for the region above rated wind speed switches into operation when the wind speed exceed the rated speed and the other controller for the region below rated wind speed switches into operation when the wind speed goes below the rated wind speed.

In the literature, a more practical wind turbine controller switching criteria is proposed (Odgaard, Stoustrup and Kinnaert, 2013). In this approach, the switching is based on both the generated power and generator speed rather than the rated wind speed as described below.

The controller for the region above rated wind speed switches into operation if:

$$P_g(t) \geq P_{gr} \quad \text{or} \quad \omega_g(t) \geq \omega_{gr}$$

The controller for the region below rated wind speed switches into operation if:

$$\omega_g(t) < \omega_{gr} - \Delta\omega$$

$\Delta\omega = 15$ is an offset providing for some hysteresis in order to avoid frequent switching of controllers. Hence, the simultaneous activation of the above two conditions is

avoided during the turbine operation. The wind turbine frequently switches between the two controllers during operation. This is because the captured wind power is a cubic function of wind speed as shown in (3-14). Therefore, P_g varies greatly and exceeds or goes below P_{gr} frequently with the changing wind speed. The schematic diagram of the wind turbine control system is shown in Figure 3-3.

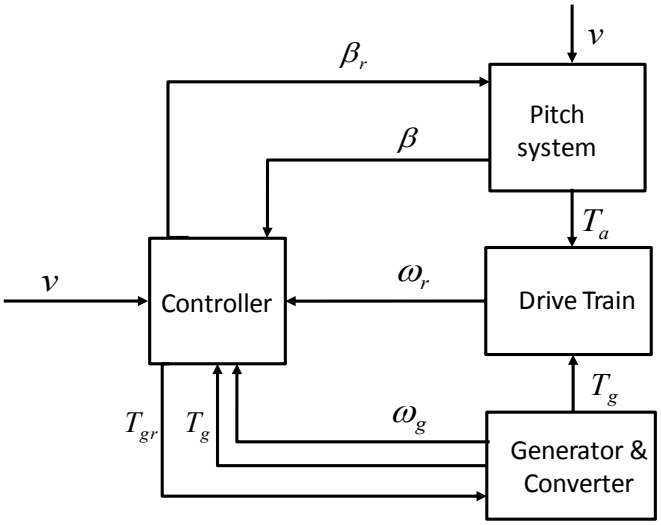

Figure 3-3 diagram of wind turbine control system

However, it is shown in Chapters 5 that the wind turbine control in different operating regions can be achieved using a single controller in the framework of MPC.

3.6 Conclusions

In this Chapter, the modelling of a modern large variable speed wind turbine is presented. Models of all the three wind turbine subsystems and the blade aerodynamics are described. The wind turbine model is shown to be nonlinear due to the high nonlinearity of the blade aerodynamics. The turbine model presented in this Chapter is used in the simulation studies presented in Chapters 4, 5, 6 & 7 to test the proposed AFTC approaches in the presence of various wind turbine faults.

The modelling of turbine faults is also presented in this Chapter including modelling for actuator, sensor and component faults. These models of faults are important since model-based AFTC approaches are designed based on joint models combining the

original turbine model with the appropriate fault model(s). It should be noted that different forms of fault (i.e. additive and multiplicative faults) are equivalent in some FE approaches.

Finally, the turbine operating principles and control strategy is outlined in this Chapter. It is shown that wind turbine control is a dual control goal problem since two different control goals should be achieved within different operation regions. This dual control goal problem should be taken into account for the turbine controller design.

The nonlinear wind turbine model described in this Chapter is simplified and linearized in Chapter 4. Based on this simplified wind turbine system, an AFTC approach for wind turbine operating in the region below rated wind speed is proposed to tolerate wind speed sensor faults.

Chapter 4: FTC for wind speed sensor faults via LSSVM and robust MPC

4.1 Introduction

The wind speed sensor mounted on the top of the turbine nacelle is a special kind of sensor from the perspective of wind turbine control since it is used to provide the control system with the reference signal rather than a feedback signal.

Theoretically, the reference signal to be tracked by the controller is the optimal rotor speed and can be calculated from the EWS as shown in (3-17). However, the EWS is a variable that cannot be measured. Therefore, the measurement from the wind speed sensor is used in practice as an approximation to the EWS to calculate the approximated optimal rotor speed. Furthermore, this measurement can be calibrated to improve the accuracy of the approximated EWS (Odgaard and Johnson, 2012). The approximated optimal rotor speed is calculated as follows:

$$\hat{\omega}_{r\_opt}(t) = \lambda_{opt} \frac{v_m(t)}{R} \tag{4-1}$$

where $v_m(t)$ is the measured wind speed from the wind speed sensor. $\hat{\omega}_{r\_opt}(t)$ is the approximated optimal rotor speed and is used as the reference signal to be tracked.

The wind speed sensor is prone to faults since it is located outside the turbine nacelle and affected by environmental factors. A strike by lightning can act as a typical cause of the wind speed sensor fault or even failure as shown in Figure 4-1.

Figure 4-1 Lightning strike on wind turbine

Furthermore, icing at low temperature is another cause of wind speed sensor faults. Salt corrosion is also a cause of faults for offshore wind turbines. In practice, there is always one or even two redundant wind speed sensors installed on the top of the wind turbine as a precaution against potential wind speed sensor faults or failures, as illustrated in Figure 4-2.

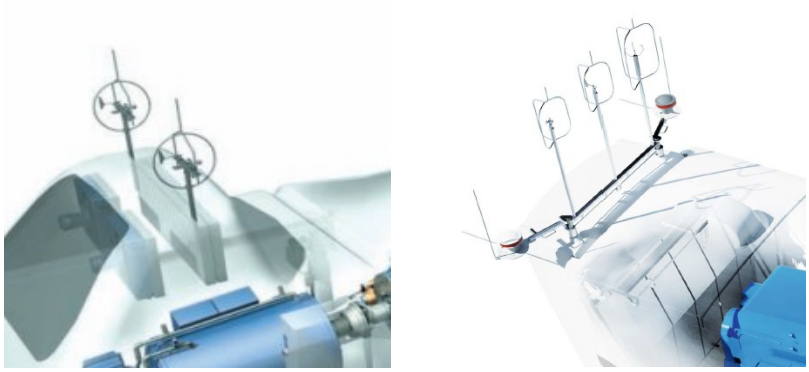

Figure 4-2 Redundant wind speed sensors (Nordex, 2013)

However, the sensor and its redundant counterpart are located in the same location in the turbine and thus exposed to the same environment factors. Therefore, these sensors are all prone to same potential faults and can even become faulty together. Furthermore, it is difficult to identify the faulty sensor. In the case of one wind speed sensor becoming faulty, the sensor fault can only be detected by comparing the measurement between the sensors. However, it's difficult to tell which sensor is faulty without using an FDI or FE unit. Thus the strategy of using only simple hardware redundancy has limited improvement in the reliability of wind speed sensors.

In this Chapter, an AFTC scheme for wind turbine operating in the region below rated wind speed is proposed for wind speed sensor faults. In this scheme, a practical FDI unit utilizing both available hardware redundancy (i.e. redundant wind speed sensor) and analytical redundancy (i.e. estimated EWS) is proposed for wind speed sensor faults. EWS estimation is achieved through the use of the least-squares support vector machine (LSSVM).

Based on the FDI unit, an AFTC approach through robust MPC is proposed. This MPC approach is robust against the estimation error of EWS. Besides, the constraints in the wind turbine system are also considered externally in this MPC approach.

The remainder of this Chapter is organized as follows: the principle of the LSSVM for function identification and classification is introduced in Section 4.2. FDI for wind speed sensor fault through LSSVM is presented in Section 4.3. The background and principle of MPC are described in Section 4.4. The wind turbine controller based on robust MPC is also proposed in Section 4.4. Simulation results of the designed AFTC scheme are shown in Section 4.5. Conclusions are drawn in Section 4.6.

4.2 Preliminary of least square support vector machine

The support vector machine (SVM) is a relatively new machine learning method originated in the late 1990s for function estimation and classification (Cortes and Vapnik, 1995; Vapnik, Golowich and Smola, 1997). It was developed from the areas of statistical learning and structural risk minimization (Vapnik, 1995). Nowadays, it is widely used in the areas of feature selection, regression and time series prediction (Wang, 2005; Wang, Men and Lu, 2008) due to its outstanding generalization performance. Compared with neural network approaches, SVM has several advantages. Firstly, it solves a convex optimization problem and thus the local minimum problem occurring in the neural network algorithm is obviated. Secondly, the number of hidden units in the SVM comes naturally from solving a convex optimization problem. On the other hand, the choice of the number of hidden units in a neural network is still based on experience rather than theoretical methods. Finally, the over-fitting problem of neural network can be avoided in SVM.

LSSVM is the least-squares version of SVM (Suykens et al., 2002). The algorithm of LSSVM is a quadratic programming problem with constraints and an infinite number of unknown parameters. However, the constrained quadratic programming problem can be transformed from the primal space into a dual space using the method of Lagrange multipliers so that the problem of an infinite number of unknown parameters can be avoided. The Mercer's condition for mapping a low-dimensional space to a high dimensional space is applied during this transformation (Steinwart and Christmann, 2008).

Compared with SVM, the optimization problem solved by LSSVM is simpler. SVM solves an optimization problem with inequity constraints. Therefore, numerical methods

like interior point methods have to be used to solve this problem. This can result in a great burden in computation when a large quantity of training samples is used. However, LSSVM solves an optimization problem with equality constraints. It is shown in Section 4.2.1 that an analytical form of the solution for this optimization problem can be obtained if this problem is transformed into a dual space.

Another advantage of LSSVM is that it is easier to design a modified version of LSSVM due to its simpler formulation, such as a weighted LSSVM for improving the robustness in nonlinear function estimation (Suykens, De Brabanter, Lukas and Vandewalle, 2002).

LSSVM is widely used to deal with both static and dynamic problems while SVM is proposed for only static problems. Therefore, LSSVM is used in recurrent modelling (Suykens and Vandewalle, 2000) and optimal control (Suykens, Vandewalle and De Moor, 2001). Some control methods based on online LSSVM are also proposed in recent years (Wang, Zhang and Mao, 2012; Gao et al., 2013).

4.2.1 LSSVM for classification

The principle of Classification based on LSSVM is to map two classes of data into a higher dimensional feature space such that the non-separable data in the original space become linearly separable in the higher dimensional feature space. This process is illustrated in Figure 4-3.

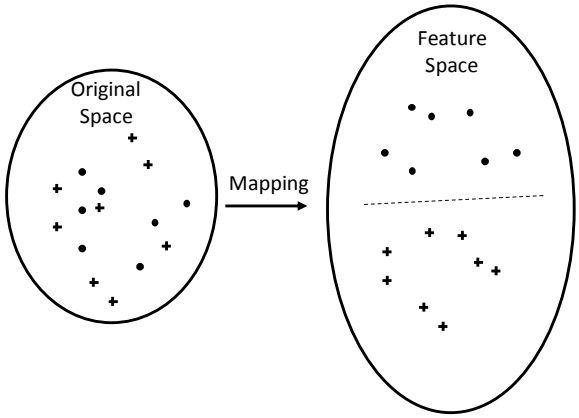

Figure 4-3 Principle of LSSVM for classification

Classification based on LSSVM is achieved in two steps. First of all, a series of training data are acquired and used to train the classifier. The training process is actually an algorithm for solving a quadratic programming problem with equality constraints. Secondly, the parameters of the identification function are then obtained from the solution of this optimization problem. The identification function is then used online for classification. The detailed principle of classification with LSSVM is described below (Suykens et al., 2002).

Given a training data set $(x_i, y_i)\ \ i = 1,2,3,.....N$ with input $x_i \in \mathbb{R}^n$ and output $y_i \in \{-1,1\}$ being the binary label for two classes, the identified classifier via LSSVM takes the form as:

$$y = sign[w^T \varphi(x) + b] \tag{4-2}$$

in which $\varphi(x) : \mathbb{R}^n \to \mathbb{R}^m$ is a nonlinear mapping from the input space to a higher dimensional feature space. The analytical form of $\varphi(x)$ is not defined explicitly. *b* is a bias term and *w* is the weighting vector. It should be noted that the dimension m of the feature space is defined implicitly. Therefore, the value of m is not known and it can even be infinity. *w* and *b* are the parameters to be calculated.

Before the classifier is being trained, the following assumption is applied on the training samples:

$$\begin{aligned} w^T \varphi(x_i) + b \geq +1 \qquad & if \quad y_i = +1 \\ w^T \varphi(x_i) + b \leq -1 \qquad & if \quad y_i = -1 \end{aligned} \tag{4-3}$$

$$i = 1,2,3,.....N$$

(4-3) can be reformulated as:

$$y_i[w^T \varphi(x_i) + b] \geq 1$$

$$i = 1,2,3,..., N$$

w and b are calculated through training, which is a process of solving the following optimization problem:

$$\min_{w,b,e} J(w,e) = \frac{1}{2} w^T w + \frac{1}{2} \mu \sum_{i=1}^{N} e_i^{\,2} \tag{4-4}$$

subject to constraints:

$$y_i[w^T \varphi(x_i) + b] = 1 - e_i$$

$$i = 1,2,3,...,N$$

(4-4) is a cost function with square error $e_i^{\,2}$. To solve (4-4), the following Lagrange function is considered:

$$L(w,e_i,b,\alpha_i) = J(w,e_i) - \sum_{i=1}^{N} \alpha_i \{y_i[w^T \varphi(x_i) + b] - 1 + e_i\} \tag{4-5}$$

where α_i are the Lagrange multipliers. Using the method of Lagrange multipliers, the following equations can be obtained:

$$w = \sum_{i=1}^{N} \varphi(x_i) \alpha_i y_i \tag{4-6}$$

$$\sum_{i=1}^{N} \alpha_i y_i = 0 \tag{4-7}$$

$$\alpha_i = \mu e_i \tag{4-8}$$

$$y_i[w^T \varphi(x_i) + b] - 1 + e_i = 0 \tag{4-9}$$

$$i = 1,2,3,...N$$

b, α_i can be calculated from (4-6) to (4-9). However, it is shown that the term $\varphi(x_i)^T \varphi(x_j) \quad i, j = 1,2,3,...,N$ appears when (4-6) is substituted into (4-9).

Therefore, (4-6) to (4-9) cannot be solved at this point since the analytical form of $\varphi(x): \mathbb{R}^n \to \mathbb{R}^m$ is undefined. To solve this problem, a mathematical rule called Mercer's condition is used (Mercer, 1909). Any analytical function satisfying Mercer's condition can be used to represent $\varphi(x_i)^T \varphi(x_j)$. Therefore, the following radial basis function (RBF) kernel can be used to represent $\varphi(x_i)^T \varphi(x_j)$:

$$\varphi(x_i)^T \varphi(x_j) = \exp\left(\frac{-\|x_i - x_j\|_2^2}{\sigma^2}\right) \tag{4-10}$$

(4-10) is the so called RBF kernel which satisfies Mercer's condition. It should be noted that there are several types of function satisfying Mercer's condition and thus the choice of kernel function is not unique. However, the RBF kernel is the most widely used kernel function and Mercer's condition holds for all possible values of σ. Using the RBF kernel, b and α_i can now be calculated from (4-6) to (4-9). Thus the identification function of LSSVM can now be obtained by substituting the calculated value of b, α_i and Equations (4-6) and (4-10) into Equation (4-2), which is given as:

$$y = sign\left[\sum_{i=1}^{N} \alpha_i y_i \exp\left(\frac{-\|x_i - x\|_2^2}{\sigma^2}\right) + b\right] \tag{4-11}$$

(4-11) is the final identification function and can be used for classification.

Remark 4-1: μ in (4-4) and σ in (4-10) are two tuning parameters which affects the classification performance of LSSVM.

Remark 4-2: It is shown that the original classifier (4-2) has only theoretical value. The applicable classifier is actually (4-11) which is an explicit analytical form of (4-2).

4.2.2 LSSVM for function identification

Function identification based on LSSVM is achieved with two steps which are similar with the steps of classification using LSSVM. First of all, a series of training data are acquired and used to train the identification function offline. Secondly, the parameters of the identification function are then obtained from the training. The identification

function is then used online for prediction. The detailed principle of function identification with LSSVM is described below.

Given a training data set $(x_i, y_i)\ \ i = 1,2,3,.....N$ with input $x_i \in \mathbb{R}^n$ and output $y_i \in \mathbb{R}$, the identified function via LSSVM takes the form:

$$y = w^T \varphi(x) + b \tag{4-12}$$

where $\varphi(x): \mathbb{R}^n \to \mathbb{R}^m$ is a nonlinear mapping from the input space to a higher dimensional feature space, b is a bias term and w is the weighting vector. Again, the value of m is not known and can even be infinity. w and b are the parameters to be calculated.

The parameters in (4-12) are obtained by solving the following optimization problem:

$$\min_{w,b,e} J(w,e) = \frac{1}{2} w^T w + \frac{1}{2} \mu \sum_{i=1}^{N} e_i^{\,2} \tag{4-13}$$

subject to:

$$y_i = w^T \varphi(x_i) + b + e_i$$

$$i = 1,2,3,..., N$$

(4-13) is a cost function with square error $e_i^{\,2}$ and a bias term b, which is a form of ridge regression (Golub and Van Loan, 2012). μ is the weighting factor, which is a tuning parameter.

To solve (4-13), the following Lagrange equation is considered:

$$L(w, e_i, b, \alpha_i) = J(w, e_i) - \sum_{i=1}^{N} \alpha_i [w^T \varphi(x_i) + b + e_i - y_i] \tag{4-14}$$

where α_i are Lagrange multipliers. Again, using the method of Lagrange multiplier and Mercer's condition, b , α_i can be calculated .

If the RBF kernel in (4-10) is used, the identification function of LSSVM can now be obtained which is given as:

$$y = \sum_{i=1}^{N} \alpha_i \exp\left(\frac{-\|x_i - x\|_2^2}{\sigma^2}\right) + b \tag{4-15}$$

(4-15) is the final identification function and can be used for function estimation or time series prediction.

Remark 4-3: μ in (4-13) and σ in (4-10) are two tuning parameters which affect the function estimation performance of the LSSVM. Compared with standard SVM, LSSVM has less tuning parameters for the case of function estimation since SVM has three tuning parameters (Suykens, 2001).

Remark 4-4: It is shown that the original identification function (4-12) has only theoretical value. The applicable identification function is actually (4-15) which is an explicit analytical form of (4-12).

4.3 FDI for wind speed sensor faults

Wind speed sensors are important "eyes" for wind turbine control since they provide the means to calculate the optimal rotor speed as the reference for the controller as outlined in Section 4.1. Since the wind speed measurements are critical for operation of the wind turbine, there are at least two of them working together in redundancy in case one malfunctions or fails.

Hence, it is important to have some form of wind speed sensor FDI scheme, which is proposed in this Section. This scheme comprises two units. The first unit is a EWS estimation unit which uses the time-series prediction ability of the LSSVM for wind speed estimation. The second unit is an FDI unit to detect and isolate the wind speed sensor faults which utilizes the classification ability of LSSVM. Fault isolation is achieved by comparing the measurements from both wind speed sensors with the

estimated EWS. Therefore, it is assumed the measurements from two wind speed sensors are available in this scheme.

4.3.1 EWS estimation based on LSSVM

Some EWS estimation methods based on the measurements of generator speed and turbine rotor speed sensors rather than that of the wind speed sensor are proposed in (Xin-Fang, Da-Ping and Yi-Bing, 2004; Abo-Khalil and Lee, 2008; Sami and Patton, 2012a). These methods are used as analytical redundancy approaches for FDI or FE of wind speed sensor faults. However, as the rated power capacity of wind turbines has increased rapidly in recent years, more and more newly built turbines have large rotors with rated powers of several megawatts. This is especially the case for wind turbines designed for the offshore environment which have large rotor blades that weigh several tens of tonnes (Jonkman and Buhl Jr, 2005). Although these large wind turbine systems are capable of generating large amounts of power, they suffer from large rotor inertia and thus the rotor speed cannot respond quickly enough to the changing EWS (Xu, Hu and Ehsani, 2012). Therefore, for a wind turbine with a very large rotor, the accuracy of the EWS estimation decreases if the estimation uses measurement from the rotor speed sensor. It seems logical that for large-scale wind turbines, the EWS estimation method should take into account the inertia of the rotor. More recently, rotors are made larger by using lighter composite materials so that newer wind turbines have reduced inertia and are more able to respond quickly to the changing EWS. However, the downside is that these new composite structures induce “blade flapping” and this brings on a requirement for a more complicated control problem involving load and vibration control (Bossanyi, 2003; Kong, Bang and Sugiyama, 2005; Soltani, Wisniewski, Brath and Boyd, 2011). This last topic is beyond the scope of this thesis.

In the EWS estimation method proposed in this Section, the inertia of the wind turbine is considered by careful use of the rotor and generator speed sensor signals. The signals on a time window of three recent time instants are used. Details of this approach are given below.

First of all, the choice of the most suitable input and output pairs (x, y) of the LSSVM should be decided. This choice will affect the EWS prediction performance. The output

of the LSSVM is the estimated EWS v_e. In this approach, signals corresponding to the three most recent time instants from the rotor and generator speed sensors are used as the LSSVM inputs. The resulting form of (x, y) is given as:

$$\begin{aligned} x &= [\phi_r \quad \Delta\phi_r \quad \phi_g \quad \Delta\phi_g] \\ y &= v_e \end{aligned} \tag{4-16}$$

The elements of the input vector x are defined as:

$$\phi_r = [\hat{\omega}_r(k) \quad \hat{\omega}_r(k-1) \quad \hat{\omega}_r(k-2)]$$

$$\Delta\phi_r = [\hat{\omega}_r(k) - \hat{\omega}_r(k-1) \quad \hat{\omega}_r(k-1) - \hat{\omega}_r(k-2)]$$

$$\phi_g = [\hat{\omega}_g(k) \quad \hat{\omega}_g(k-1) \quad \hat{\omega}_g(k-2)]$$

$$\Delta\phi_g = [\hat{\omega}_g(k) - \hat{\omega}_g(k-1) \quad \hat{\omega}_g(k-1) - \hat{\omega}_g(k-2)]$$

k is the current time instant. $\hat{\omega}_r(k)$ denotes the filtered signal from the rotor speed sensor and $\hat{\omega}_g(k)$ is the filtered signal from the generator speed sensor. The generator and rotor speed sensor data are processed by simple low-pass filters to mitigate the contaminating effect of noise. Hence, the signals in (4-16) correspond to the appropriately filtered measurements which are chosen as the inputs and outputs of the LSSVM algorithm and used as training data.

It is shown in (Wang and Hu, 2005) that the LSSVM is more robust against noise pollution compared with the standard SVM, which is also an advantage of using LSSVM for EWS estimation.

After the input and output data pairs are selected, the LSSVM parameters are acquired by obtaining a series of training data as input and output pairs (x_i, y_i) and substituting these data into (4-13) to solve the optimization problem with the algorithm described in Section 4.2.2. Then the LSSVM can be used online for estimating the EWS.

Remark 4-5: The inertia of a large wind turbine affects the time response of the measured rotor speed. Hence, the data corresponding to the most recent time instants from the generator and rotor speed sensors are used as the inputs of the LSSVM. The effect of the inertia is thus considered using 3 instants of delay in the discrete-time sense, giving a suitable EWS estimation.

4.3.2 FDI of wind speed sensor fault based on LSSVM

As explained in Section 4.3.1, EWS estimation methods using only the rotor speed at current sampling time suffer from the problem of inertia in large wind turbines since the rotor speed can not respond quickly to the fast changing wind speed. On the other hand, wind speed sensors directly measure the wind speed and thus respond quickly to the fast changing wind speed. Therefore, the estimation problem caused by the turbine inertia can be mitigated if wind speed sensor data are used to approximate the EWS. Therefore, the measurements from these sensors can be used to shorten sensor fault detection time. Furthermore, wind speed sensors can also be calibrated to improve the accuracy of the approximated EWS.

Although the wind speed sensor fault can be detected quickly by comparing the measurements between the two wind speed sensors, it's difficult to determine which sensor is faulty. On the other hand, the estimated EWS can serve as a benchmark to isolate the faulty sensor. Therefore, an FDI approach for wind speed sensor faults using both analytical redundancy (i.e. estimated EWS) and hardware redundancy (i.e. multiple wind speed sensors) is proposed in this Section.

Hence, the proposed FDI scheme actually comprises two FDI units corresponding to each of the two wind speed sensors. The schematic diagram of this FDI scheme is illustrated in Figure 4-4.

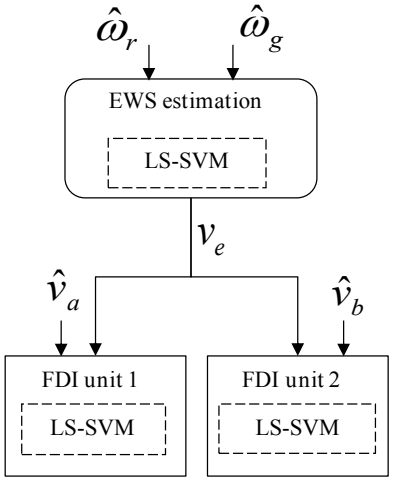

Figure 4-4 Principle of LSSVM for FDI

Consequently, the FDI strategy is realized in two steps. In the first step, the EWS wind speed is estimated via the LSSVM procedure described in Section 4.3.1. In the second step, the filtered signals from the two wind speed sensors $\hat{v}_a$ and $\hat{v}_b$ are compared with the estimated EWS v_e separately. This comparison is made using the classification ability of LSSVM. Therefore, two classifiers are designed for the two FDI units separately. The outputs of the two LSSVM classifiers have the form of a binary indication $\{-1,+1\}$ with +1 indicating the sensor is faulty and -1 otherwise. The fault in the sensor is identified if the difference between the sensor signal and the estimated EWS exceeds a threshold. This threshold is acquired implicitly through the LSSVM training. The design of the classifier using LSSVM in the second step of this FDI strategy is outlined below.

First of all, the form of input and output pairs (x, y) of the LSSVM classifier should be determined. In this approach, the output of the LSSVM classifier is a binary set $\{-1,+1\}$ indicating whether the sensor is faulty or healthy. The filtered EWS estimates and the signals of 2 recent time instants from the wind speed sensor are chosen as the inputs of the LSSVM classifier. The form of (x, y) for the two sensors is given as:

$$\begin{cases} x_a = [\hat{v}_e(k) - \hat{v}_a(k) \quad \hat{v}_e(k-1) - \hat{v}_a(k-1)] \\ y_a = +1 \quad or \quad -1 \end{cases} \qquad sensor\ a \qquad (4\text{-}17)$$

$$\begin{cases} x_b = [\hat{v}_e(k) - \hat{v}_b(k) \quad \hat{v}_e(k-1) - \hat{v}_b(k-1)] \\ y_b = +1 \quad or \quad -1 \end{cases} \quad sensor\ b \qquad (4\text{-}18)$$

in which $\hat{v}_a(k)$ and $\hat{v}_b(k)$ are the filtered wind speed signals from the two sensors and $\hat{v}_e(k)$ is the filtered EWS estimation.

After the form of input and output of the classifier is determined, the LSSVM parameters can then be acquired by obtaining a series of training data as input pairs (x_i, y_i) and substituting these data into (4-4) to solve the optimization problem with the algorithm described in Section 4.2.1. The LSSVM can then be used online for fault detection. Gain factor error faults and offset faults result in a difference between the filtered wind speed sensor data and the filtered EWS. Therefore, these two types of fault can be detected by analyzing this difference using the LSSVM classifier, which is shown in (4-17) and (4-18).

Remark 4-6: Two FDI units are designed for each of the two wind speed sensors separately in this approach and thus this FDI scheme is able to detect and isolate either single or multiple sensor faults.

4.3.3 Simulation study

A simulation example of FDI for wind speed sensor fault using LSSVM is considered here. The performance of the FDI method proposed in Section 4.3.2 is demonstrated using this example.

The wind speed data used in simulation are taken from the Simulink wind turbine benchmark model (kk-electronic, 2011), which comprise both a genuine wind data measured in a wind farm and a EWS data. It is assumed that two wind speed sensors are available for hardware redundancy. A realistic wind speed sensor is always affected by sensor noise. Therefore, the signals from the two wind speed sensors are simulated by applying a random noise with variance of 0.5 m/s to the raw wind speed data.

A series of wind turbine sensor data and EWS data are obtained from the simulation and used in Equation (4-16) to construct the training samples for the LSSVM. Then, the

algorithm described in Section 4.2.2 is used to train the LSSVM for the EWS estimation. Through simulation, it is shown that the following choice of parameters can achieve satisfactory EWS estimation performance. The tuning parameter in Equation (4-13) is chosen as $\mu = 159.3$ and the tuning parameter for the RBF kernel in (4-10) is chosen as $\sigma = 0.86$. The generator speed sensor data are filtered by a first order filter with the time constants of 1s while the rotor speed sensor data are filtered by a first order filters with the time constant of 0.9s. The trained LSSVM is then tested on other wind turbine sensor data sets and the corresponding EWS data. The performance of the EWS estimation is presented in Figure 4-5.

The EWS estimation performance is analyzed in terms of the estimation error using the following performance indicator:

$$e(t) = \frac{v_e(t) - v(t)}{v_e(t)} \tag{4-19}$$

The EWS estimation error corresponding to the estimation result in Figure 4-5 is shown in Figure 4-6, using the indicator of (4-19).

Different EWS speed data sets are used in the simulation to find suitable bounds for the estimation error. It is found that the maximum estimation error of the proposed LSSVM is 8%.

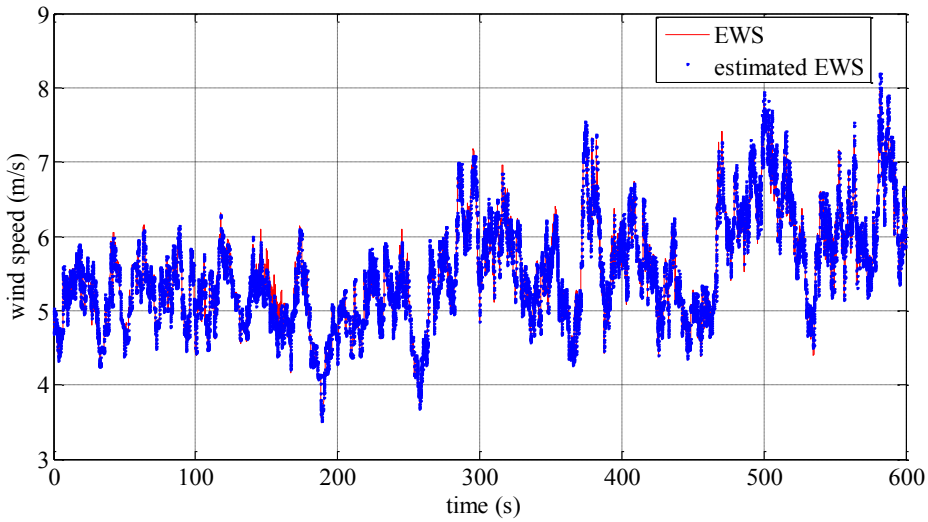

Figure 4-5 EWS estimation

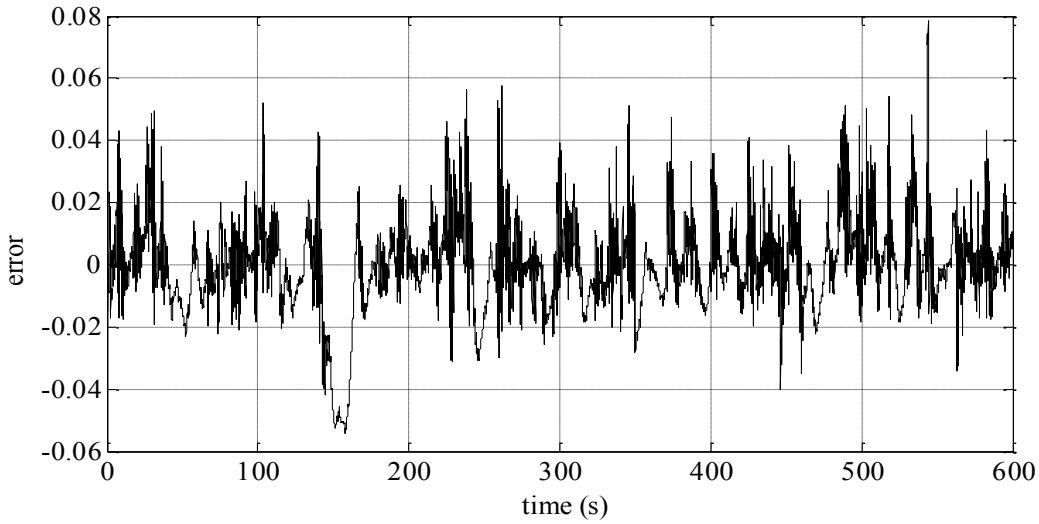

Figure 4-6 EWS estimation error

The FDI function for wind speed sensor fault can now be achieved based on the estimated EWS. Both the faulty sensor data (i.e. data from sensors subject to gain factor error faults or offset faults) and healthy sensor data are acquired from the simulation and used to construct the training samples according to (4-17) and (4-18). The classifier is then trained by the algorithm presented in Section 4.2.1. The wind speed sensor data and estimated EWS are filtered by a first order filter with a time constant of 0.2s. The tuning parameters in Equation (4-4) are chosen as $\mu = 21.7$ and the RBF kernel parameter is chosen as $\sigma = 0.29$. The fault detection time performance of the FDI unit is shown in Table 4-1. Offset faults and gain factor error faults are both considered.

Table 4-1 Fault detection time of FDI

Fault		Maximum detection time
Offset fault	±0.8 m/s	3.25s
	±1.0 m/s	2.33s
	±1.2 m/s	1.77s
	±1.4 m/s	1.35s
Gain factor error	±0.15$v_{\alpha,b}$	4.15s
	±0.2$v_{\alpha,b}$	2.35s
	±0.25$v_{\alpha,b}$	1.74s
	±0.3$v_{\alpha,b}$	1.50s

As expected, it is shown in Table 4-1 that the fault detection time decreases when the size of fault increases.

Remark 4-7: It is shown in the simulation that the use of more than two time instants of wind speed data as training sample can slightly improve the fault detection performance, (i.e. facilitating the detection of the lower level fault) at the cost of increasing detection time. Therefore, only the recent two time instants of wind speed data are used as the training sample in (4-17) and (4-18) in order to achieve a trade-off between fault detection performance and time required for detection.

4.4 Robust MPC

Model predictive control (MPC) is one of the most successful control methods for controlling multivariable systems with constraints. It is also the most widely used advanced control technique in industry with many products and applications (Qin and Badgwell, 2000; Qin and Badgwell, 2003). MPC has developed considerably since its advent in the 1970s and is still being widely studied in recent years (Rawlings and Mayne, 2009; Mayne, Kerrigan and Falugi, 2011; Lee, 2011; Bemporad, Oliveri, Poggi and Storace, 2011). It should be noted that MPC is not referred to as a specific control method but a range of control methods which use the model of the process to predict future system dynamics and calculate the control inputs according to predicted future system dynamic behaviour.

The ability to deal with system constraints explicitly is one of the prime advantages of MPC over other control methods. In practice, all physical systems are subject to some kind of constraints. These constraints may be due to physical limitations, economic considerations, system safety or performance requirements, etc. Actuators like valves have a limited range of action and slew rate. Process variable like levels in tanks and flows in pipes are also constrained. These practical constraints should all be considered by the controller. In the literature, various approaches can be used to externally consider the constraints in the MPC framework (Tarbouriech and Garcia, 1997; Maciejowski, 1999; Casavola, Giannelli and Mosca, 2000). Therefore, the constraint handling ability of MPC is the major reason for the widespread practical use of MPC in industry.

Another advantage of MPC is that its principle for predicting future system dynamic behaviour is intuitive and easy to understand, even when the considered system is a multivariable systems with cross-couplings between inputs and outputs. Currently, most research on MPC is based on state space models with multiple inputs and outputs. In the early days, MPC research was based on the use of the transfer function of a dynamic system. However, the intuitive prediction principle of MPC has been maintained from transfer function based MPC in the early stages to the more recent state space model-based MPC methodologies (Camacho and Bordons, 2004).

MPC also has the advantage of considering time-delay systems in a straightforward formulation. This ability facilitates the controller design for time-delay systems in the framework of MPC, which is attractive for real application as many process systems (e.g. in chemical reactors etc.) involve time-delay dynamics.

4.4.1 Preliminary of MPC

The principle of MPC comprises two steps. The first step is to utilize the model of the system and current system states to predict the future system behaviour over a so-called *prediction horizon* starting from current time instant (i.e. in the case of discrete-time systems). In the second step, the predicted future system behaviour is used to formulate an optimization problem in which the desired control goals or objectives are considered. The required control actions over the prediction horizon are obtained from the solution of this optimization problem. Then, only the first control action corresponding to the current time instant is used as the control input. At the next time instant, the above two steps are repeated. Therefore, MPC requires online solving an optimization problem at each time instant using a moving window of control actions. An illustration of this principle is shown in Figure 4-7 (Kwon and Han, 2006).

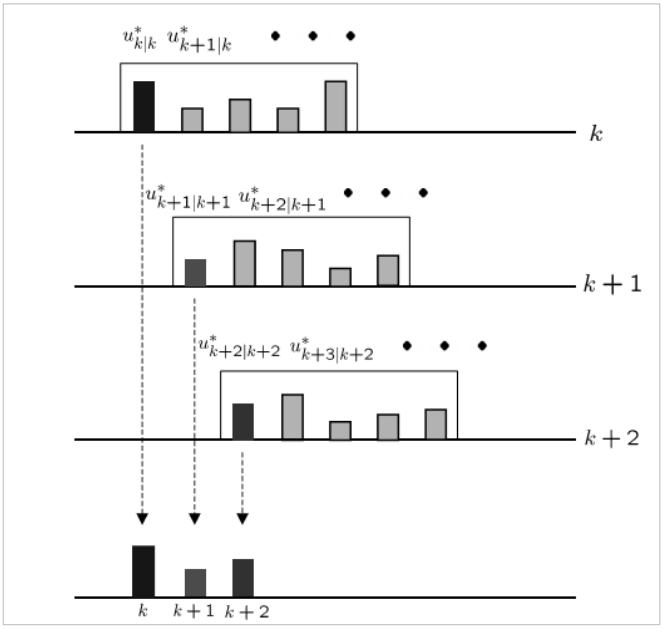

Figure 4-7 Principle of MPC

The principle for MPC based on a discrete-time state space model formulation is presented here for the following reasons. First of all, MPC in state space form is widely studied in recent years due to its advantage in dealing with multivariable systems, which is the case of wind turbine control problem. Secondly, many well known control theorems and filter theorems in the framework of the dynamic state space model can be utilized in state space model-based MPC. Thirdly, it will be shown in Chapters 5, 6 & 7 that the online optimization nature of the discrete-time MPC can be used to combine with other online algorithms to strengthen MPC in terms of FTC ability. The basic principle of MPC is described as follows (Maciejowski, 1999).

Consider the following linear discrete-time state space model of a system to be controlled:

$$x(k+1) = Ax(k) + Bu(k) \tag{4-20}$$

$$y(k) = Cx(k) \tag{4-21}$$

subject to the following system constraints:

$$u_{\min} \le u(k+j|k) \le u_{\max}$$

$$\Delta u_{\min} \le \Delta u(k+j|k) \le \Delta u_{\max} \tag{4-22}$$

$$y_{\min} \le y(k+j+1|k) \le y_{\max}$$

$j = 0,1,2,...N$

in which $x(k) \in \mathbb{R}^n$ is the state vector, $u(k) \in \mathbb{R}^l$ is the input vector and $y(k) \in \mathbb{R}^m$ is the measured outputs. A, B and C are system matrices with proper dimensions. $x(k+j|k)$ or $u(k+j|k)$ are the predicted future system states or inputs at the time instant $k+j$ using the information at the current time instant k. $u_{\min}$, $u_{\max}$, $\Delta u_{\min}$ and $\Delta u_{\max}$ are the constraints on inputs and the gradient of inputs. $y_{\min}$ and $y_{\max}$ are the constraints on system outputs. N is the length of *prediction horizon* formed by predicted future outputs $y(k+j+1|k)$, $j = 0,1,2,...N$ and also the length of *control horizon* formed by predicted present and future inputs $u(k+j|k)$, $j = 0,1,2,...N$. Therefore, a simple case of the prediction horizon and control horizon being equal is considered here.

In order to apply MPC to the system (4-20) and (4-21), there must be a method to predict future system behaviour using current system information. This future system behaviour can be acquired by substituting the current system states $x(k)$ into (4-20) and using (4-20) recursively as follows:

$$x(k+1|k) = Ax(k) + Bu(k|k)$$

$$x(k+2|k) = A^2x(k) + ABu(k|k) + Bu(k+1|k) \tag{4-23}$$

$$\vdots$$

$$x(k+N+1|k) = A^Nx(k) + A^{N-1}Bu(k|k) + ... + Bu(k+N|k)$$

The predicted outputs over the prediction horizon can be obtained by substituting (4-23) into (4-21) and given as follows:

$$y(k+1|k) = CAx(k) + CBu(k|k)$$

$$y(k+2|k) = CA^2x(k) + CABu(k|k) + CBu(k+1|k) \tag{4-24}$$

$$\vdots$$

$$y(k+N+1|k) = CA^Nx(k) + CA^{N-1}Bu(k|k) + ... + CBu(k+N|k)$$

As shown in (4-23) and (4-24), the future system behaviour and outputs are formulated in terms of the current state variable $x(k)$ and future control inputs $u(k+j|k)$, $j = 0,1,2,...N$.

For simplicity of notation, define the following vectors:

$$U(k) = \begin{bmatrix} u(k|k) \\ u(k+1|k) \\ \vdots \\ u(k+N|k) \end{bmatrix} \quad \Delta U(k) = \begin{bmatrix} \Delta u(k|k) \\ \Delta u(k+1|k) \\ \vdots \\ \Delta u(k+N|k) \end{bmatrix}$$

$$X(k) = \begin{bmatrix} x(k+1|k) \\ x(k+2|k) \\ \vdots \\ x(k+N+1|k) \end{bmatrix} \quad Y(k) = \begin{bmatrix} y(k+1|k) \\ y(k+2|k) \\ \vdots \\ y(k+N+1|k) \end{bmatrix}$$

$$U_{\min} = \begin{bmatrix} u_{\min} \\ u_{\min} \\ \vdots \\ u_{\min} \end{bmatrix} \quad U_{\max} = \begin{bmatrix} u_{\max} \\ u_{\max} \\ \vdots \\ u_{\max} \end{bmatrix} \quad \Delta U_{\min} = \begin{bmatrix} \Delta u_{\min} \\ \Delta u_{\min} \\ \vdots \\ \Delta u_{\min} \end{bmatrix} \quad \Delta U_{\max} = \begin{bmatrix} \Delta u_{\max} \\ \Delta u_{\max} \\ \vdots \\ \Delta u_{\max} \end{bmatrix}$$

$$Y_{\min} = \begin{bmatrix} y_{\min} \\ y_{\min} \\ \vdots \\ y_{\min} \end{bmatrix} \quad Y_{\max} = \begin{bmatrix} y_{\max} \\ y_{\max} \\ \vdots \\ y_{\max} \end{bmatrix}$$

where $U_{\min}$, $U_{\max}$, $\Delta U_{\min}$, $\Delta U_{\max}$, $Y_{\min}$ and $Y_{\max}$ are block vectors with N vectors of the constraint bounds defined in (4-22).

Now (4-23) and (4-24) can be written in the following compact form:

$$X(k) = \Lambda\, x(k) + \Xi U(k) \tag{4-25}$$

$$Y(k) = \Gamma\, \mathrm{X}(k) \tag{4-26}$$

in which

$$\Lambda = \begin{bmatrix} A \\ A^2 \\ A^3 \\ \vdots \\ A^N \end{bmatrix} \qquad \Xi = \begin{bmatrix} B & 0 & 0 & \cdots & 0 \\ AB & B & 0 & \cdots & 0 \\ A^2B & AB & B & \cdots & 0 \\ \vdots & \vdots & \vdots & \ddots & 0 \\ A^{N-1}B & A^{N-2}B & A^{N-3}B & \ldots & B \end{bmatrix}$$

$$\Gamma = \begin{bmatrix} C & 0 & 0 & \cdots & 0 \\ 0 & C & 0 & \cdots & 0 \\ 0 & 0 & C & \cdots & 0 \\ \vdots & \vdots & \vdots & \ddots & 0 \\ 0 & 0 & 0 & \cdots & C \end{bmatrix}$$

(4-25) and (4-26) show how the future system states and outputs are represented as a function of the current state variable $x(k)$ and the future control inputs $U(k)$. If MPC is designed for an unconstrained system and if a quadratic cost function is used, $U(k)$ can be directly calculated using (4-25) and (4-26) and a static feedback control law can be obtained.

It is assumed in (4-25) that full state measurement is available, otherwise state estimation methods are used to estimate the current system states.

The control input from MPC is obtained from the solution of an online optimization problem, which minimizes a cost function involving future system states and control inputs. The control goal of MPC is represented in this cost function. If the control goal is tracking a reference trajectory, the cost function is formulated to penalize the

deviations of the predicted outputs from the reference trajectory. Furthermore, penalizing the deviation of control input from a reference can also be formulated into the cost function. Penalties for inputs can be used to achieve economic goals or other practical concerns for actuators. The general form of the online optimization problem of MPC is formulated as:

$$\min_{U(k)} J(U(k), X(x)) \tag{4-27}$$

subject to:

$$\left.\begin{aligned} X(k) &= \Lambda x(k) + \Xi U(k) \\ Y(k) &= \Gamma X(k) \end{aligned}\right\} \tag{4-28}$$

$$U_{\min} \le U(k) \le U_{\max} \tag{4-29}$$

$$\Delta U_{\min} \le \Delta U(k) \le \Delta U_{\max} \tag{4-30}$$

$$Y_{\min} \le Y(k) \le Y_{\max} \tag{4-31}$$

in which $J(U(k), X(k))$ is the cost function to be minimized. (4-29) to (4-31) are the constraints in element-wise inequalities. Different types of cost function can be used in the optimization problems, including quadratic cost function, 1-norm cost function and ∞-norm cost function (Maciejowski, 1999).

To obtain the control input, the optimization problem (4-27) is solved. The methods for solving this problem depend on the form of the cost function. If a quadratic cost is used, active set methods or interior point methods can be used to solve (4-27) and the solution is global and unique since (4-27) is a convex problem using the quadratic cost function. If the cost function is linear, mature algorithms like simplex methods or interior point methods can be used to solve (4-27) (Bertsimas and Tsitsiklis, 1997).

After (4-27) is solved, the first element $u(k|k)$ in the vector $U(k)$ is used as the control input for the current time instant k. At the next time instant $k+1$, $x(k+1)$ is

obtained and (4-27) is solved again to obtain $u(k+1|k+1)$. Therefore, MPC functions by solving the optimization problem (4-27) online repeatedly at each time instant.

Remark 4-8: It is shown in the literature that there is an alternative formulation of MPC using $\Delta u(k|k)$ rather than $u(k|k)$ as control input, which adds an integral action to the controller. An advantage of adding this integral action is that offset free tracking in the presence of unknown constant input or output disturbance can be achieved if the controlled system is linear and the reference signal to be tracked is constant (Maciejowski, 1999). However, the wind turbine is a nonlinear system and the disturbance in the case of a wind turbine system is non-constant since the wind speed is always changing. Furthermore, the reference signal to be tracked in the region below rated wind speed (i.e. optimal rotor speed) is not constant in the wind turbine application as explained in Figure 3-2. Therefore, a straightforward MPC formulation using $u(k|k)$ as control input is presented in this Section and used all through this thesis. Details of the MPC formulation using $\Delta u(k|k)$ as control input can be found in (Maciejowski, 1999; Wang, 2009).

Remark 4-9: It is shown in the literature that the stability condition of MPC for linear discrete-time systems can be guaranteed by applying the terminal condition (Mayne, Rawlings, Rao and Scokaert, 2000). However, this terminal condition is not applied in the predictive controller designed in this Chapter due to the following two reasons. First of all, the 1-norm MPC in this Chapter is based on the 1-norm cost function. However, the terminal condition is proposed for MPC based on the quadratic cost function. Secondly, it is shown in (Wang, 2009) that the stability property can be achieved if the controlled system is stable and the prediction horizon *N* in (4-22) is long enough. The wind turbine model in this Chapter is a stable model. Meanwhile, it is shown in the simulation results in Section 4.5.3 that the prediction horizon $N = 5$ is long enough to avoid problems caused by instability and achieve satisfactory tracking performance.

Remark 4-10: The feasibility problem of MPC is caused by constraints on outputs. However, the constraints considered in the wind turbine system are the constraints on inputs defined in Table 3-2. Therefore, the predictive controller designed in this Chapter is not affected by the feasibility problem.

4.4.2 Robust MPC based on 1-norm

Robust MPC has been proposed to deal with systems with uncertainties. It has become one of the main streams of MPC research and some historical survey papers for the rich research results in this stream are available in (Morari and Lee, 1999; Bemporad and Morari, 1999). Nowadays, robust MPC is still being widely studied with some new research results (Li, Xi and Zheng, 2009; Magni, Raimondo and Allgöwer, 2009; Bumroongsri and Kheawhom, 2012; Farina and Scattolini, 2012; Zeilinger, Morari and Jones, 2014).

There are several types of robust MPC in terms of the type of cost function used. In this Section, a 1-norm robust MPC for a system described by a state space model is proposed, which is based on the robust MPC with 1-norm cost function proposed for systems described by a truncated impulse response (Camacho and Bordons, 2004). The proposed robust MPC will be used in the wind turbine control problem to consider the uncertainty due to EWS estimation error.

Consider the following constrained system with additive uncertainty, which is based on (4-20) and (4-21):

$$x(k+1) = Ax(k) + Bu(k) + Ed(k) \tag{4-32}$$

$$y(k) = Cx(k) \tag{4-33}$$

subject to the constraints defined in

(4-29) (4-30) (4-31)

in which $x(k) \in \mathbb{R}^n$ is the state vector, $u(k) \in \mathbb{R}^l$ is the input vector and $y(k) \in \mathbb{R}^m$ is the measured outputs. $d(k) \in \mathbb{R}^c$ is a bounded uncertainty satisfying $d_{\min} \le d(k) \le d_{\max}$. A, B, C and E are system matrices with proper dimensions.

The compact form of future system behaviour considering uncertainty can be obtained by using (4-32) and (4-33) recursively and given as:

$$X(k) = \Lambda x(k) + \Xi U(k) + \Phi D(k) \tag{4-34}$$

$$Y(k) = \Gamma \, \mathrm{X}(k) \tag{4-35}$$

in which $\Phi = \begin{bmatrix} E & 0 & 0 & \cdots & 0 \\ AE & E & 0 & \cdots & 0 \\ A^2E & AE & E & \cdots & 0 \\ \vdots & \vdots & \vdots & \ddots & 0 \\ A^{N-1}E & A^{N-2}E & A^{N-3}E & \cdots & E \end{bmatrix}$ and $D(k) = \begin{bmatrix} d(k) \\ d(k+1) \\ \vdots \\ d(k+N-1) \end{bmatrix}$

$D(k)$ is described by a polytope $D(k) \in \Omega$ since $d_{\min} \le d(k+i) \le d_{\max}$, $i = 0,1,2,...,N-1$ are bounded.

Consider the following cost function for system (4-32) to (4-33) in the form of 1-norm:

$$J(U(k)) = \sum_{i=1}^{N} [\lambda_i \left\| y(k+i|k) - y_r(k+i|k) \right\|_1 + \gamma_i \left\| u(k+i-1|k) \right\|_1] \tag{4-36}$$

In which $\|x\|_1 = \sum_{i=1}^{n} |x_i|$ represents the 1-norm. N is the prediction horizon and also the control horizon. $y_r(k+i|k)$ is the reference trajectory to be tracked. λ_i and γ_i with $i = 1,2,...,N$ are the weightings of the tracking error and control efforts. By minimizing (4-36), a predictive controller for tracking reference signal can be designed. However, (4-36) is not solved directly but reformulated into another cost function to simplify the optimization problem, which is described below.

If there is a series of $\zeta_i \ge 0$ and $\delta_i \ge 0$ with $i = 1,2,...,N$ such that for any $D(k) \in \Omega$, the following inequalities are satisfied:

$$\lambda_i \left\| y(k+i|k) - y_r(k+i|k) \right\|_1 \le \zeta_i \tag{4-37}$$

$$\gamma_i \left\| u(k+i-1|k) \right\|_1 \le \delta_i \tag{4-38}$$

$$i = 1,2,...,N$$

$$0 \le \sum_{i=1}^{N} \zeta_i + \sum_{i=1}^{N} \delta_i \le \eta \tag{4-39}$$

Then η becomes the upper bound of cost function (4-36). Therefore, minimizing (4-36) can be reformulated as the following optimization problem:

$$\min \quad \eta \tag{4-40}$$

subject to the constraints defined in

(4-37), (4-38) and (4-39)

(4-37) and (4-38) can be transformed into the following inequalities by expanding their 1-norm representation:

$$\lambda_i \sum_{j=1}^{m} [y_j(k+i|k) - y_{rj}(k+i|k)] \le \zeta_i \tag{4-41}$$

$$-\zeta_i \le \lambda_i \sum_{j=1}^{m} [y_j(k+i|k) - y_{rj}(k+i|k)] \tag{4-42}$$

$$\gamma_i \sum_{j=1}^{l} u_j(k+i-1|k) \le \delta_i \tag{4-43}$$

$$-\delta_i \le \gamma_i \sum_{j=1}^{l} u_j(k+i-1|k) \tag{4-44}$$

$i = 1,2,...,N$

in which $y_j(k+i|k)$, $j = 1,2,3,...,m$ are the elements in the output vector $y_j(k+i|k)$ and $u_j(k+i|k)$, $j = 1,2,3,...,l$ are the elements in the input vector.

Finally, the 1-norm robust predictive controller for system (4-32) to (4-33) can be designed by solving the following optimization problem at each time instant:

$$\min_{U(k)} \quad \eta \tag{4-45}$$

subject to:

(4-34), (4-35)

(4-39), (4-41), (4-42), (4-43) and (4-44)

(4-29), (4-30), and (4-31)

with $D(k) \in \Omega$

$i = 1,2,\ldots, N$

It is shown in the optimization problem (4-45) that both the cost function and the constraints are all linear. Therefore, (4-45) is a linear programming problem and can be solved efficiently with satisfactory computation burden. Inequality constraints (4-39), (4-41), (4-42), (4-43) and (4-44) are used to minimize the cost function (4-36). (4-34), (4-35), (4-29), (4-30) and (4-31) represents the controlled system with constraints.

Remark 4-11: (4-45) is an optimization problem subject to a large number of constraints because of the polytope description of disturbance $D(k) \in \Omega$. However, most of the constraints are redundant and can be reduced greatly due to the special form of the constraints. Therefore, (4-45) can be solved more efficiently through constraint reduction. The method for reducing the number of constraints in such linear optimization problem can be found in (Camacho and Bordons, 2004) .

Remark 4-12: The number of constraints in the optimization problem (4-45) is much higher than the number of decision variables. As pointed out in (Campo and Morari, 1987), solving the dual form of such a linear programming problem can decrease the computational burden. Therefore, the online computation burden of the proposed 1-norm robust MPC can be further decreased if the dual form of (4-45) is solved.

4.5 Robust MPC for wind speed sensor fault tolerant control

The 1-norm robust MPC in Section 4.4.2 is designed for linear systems and thus a linear wind turbine model is required in order to apply this robust MPC to wind turbine

control problems. In this Section, a linearized wind turbine model for a wind turbine operating in the region below rated wind speed is described. This linearized model is then used as the prediction model of the robust MPC.

The 1-norm robust MPC proposed in Section 4.4.2 is used here as the baseline controller for the wind turbine system. The EWS estimation error or wind speed sensor measurement error results in a bounded uncertainty in the wind turbine model and thus the robust MPC is used to deal with this uncertainty.

4.5.1 Wind turbine model linearization

As shown in (3-7), the wind turbine model is nonlinear because the aerodynamic torque T_a is a nonlinear function of β, v and ω_r. However, if only the region below rated wind speed is considered, the nonlinear turbine model can be approximated by a linear model due to the following two reasons.

First of all, the nonlinearity of the wind turbine model becomes weaker in the region below rated wind speed. As shown in Section 3.5, the turbine pitch angle β is regulated around zero below the rated wind speed and therefore it can be approximated as a constant $\beta = 0$. Thus the nonlinearity of T_a becomes weaker since it is now a nonlinear function with only two variables, i.e. v and ω_r.

Secondly, ω_r can be approximated as a constant. The turbine considered here is a modern large wind turbine with a power capacity of 4.8 MW. Such a large turbine has a rotor of tens of tonnes in weight and blades with the diameter of over fifty meters. Therefore, the rotor inertia is very large and the change of rotor speed is very slow. Furthermore, ω_r is limited to a small operation region for a large-scale wind turbine. In the case of the turbine considered here, ω_r varies between 0 to 1.9 rad/s during operation. This range is further reduced to 0 to 1 rad/s if only the region below rated wind speed is considered.

Therefore, the drive train model is used as the linearized wind turbine model and reformulated as:

$$\begin{aligned} \dot{x} &= A_{dt}x + B_{dt1}u + B_{dt2}d \\ z &= C_m x \\ y &= Cx \end{aligned} \tag{4-46}$$

in which $x = [\omega_r \quad \omega_g \quad \theta_\Delta]^{\mathrm{T}}$, $u = T_g$ and $d = T_a$.

z is the measured output. The measurements used in this model are from the turbine rotor speed sensor and generator speed sensor and therefore $z = [\omega_r \quad \omega_g]$ and $C_m = \begin{bmatrix} 1 & 0 & 0 \\ 0 & 1 & 0 \end{bmatrix}$. y is the controlled output, which is the rotor speed ω_r in this case and thus $C = [1 \quad 0 \quad 0]$. A_{dt} is the same as the system matrix of the drive train model in (3-4). B_{dt1} and B_{dt2} are first and second column of B_{dt} in (3-4).

(4-46) is a reformulation of the turbine drive train model (3-4) and thus the dynamics of both the turbine pitch system in (3-1) and the turbine generator system (3-2) are ignored in this linearized model. It is shown in the literature (Dang, Wu, Wang and Cai, 2010; Sami and Patton, 2012d; Sami and Patton, 2012a) that if the wind turbine controller is designed for the region below rated wind speed, the dynamics of both the pitch system (3-1) and the generator system (3-2) need not be considered since the pitch angle and generator torque can be regulated very well at $\beta = 0$ and $T_g = T_{gr}$, by using a PID controller. Furthermore, the influence of this assumption (i.e. $\beta = 0$ and $T_g = T_{gr}$) on wind turbine nonlinear dynamics can be ignored due to the weak nonlinearity of the wind turbine dynamics in the region below rated wind speed. The effectiveness of the linearized model (4-46) for the wind turbine operating in the region below rated wind speed is demonstrated with simulation in Section 4.5.3.

The aerodynamic torque T_g in (4-46) is considered here as a bounded disturbance given by:

$$T_a = \hat{T}_a + \Delta T_a \tag{4-47}$$

where ΔT_a is the bounded aerodynamic toque uncertainty due to bounded EWS estimation error or bounded noise in the sensor (if sensor data are used to approximate EWS). $\hat{T}_a$ is the estimated aerodynamic torque calculated from ω_r and v_e as below:

$$\hat{T}_a = \frac{1}{2}\rho\pi R^3 C_q\left(\frac{\omega_r R}{v_e}\right)v_e^{\,2} \tag{4-48}$$

(4-48) is a simplified form of the aerodynamic torque (3-7) since $\beta = 0$.

A discrete-time model of the wind turbine is now required to develop and realize the robust predictive control. Therefore, (4-46) is discretized as follows:

$$\begin{cases} x(k+1) = Ax(k) + Bu(k) + Ed(k) \\ y(k) = Cx(k) \end{cases} \tag{4-49}$$

with $A = e^{A_{dt}T}$ and $[B \quad E] = \int_0^T e^{A_{dt}\tau} B_{dt} d\tau$. T is the sampling time and chosen as $T = 0.025$s.

4.5.2 Robust MPC for wind turbine control

The 1-norm robust MPC proposed in Section 4.4.2 is used as the baseline controller for wind turbine control and given as:

$$\min_{U(k)} \quad \eta \tag{4-50}$$

subject to:

$$x(k) = \hat{x}(k) \tag{4-51}$$

(4-34), (4-35)

(4-39), (4-41), (4-42), (4-43) and (4-44)

(4-29), (4-30), and (4-31)

$$y_r(k+i|k) = \hat{\omega}_{r\_opt}(k) \tag{4-52}$$

with $D(k) \in \Omega$

$$i = 0,1,2,..., N-1$$

in which $\hat{x}(k)$ in (4-51) are the estimated system states by a Luenberger observer and thus the control scheme used here is an output feedback control strategy. (4-52) represents the optimal rotor speed-tracking. The system matrices and variables in the compact state space model (4-34) and (4-35) are defined in (4-49).

The parameters of the system matrices are defined in Table 3-1. System constraints are defined in Table 3-2.

The linear programming problem (4-50) is solved online at every time instant to calculate $U(k)$. The first element $u(k)$ in $U(k)$ is implemented as the control input for the wind turbine.

Remark 4-13: The future reference signal over the prediction horizon is unknown due to the unknown future wind speed. However, the wind speed can be approximated as constant during the prediction horizon if the sampling frequency is fast enough and the prediction horizon is short. Therefore, the future reference signal over the horizon is chosen to be the optimal rotor speed at the current time instant as shown in (4-52).

4.5.3 Simulation study

The principle of AFTC in the approach of this Chapter is to switch to a healthy redundant wind speed sensor when the faulty wind speed sensor is isolated by the LSSVM method proposed in Section 4.3. In the case of both sensors being faulty, the estimated EWS is used to provide the wind speed data. Therefore, this AFTC scheme can be used to deal with single or multiple sensor faults. The overall AFTC scheme is shown in Figure 4-8.

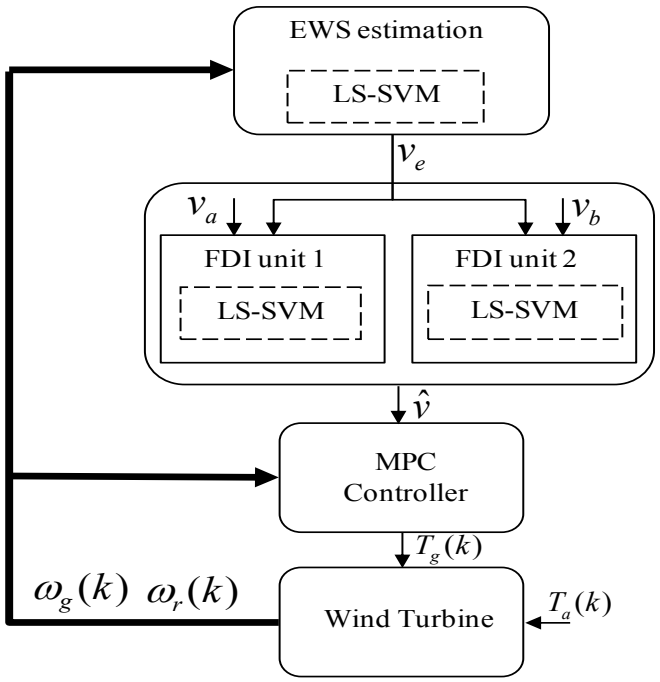

Figure 4-8 AFTC for wind speed sensor faults

This AFTC scheme is tested on the nonlinear wind turbine benchmark model described in Section 3.2. All the sensors are subject to bounded random noise.

The actual reference to be tracked is not the approximated optimal rotor speed in (4-1) but the filtered approximated optimal rotor speed which is a smoother signal. It is shown in (4-1) that $\hat{\omega}_{r\_opt}$ is highly fluctuating if the wind speed varies quickly. Trying to track such a highly fluctuating reference signal will result in heavy drive train torsion in the turbine and thus the lifetime of the drive train system will be shortened. Besides, it is found in simulation that the tracking performance deteriorates if $\hat{\omega}_{r\_opt}$ is being tracked directly. Therefore, the filtered $\hat{\omega}_{r\_opt}$ is actually being tracked.

The tracking performance of the proposed robust MPC controller in the fault-free case is shown in Figure 4-9. The controller parameters are chosen as: $N = 5$ and $\lambda_i = 1$, $i = 1,2,...,N$. In order to improve the tracking performance, the weighting on the input in (4-43) and (4-44) is chosen as $\gamma_i = 0$, $i = 1,2,...,N$ such that no penalties on the input variables are applied. The tracking performance is satisfactory as shown in Figure 4-9.

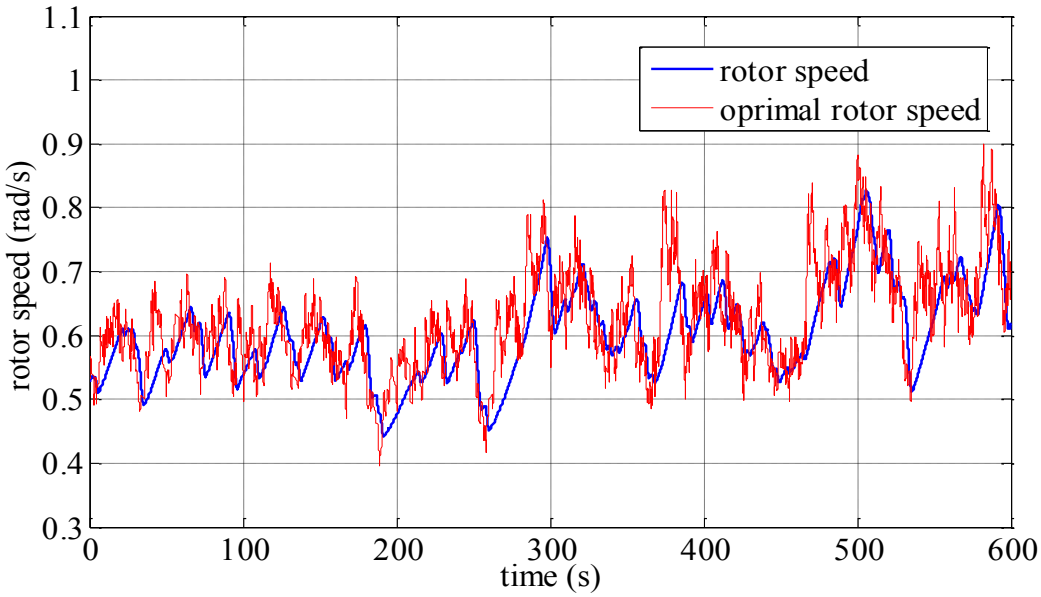

Figure 4-9 Optimal rotor speed tracking using robust MPC

The performance of a standard turbine controller used by the industry in (Abad, 2011) is also shown in Figure 4-10 for comparison. The standard controller is unable to track the reference signal closely since it is heavily influenced by the inertia of the large rotor. On the other hand, the proposed robust predictive controller considers the dynamic behaviour of the wind turbine in a period of time (i.e. in the prediction horizon) and thus the effect of the inertia is greatly mitigated.

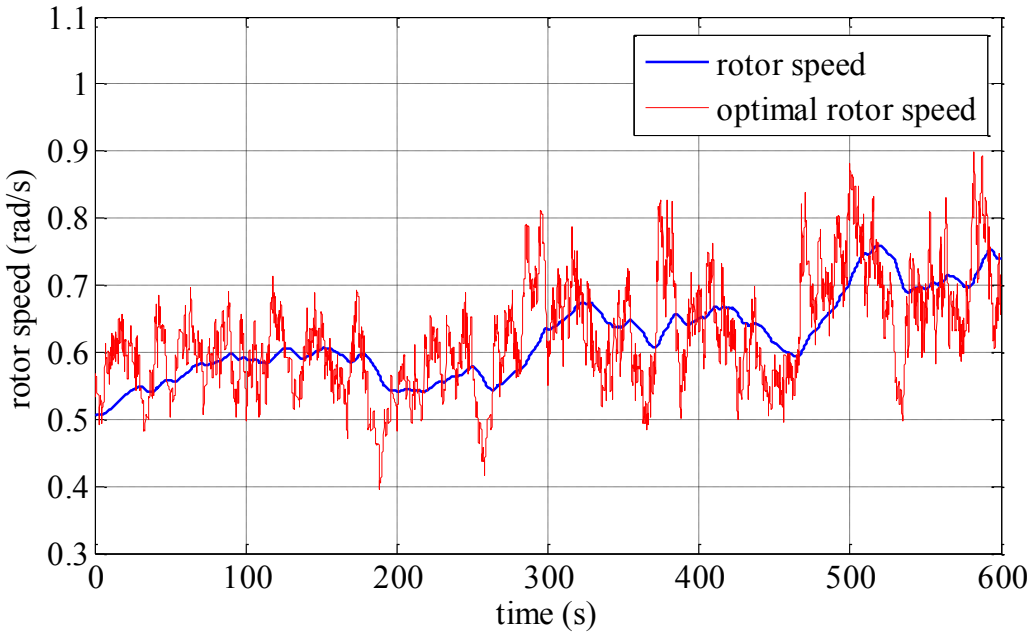

Figure 4-10 Optimal rotor speed tracking using standard controller

Figure 4-11 shows the FTC performance when a 0.2 gain factor error fault is applied on the wind speed sensor *a*. The fault is applied for 100 seconds starting at 150 seconds. A performance comparison of the robust MPC with and without the action of the FDI unit is presented. The proposed AFTC scheme switches to the healthy wind speed sensor *b* when the fault in wind speed sensor *a* is isolated by the FDI unit. The AFTC system reacts to the fault in a few seconds after the occurrence of faults. On the other hand, the rotor speed totally loses the reference signal without FDI.

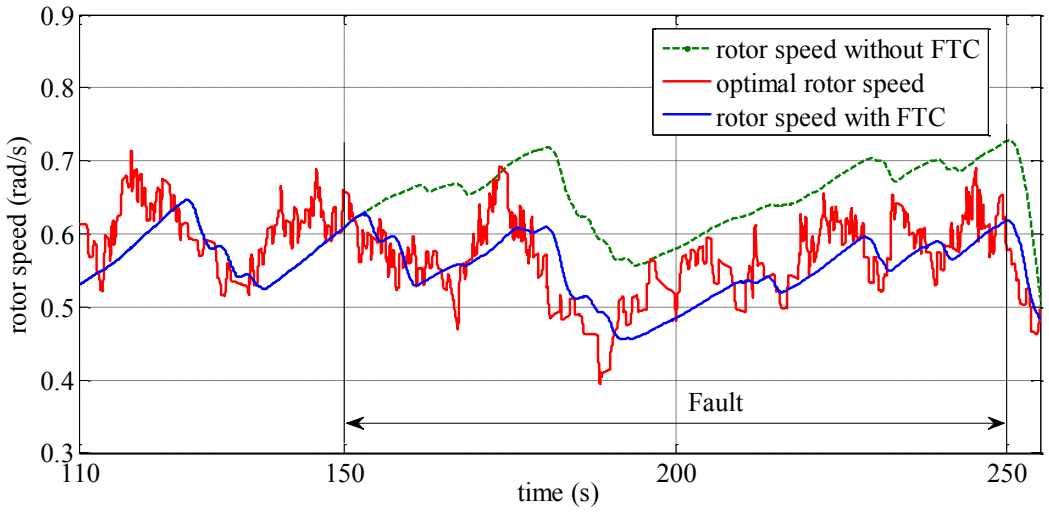

Figure 4-11 FTC performance for single sensor fault

Figure 4-12 shows the FTC performance when both of the wind speed sensors are faulty. There is a +0.8 m/s offset error in wind speed sensor *a* and a +1.0 m/s offset error in the wind speed sensor *b*. In this case, faults in both sensors are detected and the AFTC system discards data from both sensors and switches from sensor *a* to the estimated EWS to provide the reference signal. The control performance without FTC is also shown for comparison. It is shown in Figure 4-11 and Figure 4-12 that the tracking performance based on wind speed sensor data is very close to that based on estimated EWS with only slight differences.

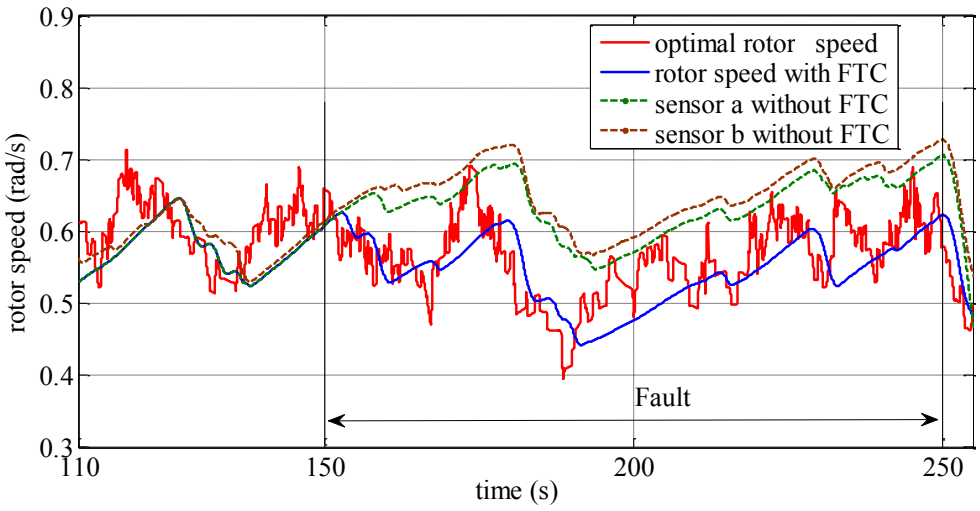

Figure 4-12 FTC performance for multiple sensor faults

The MPC prediction model is the linearized wind turbine model proposed in Section 4.5.1 while the controller is tested on the nonlinear wind turbine benchmark model described in Section 3.2. Therefore, the control performance shown in this Section justifies and demonstrates the model linearization method proposed in Section 4.5.1.

4.6 Conclusions

In this Chapter, an FDI method for wind speed sensor faults via LSSVM is proposed. Both the classification and function identification ability of LSSVM is used in this approach. The idea of combining hardware redundancy from multiple sensors and analytical redundancy from EWS estimation is used.

Based on the FDI unit, a robust 1-norm predictive controller is proposed as the baseline controller for the wind turbine to consider the EWS estimation error. The wind turbine control problem in the region below rated wind speed is considered. The robust MPC is proposed to take into account the EWS estimation error.

FTC of the wind turbine is realized by combining the FDI unit with MPC. Hardware redundancy from sensors is used first when faults occurs in one sensor. Analytical redundancy is used in the case that hardware redundancy is not available, i.e. all sensors are faulty.

A linear predictive controller is used for the nonlinear wind turbine system with satisfactory performance. Therefore, the simulation results in Section 4.5 show that the nonlinearity of the wind turbine system is weak if the operation is restricted to the region below rated wind speed.

Chapter 5 considers the AFTC problem for a wind turbine operating at wind speeds below and above the rated value. This work is thus an extension to the AFTC study in this Chapter.

Chapter 5: FTC for wind turbine sensor faults via fuzzy observer and fuzzy MPC

5.1 Introduction

AFTC methods for wind turbine operation in the region below rated wind speed can be simplified by taking advantage of the weak nonlinearity in this wind speed region. This is the strategy used in Chapter 4. If an FTC method is designed for both of the wind turbine operating regions, the following two design challenges will appear.

First of all, the nonlinearity is strong since the pitch angle is not only regulated at zero degrees in the region below rated wind speed but changes within a great range from -2 to +90 degrees in order to regulate the generator speed and power in the region above rated wind speed. Therefore, the turbine aerodynamic model (3-7) is not only a nonlinear function of two variables (i.e. v and ω_r) as in the case of Chapter 4, but a nonlinear function of three variables (i.e. v, ω_r and β) if the wind turbine is operating in both operating regions. Furthermore, the variations of v and ω_r also increase since they are varying in both turbine operating regions. Thus the nonlinearity of the wind turbine model is further increased.

Secondly, the control system design is more complex when the two operating regions are considered. For each of the two regions the system has different outputs to be controlled as explained in Section 3.5. The standard approach is to design and implement two separate control systems for each of the two operating regions.

In this Chapter, an AFTC scheme for both wind speed regions is proposed, which can be seen as an extension to the approach proposed in Chapter 4. The dynamics of the pitch system as well as the generator systems are ignored in Chapter 4. However, they are taken in to account in the controller and observer design in this Chapter since the whole dynamic behaviour of the wind turbine is required to cover the wide wind turbine operating conditions in the two operating regions.

This new approach is introduced to deal with the two challenges outlined above and the AFTC scheme comprises an FDI unit and a baseline controller. It is assumed that there is a redundant sensor that can be used when the sensor fault is detected and isolated by the FDI unit. Fault tolerance is achieved through switching to the healthy sensor in the case of sensor faults. The baseline controller in this scheme is based on MPC incorporating T-S fuzzy modelling, which is capable of accounting for the strong nonlinearity in the turbine model and controlling the wind turbine operating in both operating regions with a single controller. The FDI unit is based on a fuzzy observer using online eigenvalue assignment. The proposed wind turbine AFTC scheme utilizes both analytical and hardware redundancy.

The remainder of this Chapter is organized as follows: T-S fuzzy modelling of the wind turbine systems is shown in Section 5.2. The T-S fuzzy observer with online eigenvalue assignment is proposed in Section 5.3. The wind turbine controller based on T-S fuzzy MPC is proposed in Section 5.4. The AFTC scheme including FDI unit is described in Section 5.5. Conclusions are drawn in Section 5.6.

5.2 T-S fuzzy wind turbine model

T-S fuzzy modelling can be used to approximate a complex nonlinear dynamic model with a fuzzy model (Takagi and Sugeno, 1985; Feng, 2010). This fuzzy model has the characteristic of a simple linear time-varying system. Through this model approximation method, the controller and observer designs for the complex nonlinear model can be transformed to those for a simple linear time-varying model. Thus the controller and observer design can be simplified.

In this Section, the principle of T-S fuzzy modelling is introduced. Following this, a case study of the T-S fuzzy modelling of the nonlinear wind turbine model system is presented. The designs of the FDI unit and turbine baseline controller described in Section 5.4 and Section 5.5 is based on this wind turbine fuzzy model.

5.2.1 T-S fuzzy modelling

A T-S fuzzy dynamic model comprises two important factors: (1) fuzzy inference rules and (2) local analytical linear models. The representation of these two factors is shown as follows (Feng, 2010):

Rule p : If z_1 is F_1^p , z_2 is F_2^p , $\cdots$ and z_v is F_v^p

Then

$$x(k+1) = G_p x(k) + H_p u(k) + a_p \tag{5-1}$$

$$y(k) = C_p x(k)$$

$p = 1,2,3,....M$

where rule p denotes the p th fuzzy inference rule and M is the number of fuzzy rules. F_j^p with $j = 1,2,3,....v$ are fuzzy sets. $x(k) \in \mathbb{R}^n$ is the state vector of local models, $u(k) \in \mathbb{R}^l$ is the input vector and $y(k) \in \mathbb{R}^m$ is the measured outputs. G_p , H_p and C_p are system matrices of a discrete-time local models with proper dimensions. a_p is a constant bias term. $z = [z_1, z_2, z_3,..., z_v]$ are the so-called premise variables, which are some known variables from measurement or estimation. These premise variables can be outputs, system states or some other measurements.

(5-1) represents a series of local models in a system. The T-S fuzzy model of this overall system can be obtained from these local models by using a fuzzy inference method. If the standard fuzzy inference method is used (i.e. a singleton fuzzifier, product fuzzy inference and centre-average defuzzifier), then the T-S fuzzy model can be obtained by combining the local models in (5-1) and written as:

$$\begin{aligned} x(k+1) &= G(\eta)x(k) + H(\eta)u(k) + a(\eta) \\ y(k) &= C(\eta)x(k) \end{aligned} \tag{5-2}$$

where

$$\left.\begin{aligned} G(\eta) &= \sum_{p=1}^{M} \eta_p G_p \\ H(\eta) &= \sum_{p=1}^{M} \eta_p H_p \\ a(\eta) &= \sum_{p=1}^{M} \eta_p a_p \\ C(\eta) &= \sum_{p=1}^{M} \eta_p C_p \end{aligned}\right\} \tag{5-3}$$

η_p is the normalized membership function, which is a function of the premise variables and thus can be written as $\eta_p(z)$. This function satisfies:

$$\eta_p(z) = \frac{\xi_p(z)}{\sum_{i=1}^{M} \xi_i(z)} \tag{5-4}$$

in which:

$$\xi_p(z) = \prod_{i=1}^{v} F_i^p(z_i) \tag{5-5}$$

$F_i^p(z_i) \geq 0$ is the grade of the membership function of z_i in the fuzzy set F_i^p. (5-4) and (5-5) implies that $\eta_p(z) \geq 0$ and $\sum_{p=1}^{M} \eta_p(z) = 1$. (5-3) to (5-5) represent the fuzzy inference method for obtaining the fuzzy model (5-2).

The fuzzy inference method is important for fuzzy modelling and different inference methods are available (Feng, 2010). However, there is no theoretical method for choosing the most proper inference method for a T-S fuzzy system, so that the final choice of appropriate inference method is typical made through a "tuning" procedure. Details of fuzzy inference system theory can be found in (Kasabov, 1996; Babuska, 1998; Piegat, 2001)

Using the idea of fuzzy modelling mentioned above, a nonlinear dynamic model can be approximated by a nonlinear T-S fuzzy model which is obtained from a series of local linear models. These local models are obtained through linearizing the original

nonlinear model at a number of operating points. The procedure for this fuzzy modelling is described below.

Consider the following continuous nonlinear dynamic model:

$$\begin{aligned} \dot{x} &= f(x,u) \\ y &= Cx \end{aligned} \tag{5-6}$$

where $x(k) \in \mathbb{R}^n$ is the state vector of local models, $u(k) \in \mathbb{R}^l$ is the input vector and $y(k) \in \mathbb{R}^m$. The objective here is to obtain its approximated T-S fuzzy model in the form of (5-2). First of all, a series of local operating points should be chosen and given as $\{(x_1,u_1),(x_2,u_2),...,(x_M,u_M)\}$. Then the Taylor series expansion at the *M* local operating points is applied and the following local models can be derived:

$$\begin{aligned} \dot{x} = f(x,u) &= \left.\frac{\partial f}{\partial x}\right|_{x=x_p,u=u_p}(x-x_p) + \left.\frac{\partial f}{\partial u}\right|_{x=x_p,u=u_p}(u-u_p) + \varepsilon(x_p,u_p) \\ &= \left.\frac{\partial f}{\partial x}\right|_{x=x_p,u=u_p} x + \left.\frac{\partial f}{\partial u}\right|_{x=x_p,u=u_p} u - \left.\frac{\partial f}{\partial x}\right|_{x=x_p,u=u_p} x_p - \left.\frac{\partial f}{\partial u}\right|_{x=x_p,u=u_p} u_p + \varepsilon(x_p,u_p) \end{aligned} \tag{5-7}$$

$p = 1,2,3,....M$

$\varepsilon(x_p,u_p)$ represents higher order approximation error. (5-7) are the local linear models of (5-6) and can be reformulated as the standard state space models as follows:

$$\begin{aligned} \dot{x} &= A_p x + B_p u + c_p \\ y &= C_p x \end{aligned} \tag{5-8}$$

$p = 1,2,3,....M$

with

$$\left.\begin{aligned} A_p &= \left.\frac{\partial f}{\partial x}\right|_{x=x_p,u=u_p} \\ B_p &= \left.\frac{\partial f}{\partial u}\right|_{x=x_p,u=u_p} \\ c_p &= -\left.\frac{\partial f}{\partial x}\right|_{x=x_p,u=u_p} x_p - \left.\frac{\partial f}{\partial u}\right|_{x=x_p,u=u_p} u_p \\ C_p &= C \end{aligned}\right\} \tag{5-9}$$

The higher order approximation error $\varepsilon(x_p, u_p)$ is typically ignored in the transformation from (5-7) to (5-8).

By combining the local models in (5-8), a T-S fuzzy model of the nonlinear system (5-6) can be obtained. However, the fuzzy modelling method presented in (5-1) to (5-5) is based on discrete-time systems. Therefore, the local linear models in (5-8) are discretized as follows before being used for fuzzy inference:

$$\begin{aligned} x(k+1) &= G_p x(k) + H_p u(k) + a_p \\ y(k) &= C_p x(k) \end{aligned} \tag{5-10}$$

$p = 1,2,3,....M$

(5-10) are the local models for fuzzy inference which is the same form as the local models in (5-1).

The premise variables of the fuzzy rules for building the fuzzy model are the current system states and inputs and represented by:

$$z = [x(k), u(k)] \tag{5-11}$$

Now the fuzzy rules for T-S fuzzy modelling can be obtained from (5-10) and (5-11) and given as:

Rule p : *If* $x^1(k) = x_p^1$, $x^2(k) = x_p^2$,..., $x^n(k) = x_p^n$, $u^1(k) = u_p^1$, $u^2(k) = u_p^2, \ldots, u^l(k) = u_p^l$

$$\textit{Then} \quad x(k+1) = G_p x(k) + H_p u(k) + a_p \tag{5-12}$$

$$y(k) = C_p x(k)$$

$p = 1,2,3,....M$

in which $x^i(k)$, $i = 1,2,3,....n$ represents the i th element in the current system states and x_p^i represents the i th element in the operating point x_p used for linearization. $u^j(k)$, $j = 1,2,3,...,l$ is the j th element in the current system inputs and u_p^j , represents the j th element in the operating point u_p used for linearization.

From the fuzzy rules (5-12), the T-S fuzzy model of the nonlinear system (5-6) can be obtained by using the fuzzy inference method in (5-3) to (5-5) and represented as follows:

$$\begin{aligned} x(k+1) &= G(\eta)x(k) + H(\eta)u(k) + a(\eta) \\ y(k) &= Cx(k) \end{aligned} \tag{5-13}$$

Remark 5-1: The models in (5-12) are used to describe the nonlinear system (5-6) when the inputs and states of the system (5-6) are at any of the p operating points defined in the p fuzzy rules in (5-12). Alternatively, a linear combination of the p linear models in (5-12) is used to describe the nonlinear system (5-6) when the system inputs and states are not at any of these operating points. This linear combination is calculated by the fuzzy inference method in (5-3) to (5-5).

Remark 5-2: It is shown in (5-13) that the output matrix C is a constant and satisfies $C = C_p$, $p = 1,2,3,...,v$ as shown in (5-9). However, the output matrix $C(\eta)$ in (5-2) is not constant but depends on the membership function. This is because (5-2) is a general form of fuzzy modelling taking into account the nonlinearity in the system outputs. But the case of linear output equation is considered here as shown in (5-6).

Therefore, the output equation does not require linearization and thus the fuzzy model (5-13) and the local models (5-12) are simplified.

Remark 5-3: As shown in (5-11), the premise variables vary with the change of time instant k and are thus time-varying. On the other hand, the membership functions η in the system matrices $G(\eta)$, $H(\eta)$ and $a(\eta)$ of the fuzzy model (5-13) are calculated from these time-varying premise variables. Consequently, $G(\eta)$, $H(\eta)$ and $a(\eta)$ are also time-varying . Therefore, (5-13) is a LTV system in essence and can be represented as:

$$\begin{aligned} x(k+1) &= G(\eta_k)x(k) + H(\eta_k)u(k) + a(\eta_k) \\ y(k) &= Cx(k) \end{aligned} \tag{5-14}$$

Alternatively, if there is nonlinearity in the outputs equation, (5-14) should be rewritten as:

$$\begin{cases} x(k+1) = G(\eta_k)x(k) + H(\eta_k)u(k) + a(\eta_k) \\ y(k) = C(\eta_k)x(k) \end{cases} \tag{5-15}$$

in which η_k shows that the membership function is time-varying. The time-varying characteristic of the T-S fuzzy model is shown explicitly in (5-14) and (5-15).

Remark 5-4: It is shown in (5-11) that all the system state variables and inputs are used as premise variable. However, this is not necessary for some systems in which the nonlinearity only appears in part of the system model. For example, the nonlinear wind turbine model presented in Section 3.2 is a highly nonlinear function of three variables (i.e. β, v and ω_r) and the nonlinearity in this model only appears in the aerodynamic torque T_a. Therefore, model linearization can be applied based on only these three variables and the premise variables for building the T-S fuzzy wind turbine model are in the form of $z = [\beta(k) \quad v(k) \quad \omega_r(k)]$. Thus the inputs and other state variables in the wind turbine system are not used as premise variables. This situation is explained in the case study in Section 5.2.2

5.2.2 Case study

A case study of T-S fuzzy modelling of a wind turbine is presented in this Section. The fuzzy inference method shown in Section 5.2.1 is used for T-S fuzzy modelling of the nonlinear wind turbine system described in (3-8). The T-S fuzzy wind turbine model obtained in this Section will be used for designing the fuzzy observer in Section 5.3 and fuzzy predictive controller in Section 5.4.

Consider the following nonlinear wind turbine model in Chapter 3:

$$\begin{aligned} \dot{x} &= f(x,u,v) \\ y &= Cx \end{aligned} \tag{5-16}$$

in which $x=[\omega_r \quad \omega_g \quad \theta_\Delta \quad \dot{\beta} \quad \beta \quad T_g]^{\mathrm{T}}$, $u=[T_{gr} \quad \beta_r]^{\mathrm{T}}$ and v is the EWS. The measured outputs are the generator speed, the blade pitch angle and the generator torque and therefore $y=[\omega_g \quad \beta \quad T_g]^{\mathrm{T}}$, and $C=\begin{bmatrix} 0 & 1 & 0 & 0 & 0 & 0 \\ 0 & 0 & 0 & 0 & 1 & 0 \\ 0 & 0 & 0 & 0 & 0 & 1 \end{bmatrix}$.

The nonlinearity in (5-16) comes from the aerodynamic torque which is a nonlinear function of v, ω_r and β and represented as:

$$T_a(v,\omega_r,\beta)=\frac{1}{2}\rho\pi R^3 C_q(\lambda,\beta)v^2, \tag{5-17}$$

To obtain the T-S fuzzy wind turbine model, (5-16) should be linearized at several local operating points. However, only the aerodynamic model is nonlinear while other parts of the wind turbine model are linear as shown in (3-1), (3-2) and (3-4). Therefore, only (5-17) needs to be linearized according to the variables (v,ω_r,β). Thus (5-17) is linearized using Taylor series expansion as follows:

$$
\begin{aligned}
T_a(v,\omega_r,\beta) &= \left.\frac{\partial T_a}{\partial v}\right|_{v=v_p,\omega_r=\omega_{rp},\beta=\beta_p}(v-v_p)+\left.\frac{\partial T_a}{\partial \omega_r}\right|_{v=v_p,\omega_r=\omega_{rp},\beta=\beta_p}(\omega_r-\omega_{rp})+ \\
&\left.\frac{\partial T_a}{\partial \beta}\right|_{v=v_p,\omega_r=\omega_{rp},\beta=\beta_p}(\beta-\beta_p)+\varepsilon(x_p,u) \\
&= \left.\frac{\partial T_a}{\partial v}\right|_{v=v_p,\omega_r=\omega_{rp},\beta=\beta_p} v+\left.\frac{\partial T_a}{\partial \omega_r}\right|_{v=v_p,\omega_r=\omega_{rp},\beta=\beta_p}\omega_r+\left.\frac{\partial T_a}{\partial \beta}\right|_{v=v_p,\omega_r=\omega_{rp},\beta=\beta_p}\beta+ \\
&\left(-\left.\frac{\partial T_a}{\partial v}\right|_{v=v_p,\omega_r=\omega_{rp},\beta=\beta_p} v_p-\left.\frac{\partial T_a}{\partial \omega_r}\right|_{v=v_p,\omega_r=\omega_{rp},\beta=\beta_p}\omega_{rp}-\left.\frac{\partial T_a}{\partial \beta}\right|_{v=v_p,\omega_r=\omega_{rp},\beta=\beta_p}\beta_p\right)+\varepsilon(v,\omega_r,\beta)
\end{aligned}
\tag{5-18}
$$

$$p = 1,2,3,....M$$

in which $(v_p, \omega_{rp}, \beta_p)$, $p = 1,2,3,....M$ are some selected operating points.

The linearized drive train model in the state space form can be acquired by substituting (5-18) into (3-4) and ignoring the higher order nonlinear term $\varepsilon(v,\omega_r,\beta)$. Meanwhile, the linear turbine pitch model in (3-1) and the generator model in (3-2) can both be transformed into state space form. Thus linear models of all the three turbine subsystems in state space form are obtained. The linearized overall wind turbine model can now be obtained by formulating the two linear state space models (i.e. pitch system and generator system) and the linearized model (i.e. linearized drive train model) into one state space form as shown below:

$$
\begin{aligned}
\dot{x} &= A_p x + B_p u + E_p v + c_p \\
y &= Cx
\end{aligned}
\tag{5-19}
$$

$$p = 1,2,3,....M$$

in which x, u, y and v are same with those variables defined in the original turbine model (5-16). $A_p \in \mathbb{R}^{6\times 6}$, $B_p \in \mathbb{R}^{6\times 2}$, and $E_p \in \mathbb{R}^{6\times 1}$ are system matrices of the local linear models. $c_p \in \mathbb{R}^{6\times 1}$ is a constant term due to the constant term in the Taylor series expansion in (5-18).

In order to use the fuzzy inference method for discrete-time systems in Section 5.2.1, (5-19) is discretized as follows:

$$\begin{aligned} x(k+1) &= G_p x(k) + H_p u(k) + D_p v(k) + a_p \\ y(k) &= Cx(k) \end{aligned} \tag{5-20}$$

$p = 1,2,3,....M$

where $G_p \in \mathbb{R}^{6\times 6}$, $H_p \in \mathbb{R}^{6\times 2}$, $D_p \in \mathbb{R}^{6\times 1}$ and $a_p \in \mathbb{R}^{6\times 1}$ are the discretized system matrices corresponding to A_p, B_p, E_p and c_p.

From the local wind turbine models in (5-20) and the linearized operating points $(v_p, \omega_{rp}, \beta_p)$, the following fuzzy rules for T-S fuzzy wind turbine model can be obtained:

Rule p : *If* $v(k) = v_p$, $\omega_r(k) = \omega_{rp}$ and $\beta(k) = \beta_p$

$$\textit{Then} \quad \begin{aligned} x(k+1) &= G_p x(k) + H_p u(k) + D_p v(k) + a_p \\ y(k) &= Cx(k) \end{aligned} \tag{5-21}$$

$p = 1,2,3,....M$

Applying the fuzzy inference method in Section 5.2.1 to Equation (5-21), the T-S fuzzy wind turbine model can be derived as follows:

$$\begin{aligned} x(k+1) &= G(\eta_k)x(k) + H(\eta_k)u(k) + D(\eta_k)v(k) + a(\eta_k) \\ y(k) &= Cx(k) \end{aligned} \tag{5-22}$$

in which η_k is the membership function, which is a function of the variables used for linearization and thus can also be written as $\eta_k(v(k), \omega_r(k), \beta(k))$.

Remark 5-5: The operating points for model linearization are chosen according to the designer's knowledge of the process. In the case of this wind turbine system, four operating points are chosen and thus $M = 4$. Two operating points are chosen in the region below rated wind speed at $(v_1 = 5, \omega_{r1} = 0.56, \beta_1 = 0)$ and $(v_2 = 9, \omega_{r2} = 1.02, \beta_2 = 0)$ since in this operating region the pitch angle is regulated at

$\beta = 0$. (v_1, ω_{r1}) and (v_2, ω_{r2}) are chosen such that ω_{r1} and ω_{r1} are two optimal rotor speed values at the two wind speeds of v_1 and v_2 , separately. The other two operating points are chosen in the region above rated wind speed at $(v_3 = 13.76, \omega_{r3} = 1.7, \beta_3 = 10)$ and $(v_4 = 20, \omega_{r4} = 1.8, \beta_4 = 20)$ since for operation above the rated wind speed the pitch angle changes in the range of -2 to +90 degrees. The number of operating points is a matter of design choice. More operating points can improve accuracy but the resulting designs may have excessive complexity (Baranyi, Tikk, Yam and Patton, 2003). It is shown in the simulation results of Section 5.5 that the four operating points chosen here can produce satisfactory approximation of the nonlinearity in the wind turbine system.

Remark 5-6: It is shown in (5-22) that EWS $v(k)$ and the constant bias $a(\eta_k)$ are two disturbances. They will be treated as known disturbances and dealt with by a feed-forward strategy in the fuzzy MPC design presented in Section 5.4

5.3 T-S fuzzy observer

In order to control a system whose state variables cannot all be measured, an observer can be designed and an output feedback control strategy can be used. For a nonlinear system represented by a T-S fuzzy model with some unmeasured system states, a fuzzy observer can also be designed to estimate the state variables and hence achieve an output feedback control system. Systematic design and analysis methods for fuzzy observers are proposed in (Tanaka, Ikeda and Wang, 1998; Ma, Sun and He, 1998). The design of fuzzy observers for discrete-time systems is also introduced in (Feng, 2010). Linear matrix inequalities (LMI) are used in all these approaches for both the design and analysis of fuzzy observers.

This Section introduces the principle of the T-S fuzzy observer. In Section 5.3.1 the advantages and disadvantages of some existing T-S fuzzy observer design methods are discussed. In Section 5.3.2 a novel T-S fuzzy observer design is proposed based on online eigenvalue assignment. This observer is used for estimation of the states of the wind turbine system.

5.3.1 T-S fuzzy observer principles

Consider the following observer rules using the same rules of the T-S fuzzy system in (5-1):

Rule p : *If* z_1 is F_1^p, z_2 F_2^p, … and z_v is F_v^p

Then $\hat{x}(k+1) = G_p\hat{x}(k) + H_p u(k) + a_p + F_p[\hat{y}(k) - y(k)]$

$$\hat{y}(k) = C_p\hat{x}(k) \tag{5-23}$$

$$p = 1,2,3,....M$$

In which $\hat{x}(k)$ is the estimated state vector, $\hat{y}(k)$ is the estimated output vector. F_p, $p = 1,2,3,....M$ are the local observer gains to be determined

Using the same fuzzy inference method presented in Section 5.2.1, the following T-S fuzzy observer can be obtained:

$$\hat{x}(k+1) = G(\eta_k)\hat{x}(k) + H(\eta_k)u(k) + a(\eta_k) + F(\eta_k)[\hat{y}(k) - y(k)] \tag{5-24}$$

with $\hat{y}(k) = C(\eta_k)\hat{x}(k)$.

The dynamics of the estimation error can be obtained by subtracting the T-S fuzzy model (5-15) from the corresponding T-S fuzzy observer (5-24) and given as:

$$e(k+1) = [G(\eta_k) + F(\eta_k)C(\eta_k)]e(k) \tag{5-25}$$

where $e(k) = \hat{x}(k) - x(k)$ is the estimation error.

The observer gain $F(\eta_k)$ can be calculated by the following Theorem (Ma, Sun and He, 1998):

Theorem 5-1: The dynamics of the fuzzy observer estimation error in (5-25) is globally exponentially stable if there exist a positive definite matrix P and a series of matrices Q_p, $p = 1,2,3,....M$ such that the following LMIs are satisfied:

$$\begin{bmatrix} -P & G_p^{\mathrm{T}}P + C_j^{\mathrm{T}}Q_p^{\mathrm{T}} \\ PG_p + Q_pC_j & -P \end{bmatrix} \tag{5-26}$$

$j, p = 1,2,3,....M$

The local observer gains F_p in (5-23) are then given by:

$$F_p = P^{-1}Q_p$$

$p = 1,2,3,....M$

After the local gains F_p, $p = 1,2,3,....M$ are calculated from Theorem 5-1, the T-S fuzzy observer gain $F(\eta_k)$ in (5-24) can now be obtained using the fuzzy inference method presented in Section 5.2.1.

Theorem 5-1 is a standard approach for designing a T-S fuzzy observer for discrete-time systems. Several mature numerical methods are also available for solving the LMIs in (5-26). However, there are still several disadvantages of using the standard approach of Theorem 5-1 to design a T-S fuzzy observer. These disadvantages are explained below.

First of all, the gain of the T-S fuzzy observer cannot be assigned using Theorem 5-1. As shown in (5-26), the observer gain is calculated from the LMIs and thus only determined from the solution of the LMIs. Therefore, the eigenvalues of the fuzzy observer gain cannot be assigned. This means that designers cannot tune the fuzzy observer gain to improve the estimation performance.

Secondly, it is shown in (5-26) that the standard approach of designing a T-S fuzzy observer depends on the feasibility of the LMIs. For a very complex system with high nonlinearity, a large number of local models are needed in order to minimize the model mismatch between the original nonlinear model and the T-S fuzzy model. However, this

leads to the requirement for a significant number of LMIs and there may not be a feasible solution to satisfy so many LMIs. This highlights the well known problem of complexity in fuzzy inference modelling (Baranyi, Tikk, Yam and Patton, 2003).

Thirdly, the premise variables in (5-23) are generally chosen as variables like system states or inputs which are changing at every time instant. Meanwhile, the global T-S fuzzy observer gain in (5-24) is calculated using these premise variables. Consequently, (5-24) is also a LTV system with a time-varying observer gain. Thus the eigenvalues of the fuzzy observer gain are not fixed and are changing online at every time instant.

In order to mitigate the problems in the standard fuzzy observer design mentioned above, a method was proposed in (Chen, Lopez-Toribio and Patton, 1999) to assign the eigenvalues in a specific region of the complex plane. This method is described as follows.

Consider the following T-S fuzzy dynamic system:

$$\dot{x}(t) = A(\eta)x(t) + B(\eta)u(t) \tag{5-27}$$

with the linear output equation $y(t) = Cx(t)$.

The following T-S fuzzy observer can be designed for (5-27):

$$\dot{\hat{x}}(t) = A(\eta)\hat{x}(t) + B(\eta)u(t) + L(\eta)[\hat{y}(t) - y(t)] \tag{5-28}$$

with $\hat{y}(t) = C\hat{x}(t)$.

Its local observers are given as:

$$\dot{\hat{x}}(t) = A_p\hat{x}(t) + B_p u(t) + L_p[\hat{y}(t) - y(t)] \tag{5-29}$$

$p = 1,2,3,....M$

in which $L(\eta)$ and L_p are the fuzzy observer gain and its local observer gain separately. It is assumed that there is no nonlinearity in the outputs and thus the output matrix of each local observer is a constant matrix C. The eigenvalues of the fuzzy observer (5-28)

are assigned to lie within a suitable region of the complex plane if the following Theorem is satisfied.

Theorem 5-2 (Chen, Lopez-Toribio and Patton, 1999)**:** The fuzzy observer (5-28) has its eigenvalues in a region $S(\alpha,\beta)$, if there exist a common positive definite matrix P satisfying the following LMIs:

$$\begin{bmatrix} -\beta P & (A_p - L_p C)P \\ P(A_p - L_p C)^T & -\beta P \end{bmatrix} < 0 \tag{5-30}$$

$$(A_p - L_p C)^T P + P(A_p - L_p C) + 2\alpha P < 0 \tag{5-31}$$

$p = 1,2,3,....M$

The region $S(\alpha,\beta)$ is shown in Figure 5-1.

The eigenvalues of a T-S fuzzy observer can be confined in a region using Theorem 5-2. However, Theorem 5-2 solves more LMIs compared with Theorem 5-1. Furthermore, for a complex nonlinear system with more local models, there are more LMIs to be satisfied and (5-30) and (5-31) are very likely to be infeasible.

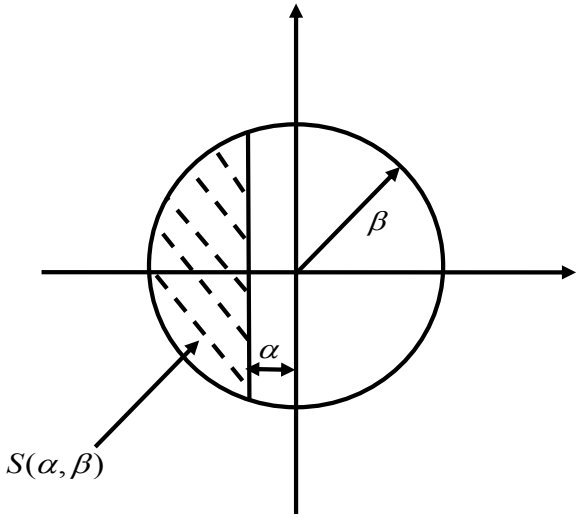

Figure 5-1 Eigenvalue region

Theorem 5-2 can only be applied to the simple situation in which there is no nonlinearity in the output of the original nonlinear system (i.e. in the case of a constant

output matrix C in the system). Hence, the application of Theorem 5-2 is limited in this way.

5.3.2 T-S fuzzy observer using online eigenvalue assignment

In this Section, an algorithm for designing a T-S fuzzy observer is proposed. Using this algorithm, the gain of the T-S fuzzy observer can be assigned through online assignment of eigenvalues. This algorithm is used online to estimate the system states at every time instant and thus it is proposed for discrete T-S fuzzy systems. The algorithm is shown as follows:

Consider the following T-S fuzzy observer designed for the fuzzy system (5-15) with its fuzzy rules in (5-12):

$$\hat{x}(k+1) = G(\eta_k)\hat{x}(k) + H(\eta_k)u(k) + a(\eta_k) + F[\hat{y}(k) - y(k)] \qquad (5\text{-}32)$$

with $\hat{y}(k) = C(\eta_k)\hat{x}(k)$.

The dynamics of the state estimation error can be obtained by subtracting the fuzzy model (5-15) from the corresponding fuzzy observer (5-32) and given as:

$$e(k+1) = [G(\eta_k) + FC(\eta_k)]e(k) \qquad (5\text{-}33)$$

where F is the fuzzy observer gain to be calculated by an algorithm, which is different with $F(\eta_k)$ calculated using standard fuzzy inference method. The algorithm for calculating F and assigning the eigenvalues of the T-S fuzzy observer gain is given as follows:

Algorithm 5-1: Online Eigenvalue Assigment for discrete T-S fuzzy observers

1 Acquire $\hat{x}(k)$ from the T-S fuzzy observer (5-32).

2 Update η_k with the corresponding premise variables using the fuzzy inference methods in Section 5.2.1.

3 Calculate $G(\eta_k), H(\eta_k), a(\eta_k)$ and $C(\eta_k)$ from η_k.

4 Calculate F from $G(\eta_k)$, $C(\eta_k)$ and the predefined eigenvalues λ of the observer gain, using a standard pole placement method.

5 $k = k + 1$, go to step 1.

in which λ is a vector of predefined eigenvalues and k is the current time instant.

The assumption of using Algorithm 5-1 is that each local model of the T-S fuzzy system (5-15) should be observable. Then the global observability of the fuzzy system (5-15) can be guaranteed through applying LMI conditions to these observable local models (Feng, 2010). Compared with the standard fuzzy observer design approach in Theorem 5-1 and the modified approach in Theorem 5-2, Algorithm 5-1 has several advantages as follows.

First of all, the use of LMIs for computing the T-S fuzzy observer gain is obviated by using Algorithm 5-1 and thus there is no problem of infeasible solution encountered in using LMIs.

Secondly, the eigenvalues of the T-S fuzzy observer are predefined by the designer in Step 4 of Algorithm 5-1 and thus they can be specified to specific points in the z-plane rather than within a range by using Theorem 5-2. Therefore, the fuzzy observer gain can be tuned by the designer using Algorithm 5-1. Furthermore, the eigenvalues obtained from Theorem 5-1 are changing online due to the time-varying behaviour of $F(\eta_k)$ in (5-25). However, the eigenvalues obtained from Algorithm 5-1 are predefined and are thus fixed.

Thirdly, Algorithm 5-1 can be applied to a wider class of fuzzy system with nonlinearity in the output equation while Theorem 5-2 can only be applied to the limited situation in which there is no nonlinearity in the output equation. This is because Algorithm 5-1 is designed for (5-15) which has nonlinearity in the output equation while Theorem 5-2 is only applied to system (5-27) without nonlinearity in the output equation.

Remark 5-7: The premise variables in Step 2 may not be all the system state variables $\hat{x}(k)$ and inputs $u(k)$. They are determined by the variables used to linearize the original nonlinear model. In the case of wind turbine, the three variables of (v, ω_r, β) are used as the premise variables, which is a combination of one known disturbance and two system state variables.

Remark 5-8: If Algorithm 5-1 is running in the Matlab/Simulink environment (MathWorks, 2011), the standard pole-placement method in Step 4 refers to the function $place(G(\eta_k)^{\mathrm{T}}, -C(\eta_k)^{\mathrm{T}}, \lambda)$ with λ being the vector of predefined eigenvalues.

5.4 T-S fuzzy model predictive control for wind turbines

As described in Section 4.4, MPC has the advantage of dealing with system constraints externally. However, most mature MPC methods are designed for linear systems. MPC design and implementation approaches for nonlinear systems require more complex algorithms and are constrained by more assumptions (Grüne and Pannek, 2011) since the optimization problem to be solved by MPC cannot be formulated as a standard linear or quadratic programming problem due to the system model nonlinearity.

On the other hand, the T-S fuzzy modelling methods can be used to transform a nonlinear system model into its approximated T-S fuzzy model which is a LTV system. From the perspective of discrete-time systems, a LTV system is a linear system at every time instant.

Therefore, combining the MPC algorithm with a T-S fuzzy prediction model can be a practical approach to simplify the MPC design for nonlinear systems. In the discrete-time system sense, the T-S fuzzy prediction model is a linear model at each time instant. Thus the standard linear or quadratic programming algorithms can still be applied to a T-S fuzzy model. It is important to note here that the advantages of MPC for linear systems, such as taking into account constraints and future system behaviour, are retained in this new framework of T-S fuzzy MPC.

In this Section, a novel T-S fuzzy MPC approach for controlling the nonlinear wind turbine systems is proposed. The prediction model used in this framework is a T-S fuzzy model of the original nonlinear wind turbine system. Meanwhile the MPC

algorithm of this new framework minimizes a quadratic cost function subject to a series of constraints at every time instant. This T-S fuzzy MPC approach is used in Section 5.5 as a baseline controller for AFTC of wind turbine systems.

5.4.1 T-S fuzzy model predictive control

Consider the following constrained discrete-time nonlinear system:

$$\begin{aligned} x(k+1) &= f(x(k), u(k)) \\ y(k) &= g(x(k)) \end{aligned} \tag{5-34}$$

subject to:

$$\begin{aligned} u_{\min} \le u(k+j|k) \le u_{\max} \\ \Delta u_{\min} \le \Delta u(k+j|k) \le \Delta u_{\max} \\ y_{\min} \le y(k+j+1|k) \le y_{\max} \end{aligned} \tag{5-35}$$

$j = 0,1,2,...N$

with its T-S fuzzy model given as follows:

$$\begin{aligned} x(k+1) &= G(\eta_k)x(k) + H(\eta_k)u(k) + a(\eta_k) \\ y(k) &= C(\eta_k)x(k) \end{aligned} \tag{5-36}$$

where $x(k) \in \mathbb{R}^n$ and $u(k) \in \mathbb{R}^l$ are the state vector and input vector. $y(k) \in \mathbb{R}^m$ are the measured outputs. $u_{\min}$, $u_{\max}$, $\Delta u_{\min}$, $\Delta u_{\max}$, $y_{\min}$ and $y_{\max}$ are system constraints.

The original MPC problem for (5-34) is shown as follows:

$$\min_{U(k)} J(U(k),\ X(k)) \tag{5-37}$$

subject to:

$$\begin{aligned} x(k+j+1|k) &= f(x(k+j|k), u(k+j|k)) \\ y(k+j|k) &= g(x(k+j|k)) \end{aligned} \tag{5-38}$$

$$U_{\min} \le U(k) \le U_{\max}$$

$$\Delta U_{\min} \le \Delta U(k) \le \Delta U_{\max} \tag{5-39}$$

$$Y_{\min} \le Y(k) \le Y_{\max}$$

$j = 0,1,2,\ldots N$

in which (5-39) are the compact form of system constraints as defined in Section 4.4.1. N is the control horizon and also the prediction horizon. (5-37) is difficult to solve due to the nonlinearity in (5-38). However, this optimization problem can be simplified if the original nonlinear prediction model (5-38) is replaced with its T-S fuzzy model. Therefore, the original optimization problem (5-37) is transformed into the following optimization problem with T-S fuzzy prediction model:

$$\min_{U(k)} J(U(k),\ X(k)) \tag{5-40}$$

subject to:

$$\begin{aligned} x(k+j+1|k) &= G(\eta_{k+j|k})x(k+j|k) + H(\eta_{k+j|k})u(k+j|k) + a(\eta_{k+j|k}) \\ y(k+j|k) &= C(\eta_{k+j|k})x(k+j) \end{aligned} \tag{5-41}$$

(5-39)

$j = 0,1,2,\ldots N$

in which (5-41) is derived from the (5-36). If $J(U(k),\ X(k))$ in (5-40) is a quadratic or linear cost function, (5-40) becomes a standard quadratic or linear programming

problem since the prediction model (5-41) is a linear system at every time instant. Then (5-40) can be solved using the methods presented in Section 4.4.1.

Remark 5-9: As shown in (5-41), the system matrices $G(\eta_{k+j|k})$, $H(\eta_{k+j|k})$, $a(\eta_{k+j|k})$ and $C(\eta_{k+j|k})$ are based on the assumption that future membership functions $\eta_{k+j|k}$, $j = 0,1,2,...N$ over the horizon are known in advance. This means that the future premise variables should also be known in advance since $\eta_{k+j|k}$ are calculated from the future premise variables. However, future premise variables are not readily known in most cases. A method to solve this problem is to approximate $G(\eta_{k+j|k})$, $H(\eta_{k+j|k})$, $a(\eta_{k+j|k})$ and $C(\eta_{k+j|k})$, $j = 0,1,2,...N$ with $G(\eta_k)$, $H(\eta_k)$, $a(\eta_k)$ and $C(\eta_k)$ provided that the system dynamics are not very fast and the sampling period of the discrete-time system is fast enough. Therefore, the prediction model (5-41) is replaced with the following prediction model:

$$\begin{aligned} x(k+j+1|k) &= G(\eta_k)x(k+j|k) + H(\eta_k)u(k+j|k) + a(\eta_k) \\ y(k+j|k) &= C(\eta_k)x(k+j) \end{aligned} \tag{5-42}$$

Remark 5-10: The terminal condition proposed in (Mayne, Rawlings, Rao and Scokaert, 2000) is not used in the T-S fuzzy MPC proposed in this Section to achieve stability due to the following two reasons. First of all, the terminal condition is proposed for systems without variation in the model parameters. However, the T-S fuzzy model in (5-36) is a linear time varying system and thus the parameters in the model are changing at every time instant. Therefore, the terminal condition cannot be applied to the T-S fuzzy MPC proposed in this Chapter. Secondly, the stability property can be achieved if the controlled system is stable and the prediction horizon is long enough, as explained in Remark 4-9. The wind turbine model in this Chapter is a stable T-S fuzzy model satisfying the stability condition of T-S fuzzy system presented in (Feng, 2010). Meanwhile, it is shown in the simulation results in Section 5.5.3 that the prediction horizon $N = 6$ is long enough to avoid problems caused by instability and achieve satisfactory tracking performance. The feasibility problem is avoided as explained in Remark 4-10.

5.4.2 T-S fuzzy model predictive control for wind turbines

FTC strategies for wind turbine systems based on T-S fuzzy modelling are presented in (Sami and Patton, 2012b; Sami and Patton, 2012a). However, these studies only consider the region below rated wind speed. A wind turbine is frequently switching between two operation regions during operation and thus duplex controllers can be used. As shown in (Maciejowski, 1999), MPC has the advantage of simplifying multiple controller designs if different outputs are to be regulated at different time instants. Therefore, a T-S fuzzy MPC scheme for control of wind turbines is designed in this Section to deal with the nonlinearity and simplify the multiple controller design in the wind turbine system.

Using a quadratic cost function and the T-S fuzzy wind turbine model in (5-22), the T-S fuzzy MPC for the wind turbine is formulated as the following optimization problem:

$$\min_{u(k),u(k+1),,,u(k+N-1)} \sum_{i=1}^{N} \left\| x(k+i) - x_r(k) \right\|_R \tag{5-43}$$

subject to:

$$x(k) = \hat{x}(k) \tag{5-44}$$

$$x(k+i+1|k) = G(\eta_k)x(k+i|k) + H(\eta_k)u(k+i|k) + D(\eta_k)v(k+i|k) + a(\eta_k) \tag{5-45}$$

$$\begin{aligned} &\beta_{\min} \le \beta_r(k+i|k) \le \beta_{\max} \\ &\Delta\beta_{\min} \le \beta_r(k+i|k) - \beta_r(k+i-1|k) \le \Delta\beta_{\max} \\ &T_{\min} \le T_{gr}(k+i|k) \le T_{\max} \\ &\Delta T_{\min} \le T_{gr}(k+i|k) - T_{gr}(k+i-1|k) \le \Delta T_{\max} \end{aligned} \tag{5-46}$$

$i = 0,1,2,...N-1$

where N is the MPC prediction horizon, $x_r(k) = [\hat{\omega}_{r\_opt}(k) \quad \omega_{gr} \quad 0 \quad 0 \quad \beta_{opt} \quad \frac{P_{gr}}{\eta_g \omega_g(k)}]^{\mathrm{T}}$ is the reference signal and $\|x\|_R = x^T R x$. η_k is the membership function. At each time instant, (5-43) is solved and the calculated $u(k)$ are used as control inputs.

The weighting matrix $R \in \mathbb{R}^{6\times 6}$ in (5-43) depends on the turbine operating region given as:

$$R = \begin{cases} diag(1 \quad 0 \quad 0 \quad 0 \quad 1 \quad 0) & region \quad below \quad rated \quad wind \quad speed \\ diag(0 \quad 1 \quad 0 \quad 0 \quad 0 \quad 1) & region \quad above \quad rated \quad wind \quad speed \end{cases} \tag{5-47}$$

By changing the weighting matrix R, different references in $x_r(k)$ are tracked and thus different control goals in the two wind speed regions can be achieved. Therefore, the design of multiple wind turbine controllers for different wind speed regions is greatly simplified using MPC, since it is realized by only changing the weighting matrix.

One reference to be tracked in $x_r(k)$ is $T_{g\_opt}(t) = \dfrac{P_{gr}}{\omega_g(t)\eta_g}$. As discussed in (3-18), tracking $T_{g\_opt}(t)$ is an indirect way to regulate generated power around P_{gr}.

During turbine operation, the range of control inputs is limited by physical constraints imposed by the turbine actuators due to hardware specifications of the hydraulic system and the power converter. Hence, these constraints should be considered in the design of the turbine controller. In the framework of T-S fuzzy MPC, these turbine constraints are considered externally and formulated as the constraints of the quadratic programming problem (5-43) as shown in (5-46). $\beta_{\min}$, $\beta_{\max}$, $\Delta\beta_{\min}$, $\Delta\beta_{\max}$, $T_{\min}$, $T_{\max}$, $\Delta T_{\min}$ and $\Delta T_{\max}$ are the constraints on turbine blade pitch angle and generator torque reference, which is given in Table 3-2。

Equation (5-45) is the T-S fuzzy prediction model derived from the fuzzy wind turbine model in (5-22). (5-43) is now a standard quadratic programming problem at every time instant due to the T-S fuzzy prediction model. Therefore, it can be solved online with mature numerical methods.

(5-44) shows that this is an output feedback control strategy requiring the use of an observer. At each time instant, the system states are estimated by the T-S fuzzy observer with online eigenvalue assignment proposed in Section 5.3.2.

As described in Section 5.2.2, the wind turbine model is linearized according to the variables (v, ω_r, β). Therefore, the membership functions η_k are functions of (v, ω_r, β) and thus can be rewritten as $\eta_k(v(k), \omega_r(k), \beta(k))$. However, it is shown in the turbine model (5-16) that the turbine rotor speed $\omega_r(k)$ is not measured. Therefore, the estimate of $\omega_r(k)$ from the T-S fuzzy observer is used as the premise variable. Meanwhile, the EWS in the premise variables can be obtained by the EWS estimation method proposed in Section 4.3.1 or some other EWS estimation methods (Xin-Fang, Da-Ping and Yi-Bing, 2004; Abo-Khalil and Lee, 2008; Sami and Patton, 2012a).

5.5 Wind turbine FTC for sensor faults

In this Section, a wind turbine AFTC scheme for sensor faults is considered. The sensors considered here are the three output sensors defined in the wind turbine model (5-16). The FDI unit in this scheme is based on a residual generation method. AFTC is achieved by switching to the healthy sensor when the faulty sensor is isolated by the FDI unit. Therefore, hardware redundancy (i.e. redundant sensors) is used in this scheme.

Both the AFTC schemes in Chapter 4 and this Chapter use the idea of combining hardware and analytical redundancies. However, the method in Chapter 4 is only valid for the wind turbine operation in the region below rated wind speed. Hence, the AFTC method proposed in this Section can be seen as an extension to the AFTC approach of Chapter 4 since both operating regions are considered.

5.5.1 FDI of wind turbines using residual generation

A method of FDI by using residuals generated from a bank of fuzzy observers was proposed in (Chen, Lopez-Toribio and Patton, 1999). Each fuzzy observer is based on a reduced number of measurements taken from the system outputs. This method is based on the standard *Generalized Observer* approach (Patton, Frank and Clarke, 1989). A limitation of this method is that each observer based on the reduced number of system outputs must be observable. However, the local models of the T-S fuzzy turbine model in (5-20) are not observable if the number of system outputs are reduced (i.e. using only the output set of (ω_g, β), (ω_g, T_g), or (β, T_g) to design local observers).

In this Section, an FDI approach based on residual generation using the T-S fuzzy observer is proposed. Compared with a similar method proposed in (Chen, Lopez-Toribio and Patton, 1999), this approach uses only one T-S fuzzy observer rather than a bank of observers. The fault is isolated by analyzing the response of the residual to different sensor faults.

The first step of the proposed FDI method makes use of a T-S fuzzy observer along with the measurements to generate the residual signals. The T-S fuzzy observer designed by Algorithm 5-1 for wind turbine system (5-22) is given as follows:

$$\hat{x}(k+1) = G(\eta_k)\hat{x}(k) + H(\eta_k)u(k) + D(\eta_k)v(k) + a(\eta_k) + F[\hat{y}(k) - y(k)] \quad (5\text{-}48)$$

In which $\hat{x}(k)$ are the estimated wind turbine system states.

Once $\hat{x}(k)$ is obtained from (5-48), the sensor faults can then be detected by a residual vector generated from $\hat{x}(k)$ and the sensor outputs as follows:

$$\varepsilon(k) = [r_\omega(k) \quad r_\beta(k) \quad r_T(k)] \quad (5\text{-}49)$$

where

$$r_\omega(k) = \left|\hat{\omega}_g(k) - \omega_g(k)\right|$$

$$r_\beta(k) = \left|\hat{\beta}(k) - \beta(k)\right| \quad (5\text{-}50)$$

$$r_T(k) = \left|\hat{T}_g(k) - T_g(k)\right|$$

$r_\omega(k)$, $r_\beta(k)$ and $r_T(k)$ are residual signals. $\hat{\omega}_g(k)$, $\hat{\beta}(k)$ and $\hat{T}_g(k)$ are the estimated system states from the T-S fuzzy observer.

Theoretically, sensor faults can be detected if the values of the residuals in (5-50) are not zero. However, the values of these residuals are not zero in practice even when there are no sensor faults. This is because of the following three reasons. First of all, there are some uncertain effects including: (1) the estimation error of EWS or error in wind speed sensor measurement (if wind speed sensor is used to obtain wind speed data), (2) the

ignored high order term $\varepsilon(v, \omega_r, \beta)$ in (5-18), and (3) the model mismatch between the T-S fuzzy model and the original nonlinear wind turbine model. Secondly, there is noise in all the three output sensors. Therefore, the residual vector $\varepsilon(k)$ always lies within a threshold ε_r, even when there are no sensor faults. This threshold is used as the fault indicator such that faults are detected when the residual vector $\varepsilon(k)$ exceeds ε_r.

Using a very small value of the threshold ε_r is likely to increase the chance of false alarms. On the other hand, small faults cannot be detected if ε_r is set too large. Therefore, ε_r should be carefully tuned to achieve a trade-off between the chance of false alarms and the detectable level of faults.

Faults can be detected using the residual generation method mentioned above. However, the faulty sensor cannot be isolated. Isolation of faults is realized in the second step of this FDI method, which is a process of analyzing the sensitivity of the residuals to the different faults. It is found out in simulation that the sensitivity of each residual to different sensor faults is different. One residual can be very sensitive to faults in a particular sensor and produce a residual signal with very large magnitude while it may be insensitive to faults in another sensor and produce a subtle residual which is difficult to observe. An FDI logic table for isolating faults can then be obtained from the sensitivity characteristic of different residuals.

The following example is given in order to show the sensitivity characteristic of residual signals. The response of $r_T(k)$ to faults in the generator speed sensor and generator torque sensor is shown in Figure 5-2, using the T-S fuzzy observer proposed in Algorithm 5-1. The faults are applied from 200 seconds to 300 seconds.

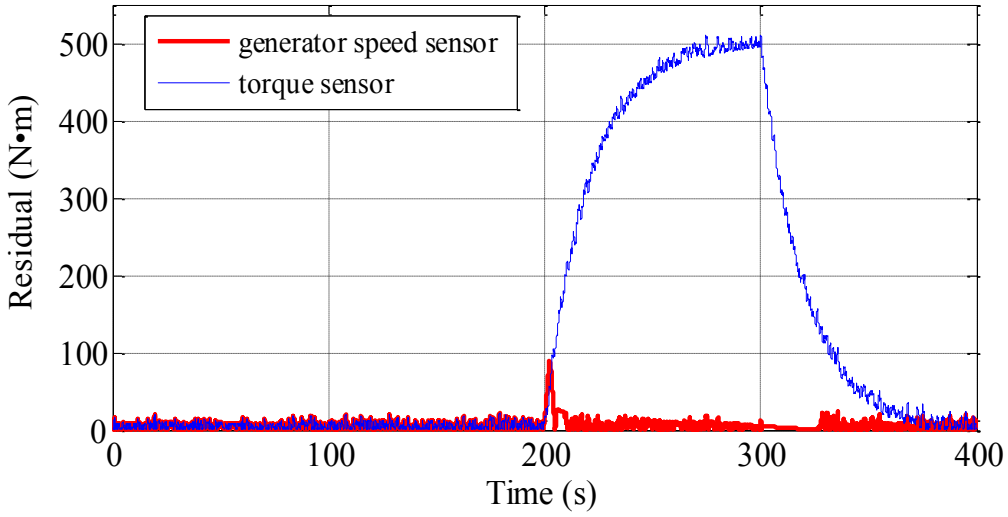

Figure 5-2 Response of $r_T(k)$ to faults in different sensors

The range of the generator speed is 0 to 186 rad/s and the range of the generator torque is 0 to 3.6×10^4 N·m as defined in Table 3-2. In Figure 5-2, only a subtle offset fault of 3.6×10^2 N·m is applied to the generator toque sensor, which is only 1% of the generator torque range. On the other hand, a great offset fault value of 10 rad/s is applied to the generator speed sensor. It is shown in Figure 5-2 that the residual $r_T(k)$ is very sensitive to the generator torque sensor fault and has a large magnitude. However, $r_T(k)$ is not very sensitive to the generator speed sensor fault and thus has a much smaller magnitude.

By analyzing the result in Figure 5-2, two different thresholds r_T^1 and r_T^2 can be set to isolate these two types of sensor faults. r_T^1 is used to isolate generator speed sensor faults while r_T^2 is used to isolate generator torque sensor faults and it is set much larger than r_T^1. The generator speed sensor is faulty if the residual $r_T(k)$ exceeds r_T^1 but below r_T^2.On the other hand, the generator torque sensor is faulty if the residual $r_T(k)$ exceeds r_T^2.

Another example is given here in order to show that the response of the residual signal to some faults is difficult to observe. The response of $r_\beta(k)$ to the generator torque sensor offset fault of 3.6×10^3 N·m is shown in Figure 5-3, using the T-S fuzzy observer

proposed in Algorithm 5-1. The fault is applied from 200s to 300s. It is shown in Figure 5-3 that the residual $r_\beta(k)$ is not sensitive to the generator torque sensor fault and thus it is difficult to observer an obvious residual response to this kind of fault.

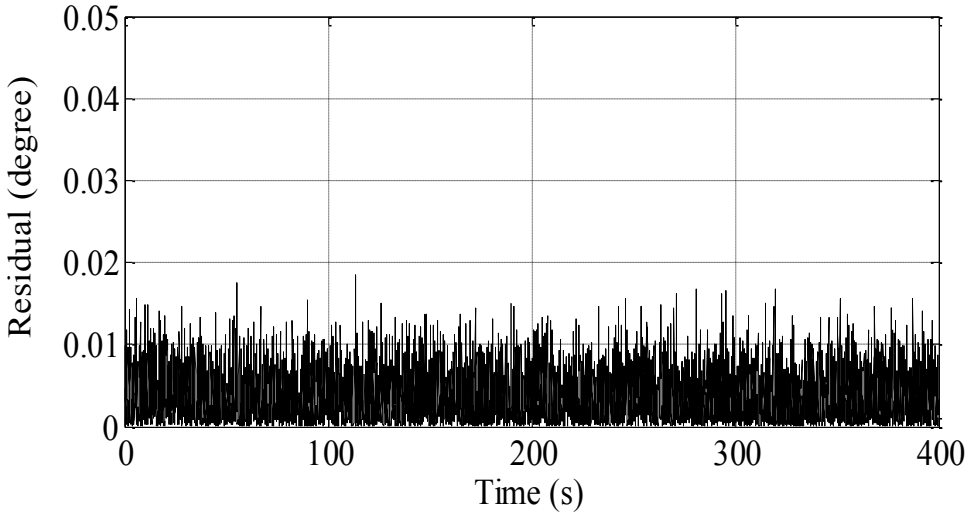

Figure 5-3 Response of $r_\beta(k)$ to faults in generator torque sensor

Figures 5-2 and 5-3 are two examples showing the sensitivity characteristics of the residuals. An FDI logic unit can then be obtained by analyzing this characteristic of all the residuals in the residual vector (5-49) and setting proper thresholds for different residuals. The FDI logic and the responses for detecting faults are given in Table 5-1，in which $r_\omega(k)$ $r_\omega(k)$ of 0.5 rad/s and $r_T(k)$ of 30 N·m correspond to the thresholds for detecting the generator speed sensor fault with the size of 7 rad/s or above and 3 rad/s or above respectively, $r_\beta(k)$ of 0.4 degree corresponds to the threshold for detecting the pitch angle sensor fault with the size of 2 degrees or above, $r_T(k)$ of 500 N·m corresponds to the thresholds for detecting the generator torque sensor fault with the size of 600 N·m or above. "×" means the residual in the corresponding column is not sensitive to the fault in the corresponding row.

Table 5-1 FDI logic

	$r_\omega(k)$	$r_\beta(k)$	$r_T(k)$
Generator speed sensor fault	0.5 rad/s	×	30 N·m
Pitch angle sensor fault	×	0.6 degree	×
Generator torque sensor fault	×	×	500 N·m

It is shown in Table 5-1 that $r_\omega(k)$ is not sensitive to the pitch angle sensor fault and the generator torque sensor fault, and thus only $r_\beta(k)$ and $r_T(k)$ are used to isolate these two faulty sensors. The pitch angle sensor fault can be detected and isolated by $r_\beta(k)$ since neither $r_\omega(k)$ nor $r_T(k)$ is sensitive to faults in the pitch angle sensor. Meanwhile, the generator speed sensor fault can be detected by $r_T(k)$ or $r_\omega(k)$. If only $r_T(k)$ is used, isolation of the generator speed sensor or the generator torque sensor faults can be achieved by setting one threshold r_T^1 for the generator speed sensor faults and a much larger threshold r_T^2 for the generator torque sensor faults as mentioned in the above discussion of Figure 5-2.

5.5.2 FTC of wind turbines using T-S fuzzy MPC and T-S fuzzy observer

Based on the FDI unit designed in Section 5.5.1, an AFTC scheme is designed in this Section for wind turbine sensor faults. Both hardware redundancy (i.e. redundant sensors) and analytical redundancy (i.e. estimation by T-S fuzzy observer) are utilized. The idea of this AFTC scheme comprises the following three steps.

First of all, the T-S fuzzy MPC is used as the baseline controller for the wind turbine in order to deal with the constraints and the turbine nonlinearity due to the larger system operating region (i.e. both the regions below and above rated wind speed) compared with the operating region in Chapter 4.

Secondly, the T-S fuzzy observer with online eigenvalue assignment proposed in Section 5.3.2 is used and serves two purposes: (1) estimating the wind turbine system states and providing this estimation to the T-S fuzzy MPC such that an output feedback control strategy for wind turbine is realized, and (2) generating the residual and use the FDI logic in Table 5-1 to isolate the faulty sensor.

Finally, the controller switches to the healthy redundant sensor for feedback when the faulty sensor is isolated by the FDI unit.

The AFTC scheme for sensor faults is illustrated in Figure 5-4.

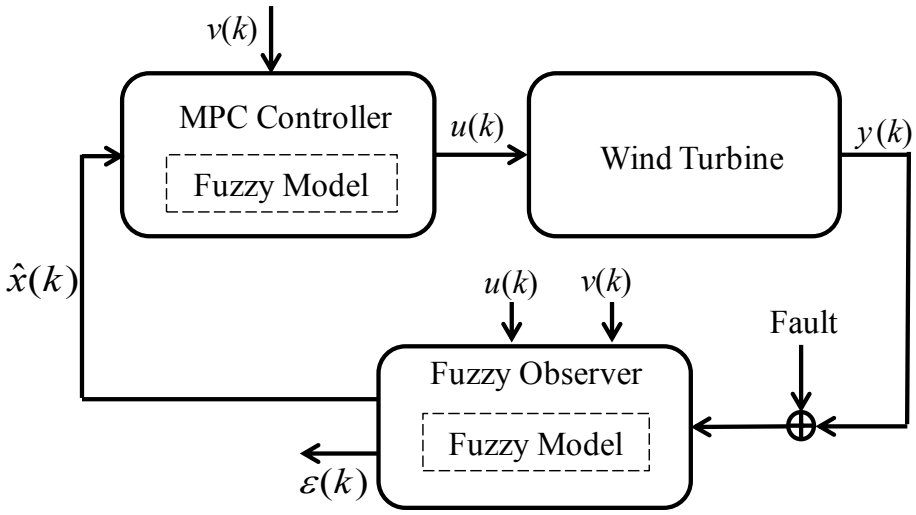

Figure 5-4 AFTC scheme

5.5.3 Simulation study

The AFTC strategy proposed in Section 5.5.2 is simulated and tested on the nonlinear wind turbine model presented in (3-8). Both offset faults and gain factor error faults in the sensors are considered. The sensors used are added with random noise as defined in Table 5-2. The rated generator power and speed are $P_{gr} = 4.8 \times 10^6$ W and $\omega_{gr} = 162$ rad/s.

Table 5-2 Sensor noise

Sensor	Mean value	Variance
Generator speed sensor noise	0	0.05 rad/s
Pitch angle sensor noise	0	0.2 degree/s
Generator torque sensor noise	0	90 N·m

The T-S fuzzy observer used in this simulation is presented in Section 5.3.2. In the FDI unit, the residual thresholds for isolating generator speed and generator torque sensor

faults are chosen as $r_T^1 = 30$ and $r_T^2 = 500$, respectively. The residual thresholds for isolating the pitch angle sensor fault is chosen as $r_\beta = 0.5$.

The turbine T-S fuzzy predictive controller used in the simulation is proposed in Section 5.4.2 with the prediction horizon chosen as $N = 6$. Switching of the weighting matrix in (5-47) is based on the switching criteria presented at the end of Section 3.5.3.

The wind speed data used in simulation cover both operating regions above and below rated wind speed in order to simulate the performance of the proposed AFTC scheme in both wind speed regions. This wind speed data are shown in Figure 5-5.

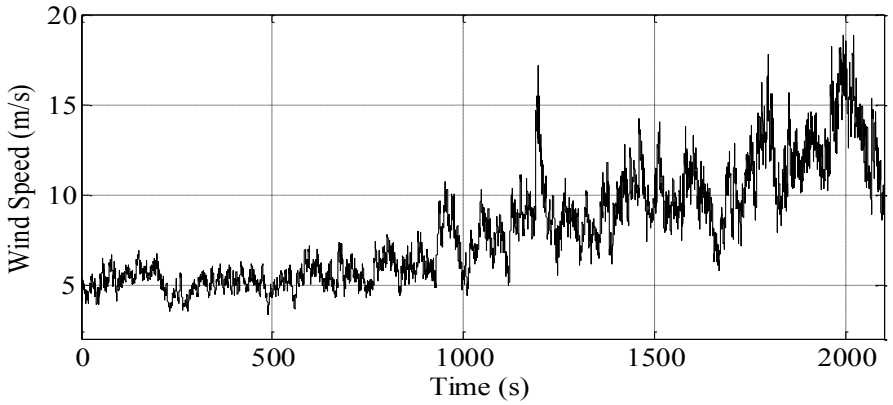

Figure 5-5 Wind speed data

Tracking of the filtered optimal rotor speed using the proposed AFTC in the fault-free case is shown in Figure 5-6. The tracking error is obvious only at peaks of the filtered optimal rotor speed curve. It is shown that the tracking performance in the region below rated wind speed is satisfactory.

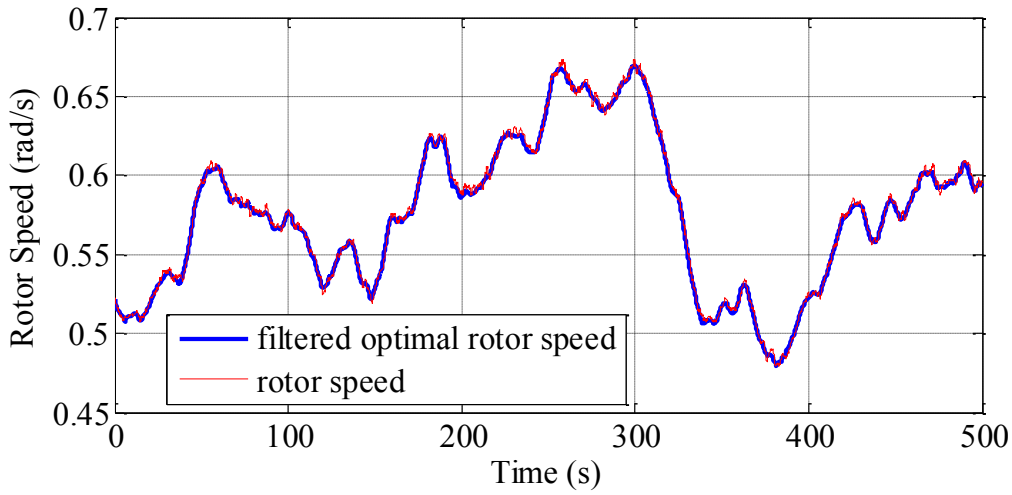

Figure 5-6 Tracking performance in fault-free case

The performance of the generator power and speed regulation in the fault-free case is shown in Figure 5-7 & 5-8. It is shown that the T-S fuzzy predictive controller switches to the generator power and speed regulation when the wind speed is high and the generated power or speed is approaching the rated value. When the wind speed is low and the generated power or speed goes below the rated value, the controller switches to the optimal rotor speed tracking. It is also shown that the controller frequently switches between the two control goals of the generator power/speed regulation and optimal rotor speed tracking around 500s, 600s and 680s since the wind speed after 400s is highly fluctuating.

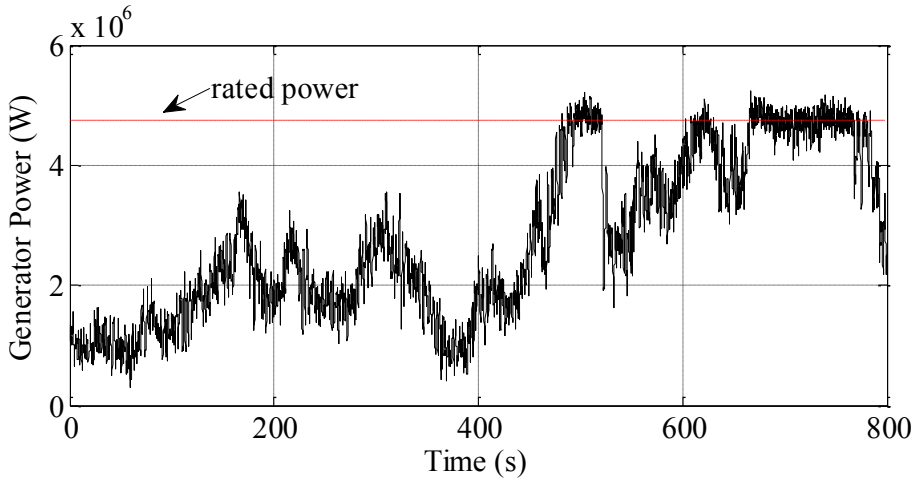

Figure 5-7 Generator power regulation in fault-free case

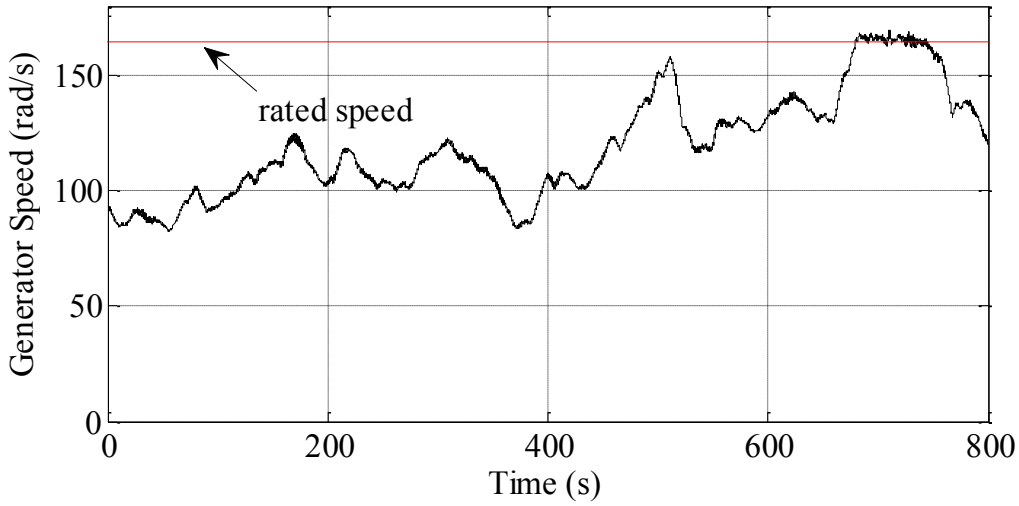

Figure 5-8 Generator speed regulation in fault-free case

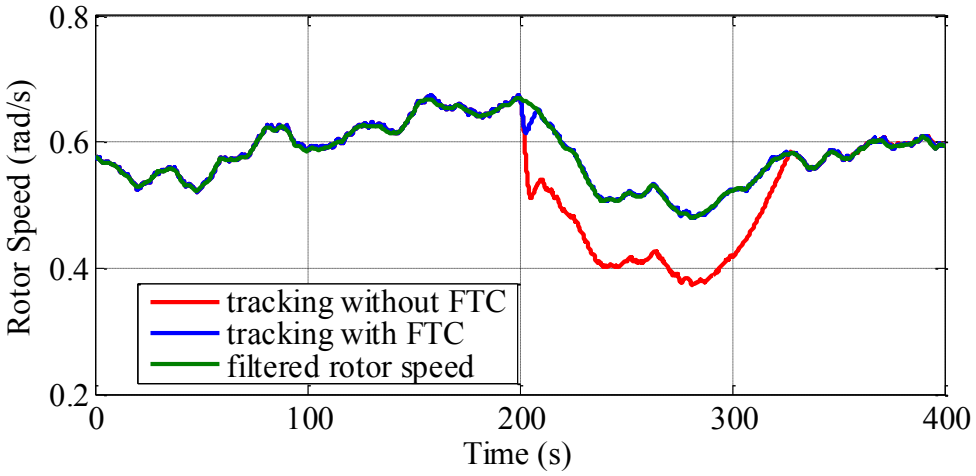

Figure 5-9 Tracking performance in the presence of generator speed sensor fault

Figure 5-9 shows the tracking of filtered optimal rotor speed with and without FTC. A generator speed sensor offset fault of 10 rad/s in the region below rated wind speed is simulated. The proposed AFTC scheme switches to the redundant healthy sensor when the fault is identified by the FDI unit. It is shown in Figure 5-9 that the rotor speed deviates greatly from the reference being tracked (i.e. filtered optimal rotor speed) without FTC.

Figure 5-10 shows the performance of FTC for a 10% gain factor error fault of generator torque sensor. It is shown that the tracking performance is insensitive to the generator torque sensor fault since the tracking error using FTC is only slightly smaller than that without using FTC.

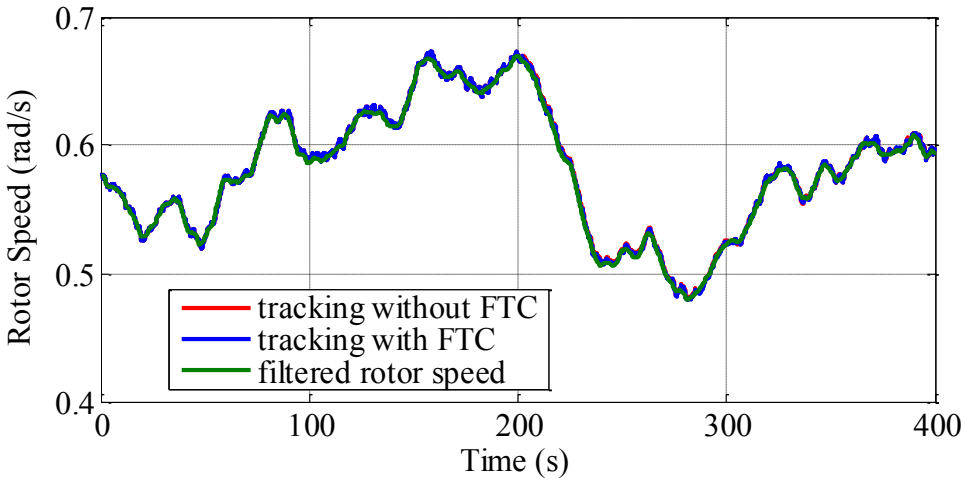

Figure 5-10 Tracking performance in the presence of generator torque sensor fault

Figure 5-11 shows the performance of FTC for a pitch angle sensor offset fault of 5 degree in the region above rated wind speed. The proposed AFTC scheme switches to the redundant healthy sensor when the faulty sensor is identified by FDI unit. As shown in Figure 5-11, the generator power exceeds 110% of P_{gr} without the AFTC action. This occurs at 200 seconds, which is not acceptable for safe operation of the generator.

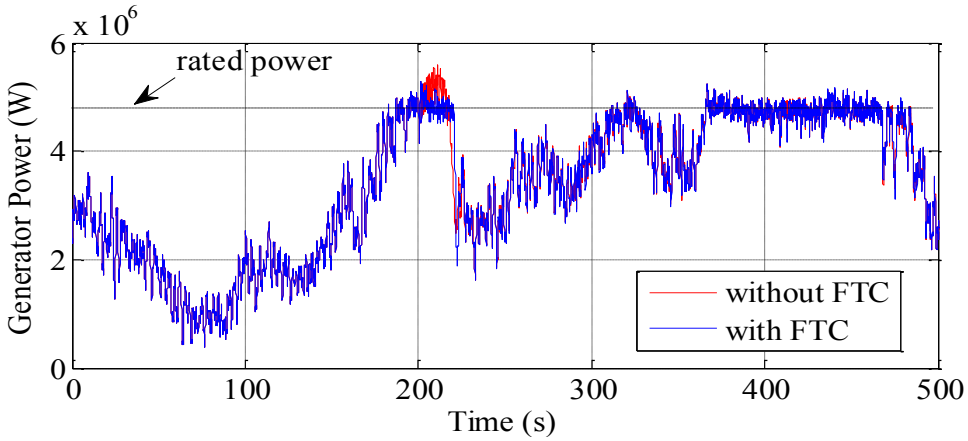

Figure 5-11 Generator power regulation in the presence of pitch angle sensor faults

5.6 Conclusions

In this Chapter, An AFTC strategy based on T-S fuzzy modelling is proposed for a nonlinear wind turbine system. A T-S fuzzy model of the wind turbine is built to approximate the original nonlinear wind turbine system such that controller and FDI designs for the complex nonlinear turbine system can be transformed to that for a linear

time-varying system. Therefore, the controller and FDI designs can be both simplified since they are dealing with an LTV model with regular model structure rather than a highly nonlinear model. The simulation results in Section 5.5.3 demonstrates that T-S fuzzy modelling can be used as a reliable model identification tool for wind turbine systems.

Based on the wind turbine T-S fuzzy model, a new fuzzy observer using online eigenvalue assignment is proposed as both the FDI unit and the state estimator. The proposed fuzzy observer has several advantages over the standard fuzzy observer due to the new feature of online eigenvalue assignment. The residual generated from the fuzzy observer is used to identify faults. Meanwhile, it is shown that fault isolation can be achieved by analyzing the responses of residuals to different faults. Therefore, only one observer rather than an observer bank is needed in this FDI approach.

The AFTC system designed in this Chapter takes into account both wind turbine operating regions and simplify the multiple controller design for the dual control goal problems in wind turbine control. The simulation results show clearly that T-S fuzzy MPC proposed in this Chapter is effective for AFTC of wind turbines.

In Chapter 6, an application scenario in which there is not enough hardware redundancy in the wind turbine systems is considered. Another AFTC scheme for wind turbine sensor faults is proposed for this scenario.

Chapter 6: FTC for wind turbine sensor faults via observers and fuzzy MPC

6.1 Introduction

The AFTC strategy for wind turbines proposed in Chapter 5 requires the use of both analytical and hardware redundancies. This approach is very dependent on the availability of sufficient redundant hardware. There must be sufficient redundant sensors to make this approach feasible. Modern wind turbine systems are equipped with several types of sensors which are arranged in redundancy (Odgaard and Stoustrup, 2012).

However, there may not be enough redundant sensors in the wind turbine system in certain cases. For example, a redundant torque sensor can be utilized for the wind turbine FDI as shown in Chapter 5. However, torque sensors are usually very expensive and difficult to install (Lu, Li, Wu and Yang, 2009; Kalinin, Leigh, Stopps and Artigao, 2013). Therefore, using redundant torque measurements may not be a proper approach in certain cases in which hardware cost and engineering complexity are major concerns.

This Chapter proposes a new AFTC scheme due to the special concerns for wind turbine systems in the case that there is not enough hardware redundancy. This scheme comprises an FDI unit, an FE unit and a baseline controller. The FE unit is designed for both generator subsystem and the pitch subsystem using a descriptor observer approach in order to consider the case that there is only one generator torque sensor in the turbine system. The FDI unit is designed for the drive train subsystem using the approach of residual generation through T-S fuzzy observer with online eigenvalue assignment, as proposed in Chapter 5. In this case the FDI unit still utilizes the available hardware redundancies of other sensors since the redundant generator speed sensor are readily available in a practical wind turbine. The overall wind turbine model presented in Chapter 3 is separated into two subsystems in this Chapter and the FE unit and the FDI unit are designed for each of these two subsystems.

The AFTC scheme proposed in this Chapter is a modification of the scheme proposed in Chapter 5 in order to deal with a specific practical case of the wind turbine system. In Section 6.5.2, it is shown in simulation that the proposed AFTC scheme is able to deal with both the cases of single and multiple sensor faults.

The remainder of this Chapter is organized as follows: Wind turbine modelling of two subsystems is described in Section 6.2. The FE unit for the generator torque sensor fault estimation is proposed in Section 6.3. The FDI for wind turbine sensor faults based on residual generation is shown in Section 6.4. The final AFTC scheme for the wind turbine system that synthesises together the FDI, FE and baseline controller systems is described in Section 6.5. Conclusions are drawn in Section 6.6.

6.2 Wind turbine subsystem modelling

The FDI and FE units described in this Chapter are designed for linear systems and nonlinear systems separately. Therefore, the overall wind turbine model in (3-8) is also divided into a linear submodel and a nonlinear submodel. The first submodel is a combined linear model of the pitch and generator subsystem, based on which an FE unit is designed. The second submodel is the nonlinear drive train model, which is then approximated by the corresponding T-S fuzzy drive train model. An FDI unit for the drive train system is designed based on this fuzzy model. These two submodels are presented in this Section.

6.2.1 Modelling of wind turbine pitch and generator subsystem

Consider the pitch subsystem model in (3-1) and the generator model in (3-2), which for convenience are reproduced here:

$$\frac{\beta(s)}{\beta_r(s)} = \frac{\omega_n^2}{s^2 + 2\zeta\omega_n s + \omega_n^2} \tag{6-1}$$

$$\frac{T_g(s)}{T_{gr}(s)} = \frac{\alpha}{s + \alpha} \tag{6-2}$$

The parameters and variables of (6-1) and (6-2) are defined in Section 3.2. The models in (6-1) and (6-2) can be readily transformed into the LTI state space form as:

$$\dot{x}_\beta = A_\beta x_\beta + B_\beta u_\beta \tag{6-3}$$

$$\dot{x}_g = A_g x_g + B_g u_g \tag{6-4}$$

(6-3) and (6-4) are the state space representations of the original transfer functions (6-1) and (6-2) separately.

The following model for both the pitch and generator subsystems can be obtained by combining (6-3) and (6-4):

$$\begin{aligned} \dot{x}_1 &= A_1 x_1 + B_1 u \\ y_1 &= C_1 x_1 \end{aligned} \tag{6-5}$$

where $\dot{x}_1 = [\dot{\beta} \quad \beta \quad T_g]^{\mathrm{T}}$ and $u = [T_{gr} \quad \beta_r]^{\mathrm{T}}$. The measured outputs of this subsystem is $y_1 = [\beta \quad T_g]$. $A_1 \in \mathbb{R}^{3\times3}$, $B_1 \in \mathbb{R}^{3\times2}$, $C_1 \in \mathbb{R}^{2\times3}$ are the corresponding system matrices as follows:

$$A_1 = \begin{bmatrix} A_\beta & 0 \\ 0 & B_g \end{bmatrix}, \quad B_1 = \begin{bmatrix} B_\beta & 0 \\ 0 & B_g \end{bmatrix} \text{ and } C_1 = \begin{bmatrix} 0 & 1 & 0 \\ 0 & 0 & 1 \end{bmatrix}.$$

The discrete submodel of the pitch and generator subsystems is obtained as follows by discretizing (6-5):

$$\begin{cases} x_1(k+1) = G_1 x_1(k) + H_1 u(k) \\ y_1(k) = C_1 x_1(k) \end{cases} \tag{6-6}$$

where $G_1 \in \mathbb{R}^{3\times3}$, $H_1 \in \mathbb{R}^{3\times2}$, $C_1 \in \mathbb{R}^{2\times3}$ are obtained by discretizing the system matrices in (6-5). $x_1(k) = \left[\dot{\beta}(k) \quad \beta(k) \quad T_g(k)\right]^{\mathrm{T}}$ and $u(k) = [T_{gr}(k) \quad \beta_r(k)]^{\mathrm{T}}$. The outputs of this submodel are $y_1(k) = [\beta(k) \quad T_g(k)]^{\mathrm{T}}$.

It is shown in (6-6) that the combined pitch and generator subsystem are now formulated as a linear system rather than the nonlinear system (3-8), through the model transformation presented above. (6-6) can be seen as a subsystem separated from the original nonlinear wind turbine system (3-8). An advantage of this transformation is that

the FE unit design for the pitch subsystem and the generator subsystem is simplified since it is now based on the linear model (6-6) rather than the nonlinear wind turbine model (3-8).

It is shown in Section 6.3 that a linear descriptor observer is designed for (6-6) to estimate the faults in the generator torque sensor and the pitch angle sensor, making use of the advantage of the above model transformation.

6.2.2 Modelling of drive train subsystem

As discussed in Chapter 3, the nonlinearity in the wind turbine model comes from the aerodynamic model (3-7), which is part of the drive train system model as presented in (3-4). Therefore, the T-S fuzzy modelling method can be applied to the drive train subsystem such that a T-S fuzzy drive train model can be obtained as described below.

Consider the wind turbine drive train and aerodynamic models in (3-4), which are rewritten here for convenience:

$$\begin{bmatrix} \dot{\omega}_r \\ \dot{\omega}_g \\ \dot{\theta}_\Delta \end{bmatrix} = A_{dt} \begin{bmatrix} \omega_r \\ \omega_g \\ \theta_\Delta \end{bmatrix} + B_{dt} \begin{bmatrix} T_a \\ T_g \end{bmatrix}. \tag{6-7}$$

Using the linearization method presented in Section 5.2.2, The aerodynamic torque T_a in (6-7) can be linearized at some operating points $(v_p, \omega_{rp}, \beta_p)$, $p = 1,2,3,....M$ in order to obtain the corresponding linearized aerodynamic model.

Substituting (5-18) into (6-7), the following local drive train models can be acquired:

$$\begin{aligned} \dot{x}_2 &= A_{2p}x_2 + B_{2p}u + E_{2p}d_2 + c_{2p} \\ y_2 &= C_2 x_2 \end{aligned} \tag{6-8}$$

$p = 1,2,3,....M$

in which $A_{2p} \in \mathbb{R}^{3\times3}$, $B_{2p} \in \mathbb{R}^{3\times2}$,and $E_{2p} \in \mathbb{R}^{3\times3}$ are system matrices of the local models. $c_{2p} \in \mathbb{R}^{3\times1}$ are the constant terms arising from the Taylor series expansion

given in (5-18). Also, $x_2 = [\omega_r \quad \omega_g \quad \theta_\Delta]^{\mathrm{T}}$ and $d_2 = [\beta \quad T_g \quad v]^{\mathrm{T}}$. The measured output is the generator speed $y_2 = \omega_g$ and thus $C_2 = [0 \quad 1 \quad 0]$.

The discrete-time local drive train models of the wind turbine system can be obtained by discretizing (6-8), leading to:

$$\begin{aligned} x_2(k+1) &= G_{2p}x_2(k) + H_{2p}u(k) + D_{2p}d_2(k) + a_{2p} \\ y_2 &= C_2x_2 \end{aligned} \tag{6-9}$$

$p = 1,2,3,....M$

in which $G_{2p} \in \mathbb{R}^{3\times3}$, $H_{2p} \in \mathbb{R}^{3\times2}$,and $D_{2p} \in \mathbb{R}^{3\times3}$ and $a_{2p} \in \mathbb{R}^{3\times1}$ are system matrices of the discretized local models. $x_2(k) = [\omega_r(k) \quad \omega_g(k) \quad \theta_\Delta(k)]^{\mathrm{T}}$ and $d_2(k) = [\beta(k) \quad T_g(k) \quad v(k)]^{\mathrm{T}}$.

From (6-9) and the linearization operating points $(v_p, \omega_{rp}, \beta_p)$, $p = 1,2,3,....M$, the T-S fuzzy rules of the discrete-time drive train system are obtained as follows:

Rule p: *If* $v(k) = v_p$, $\omega_r(k) = \omega_{rp}$ and $\beta(k) = \beta_p$

$$\text{Then} \quad \begin{aligned} x_2(k+1) &= G_{2p}x_2(k) + H_{2p}u(k) + D_{2p}d_2(k) + a_{2p} \\ y_2 &= C_2x_2 \end{aligned} \tag{6-10}$$

$p = 1,2,3,....M$

Using the fuzzy rules (6-10) and the fuzzy inference method presented in Section 5.2.1, the T-S fuzzy drive train submodel can then be obtained as follows:

$$\begin{aligned} x_2(k+1) &= G_2(\eta_k)x_2(k) + H_2(\eta_k)u(k) + D_2(\eta_k)d_2(k) + a(\eta_k) \\ y_2(k) &= C_2x_2(k) \end{aligned} \tag{6-11}$$

In which η_k are the membership functions, which are a function of the premise variables used for linearization and thus can also be written as $\eta_k(v(k), \omega_r(k), \beta(k))$.

6.3 FE of wind turbine sensor faults via descriptor observer

A method of simultaneous estimation of sensor faults and system states was proposed in (Gao and Ho, 2004), which is an effective approach for FE of sensor faults. This approach is realized in the framework of a continuous descriptor system. The idea of multiple integrals is used in this approach to estimate states and a class of unbounded output disturbances or faults. However, the estimation performance is not satisfactory if the faults or disturbances to be estimated are bounded high frequency signals. Meanwhile, an assumption of this approach is that the measurement noise should have the same form as the input disturbance, which is not practical in some cases.

A modified descriptor observer design based on the above approach is presented in (Gao and Wang, 2006) for continuous systems. In this modified approach, the derivative of the output signal is avoided by introducing a derivative gain. Although this observer is in the form of a descriptor system, it is designed for non-descriptor systems. In this approach, a non-descriptor system is transformed into a descriptor system. This transformation results in several advantages. First of all, if the system is stable, this observer can completely decouple the sensor faults from sensor signals and achieve accurate estimation of system states and sensor faults. Secondly, the fault to be estimated can even be unbounded using this approach.

In this Section, a descriptor observer approach for wind turbine sensor fault estimation is proposed such that system states and sensor faults can be estimated simultaneously. This approach is based on the modified descriptor observer mentioned above and extended for the discrete-time system case. It will be shown that sensor faults can be decoupled from the sensor outputs using this approach.

6.3.1 Descriptor observer formulation

The principle and design procedure of a descriptor observer for discrete-time systems is presented in this Section. The system with sensor faults considered here is given by:

$$x(k+1) = Gx(k) + Hu(k) \tag{6-12}$$

$$y(k) = Cx(k) + f(k) \tag{6-13}$$

in which $x(k) \in \mathbb{R}^n$ is the state vector, $u(k) \in \mathbb{R}^l$ is the input vector and $y(k) \in \mathbb{R}^m$ are the measured outputs. $f(k) \in \mathbb{R}^m$ is the sensor fault vector. G, H and C are system matrices with proper dimensions.

An augmented descriptor system can be constructed from (6-12) and (6-13) as follows:

$$\overline{E}\overline{x}(k+1) = \overline{G}\overline{x}(k) + \overline{H}u(k) + \overline{N}f(k) \tag{6-14}$$

$$y(k) = \overline{C}\overline{x}(k) = C_0\overline{x}(k) + f(k) \tag{6-15}$$

in which

$$\overline{x}(k) = \begin{bmatrix} x(k) \\ f(k) \end{bmatrix} \qquad \overline{E} = \begin{bmatrix} I_n & 0 \\ 0 & 0 \end{bmatrix}$$

$$\overline{G} = \begin{bmatrix} G & 0 \\ 0 & -I_m \end{bmatrix} \qquad \overline{H} = \begin{bmatrix} H \\ 0 \end{bmatrix}$$

$$\overline{N} = \begin{bmatrix} 0 \\ I_m \end{bmatrix} \qquad \overline{C} = \begin{bmatrix} C & I_m \end{bmatrix} \qquad C_0 = \begin{bmatrix} C & 0 \end{bmatrix}$$

(6-14) is known as a *descriptor system* due to the matrix $\overline{E}$ appearing in the left side of the state space model. The descriptor observer for the augmented discrete-time system (6-14) and (6-15) is given as follows:

$$E_n\xi(k+1) = G_n\xi(k) + \overline{H}u(k) \tag{6-16}$$

$$\hat{\overline{x}}(k) = \xi(k) + K_n y(k) \tag{6-17}$$

In which $\xi(k) \in \mathbb{R}^{n+m}$ is the states of the descriptor observer, $\hat{\overline{x}}(k)$ is the estimation of $\overline{x}(k)$. $E_n \in \mathbb{R}^{(n+m)\times(n+m)}$, $G_n \in \mathbb{R}^{(n+m)\times(n+m)}$ and $K_n \in \mathbb{R}^{(n+m)\times m}$ are parameters to be designed.

By substituting (6-15) into (6-17), the following equation can be obtained:

$$\xi(k) = \hat{\bar{x}}(k) - K_n C_0 \bar{x}(k) - K_n f(k) \tag{6-18}$$

By substituting (6-15) and (6-18) into (6-16), the following equation is obtained:

$$\begin{aligned} E_n \hat{\bar{x}}(k+1) - E_n K_n \bar{C} \bar{x}(k+1) = \\ G_n[\hat{\bar{x}}(k) - K_n C_0 \bar{x}(k) - K_n f(k)] + \bar{H} u(k) \end{aligned} \tag{6-19}$$

By subtracting (6-19) from (6-14), the following equation can be obtained:

$$\begin{aligned} (\bar{E} + E_n K_n \bar{C}) \bar{x}(k+1) - E_n \hat{\bar{x}}(k+1) = \\ (\bar{G} + G_n K_n C_0) \bar{x}(k) - G_n \hat{\bar{x}}(k) + \bar{N} f(k) + G_n K_n f(k) \end{aligned} \tag{6-20}$$

Define the estimation error as:

$$\bar{e}(k) = \bar{x}(k) - \hat{\bar{x}}(k) \tag{6-21}$$

If the following matrix equations are satisfied:

$$\bar{E} + E_n K_n \bar{C} = E_n \tag{6-22}$$

$$\bar{G} + G_n K_n C_0 = G_n \tag{6-23}$$

$$\bar{N} + G_n K_n = 0 \tag{6-24}$$

Then the following estimation error dynamics can be obtained by substituting (6-21), (6-22), (6-23) and (6-24) into (6-20):

$$E_n \bar{e}(k+1) = G_n \bar{e}(k) \tag{6-25}$$

E_n, G_n and K_n can be computed from the matrix equations (6-22) to (6-24) and given as:

$$\begin{cases} G_n = \begin{bmatrix} G & o \\ -C & -I_p \end{bmatrix} \\ K_n = \begin{bmatrix} 0 \\ I_p \end{bmatrix} \\ E_n = \begin{bmatrix} I & 0 \\ MC & M \end{bmatrix} \end{cases} \tag{6-26}$$

where $M \in \mathbb{R}^{m \times m}$ is a full rank matrix which is a parameter to be designed.

By substituting (6-26) into (6-25), the following error dynamics are obtained:

$$\begin{bmatrix} I & 0 \\ MC & M \end{bmatrix} \bar{e}(k+1) = \begin{bmatrix} G & o \\ -C & -I_p \end{bmatrix} \bar{e}(k) \tag{6-27}$$

(6-27) can be transformed into:

$$\begin{aligned} \bar{e}(k+1) &= \begin{bmatrix} I & 0 \\ MC & M \end{bmatrix}^{-1} \begin{bmatrix} G & o \\ -C & -I_p \end{bmatrix} \bar{e}(k) \\ &= \begin{bmatrix} G & 0 \\ -CG - M^{-1}C & -M^{-1} \end{bmatrix} \bar{e}(k) \end{aligned} \tag{6-28}$$

When G and $-M^{-1}$ in (6-28) are stable matrices, $\lim_{k \to \infty} \bar{e}(k) = 0$ and thus simultaneous estimation of system states and sensor faults can be achieved. Therefore, a requirement for using the descriptor observer proposed in this Section is that the system (6-12) and (6-13) should be stable.

It is shown from the observer design procedure that the descriptor observer is designed for the descriptor system (6-14) and (6-15). However, (6-14) to (6-15) are only a reformulation of the original non-descriptor system (6-12) and (6-13). Therefore, this observer is actually designed for non-descriptor systems.

Remark 6-1: It can be seen from the design procedure of this observer that the sensor fault $f(k)$ in (6-13) is naturally decoupled from the sensor outputs. Thus sensor fault compensation is not needed if this descriptor observer is used in an AFTC scheme.

6.3.2 Descriptor observer for FE of wind turbine sensor faults

As mentioned in Section 6.1, the situation when there is no redundant generator torque sensor is considered in this Chapter. The absence of the redundant torque sensor means that only analytical redundancy-based methods can be utilized. The descriptor observer approach described in Section 6.3.1 uses only analytical redundancy since faults are estimated using the system model and thus no other redundant generator torque sensor is required. On the other hand, the pitch and generator subsystem in (6-6) satisfies two requirements of using this descriptor observer approach: (1) (6-6) is a linear system and (2) the system matrix G_1 in (6-6) is a stable matrix using the wind turbine model parameter given in Table 3-1.Therefore, this descriptor observer can be used as a FE unit for faults in the generator torque sensor and pitch angle sensor. The design of this FE unit is described below.

First of all, the wind turbine submodel (6-6) with the inclusion of sensor faults is given as:

$$\begin{aligned} x_1(k+1) &= G_1 x_1(k) + H_1 u_1(k) \\ y_1(k) &= C_1 x_1(k) + f_1 \end{aligned} \tag{6-29}$$

in which $f_1 \in \mathbb{R}^{2\times 1}$ represents sensor faults in both generator torque and pitch angle sensors.

To estimate both system states and faults, the following augmented model can then be obtained from (6-29):

$$\begin{aligned} \overline{E}\overline{x}_1(k+1) &= \overline{G}_1\overline{x}_1(k) + \overline{H}_1 u(k) + \overline{N} f(k) \\ y_1(k) &= \overline{C}_1\overline{x}_1(k) = C_1^0\overline{x}_1(k) + f(k) \end{aligned} \tag{6-30}$$

in which

$$\bar{x}_1(k) = \begin{bmatrix} x_1(k) \\ f(k) \end{bmatrix}, \quad \overline{E} = \begin{bmatrix} I_3 & 0 \\ 0 & 0 \end{bmatrix},$$

$$\overline{G}_1 = \begin{bmatrix} G_1 & 0 \\ 0 & -I_2 \end{bmatrix}, \quad \overline{N} = \begin{bmatrix} 0 \\ I_{2\times 2} \end{bmatrix},$$

$$\overline{H}_1 = \begin{bmatrix} H_1 \\ 0 \end{bmatrix} \quad \overline{C}_1 = [C_1 \quad I_{2\times 2}],$$

$$C_1^0 = [C_1 \quad 0]$$

Based on (6-30), the following FE unit for the system (6-29) can be obtained:

$$\begin{aligned} E_n\zeta(k+1) &= G_{1n}\zeta(k) + \overline{H}_1 u(k) \\ \hat{\bar{x}}_1(k) &= \zeta(k) + K_n y_1(k) \end{aligned} \tag{6-31}$$

where $\varsigma(k) \in \Re^{5\times 1}$. $\hat{\bar{x}}_1(k) = \left[\hat{x}_1(k) \quad \hat{f}(k)\right]^{\mathrm{T}}$ is the estimate of $\bar{x}_1(k)$. $E_n \in \Re^{5\times 5}$, $G_{1n} \in \Re^{5\times 5}$ and $K_n \in \Re^{5\times 2}$ can be calculated using the method in Section 6.3.1.

6.4 FDI for wind turbine sensor faults via T-S fuzzy observer

In practice, the redundant generator speed sensor is readily available in a wind turbine system. This is therefore a form of hardware redundancy and is now used in the AFTC scheme to deal with the generator speed sensor faults. Hence, the principle of this AFTC strategy is to design an FDI unit to isolate the faulty generator speed sensor so that the controller can switch to the healthy sensor to obtain feedback.

In this Section, the idea of residual-based FDI proposed in Section 5.5.1 is used as the FDI unit for the generator speed senor faults. The T-S fuzzy model of the drive train system shown in Section 6.2.2 is used in this FDI unit due to the nonlinearity in the drive train system. Based on this T-S fuzzy model, a T-S fuzzy observer with online eigenvalue assignment is used for two purposes: (1) estimate the system states of the drive train system and provide these estimated states to the wind turbine controller such

that an output feedback control strategy is achieved, and (2) generate the residual using the estimated generator speed in order to detect and isolate generator speed sensor faults.

6.4.1 Design of FDI unit for wind turbine sensor faults

The T-S fuzzy observer with online eigenvalue assignment presented in Section 5.3.2 is used to design the driver train system observer which is based on the T-S fuzzy driver train system model (6-11). This observer is given as follows:

$$\begin{aligned}\hat{x}_2(k+1) &= G_2(\eta_k)\hat{x}_2(k) + H_2(\eta_k)u(k) \\ &\quad + F_2[y_2(k) - \hat{y}_2(k)] + D_2(\eta_k)d_2(k) + a(\eta) \\ \hat{y}_2(k) &= C_2\hat{x}_2(k)\end{aligned} \tag{6-32}$$

where $\hat{x}_2(k) = [\hat{\omega}_r(k) \quad \hat{\omega}_g(k) \quad \hat{\theta}_\Delta(k)]^{\mathrm{T}}$ is the estimated state vector. $F_2 \in \Re^{3\times 1}$ is the fuzzy observer gain which is calculated using Algorithm 5-1.

Generator speed sensor faults can be detected by comparing the signals from the sensor in use and the corresponding redundant sensor. However, it is difficult to isolate the faulty sensor without an FDI unit. The faulty generator speed sensor can be isolated by an FDI residual signal generated from the generator speed sensor output and the T-S fuzzy observer (6-32) as follows:

$$\varepsilon(k) = \left|\hat{\omega}_g(k) - \omega_g(k)\right| \tag{6-33}$$

In practice, $\varepsilon(k)$ lies within a threshold due to sensor noise，EWS estimation error, and model mismatch between the T-S fuzzy drive train submodel (6-11) and the original nonlinear drive train submodel (6-7). The value of $\varepsilon(k)$ will exceed the threshold when the generator speed sensor fault is present and thus the FDI scheme is based on the following logic:

$$\begin{aligned}&\varepsilon(k) \le \varepsilon_r \quad sensor \;\; is \;\; healthy \\ &\varepsilon(k) \ge \varepsilon_r \quad sensor \;\; is \;\; faulty\end{aligned} \tag{6-34}$$

Remark 6-2: It should be noted that either the disturbance term $d_2(k) = [\beta(k) \quad T_g(k) \quad v(k)]^{\mathrm{T}}$ in (6-32) or the membership functions $\eta_k(v(k), \omega_r(k), \beta(k))$ contain $\beta(k)$ and $T_g(k)$ which are the state variables not included in the drive train system. In the design of the above T-S fuzzy observer, $\beta(k)$ and $T_g(k)$ are provided by the estimation from the descriptor observer in Section 6.3.2. Therefore, the disturbance term and the membership function used in the above T-S fuzzy observer are actually $d_2(k) = [\hat{\beta}(k) \quad \hat{T}_g(k) \quad v(k)]^{\mathrm{T}}$ and $\eta_k(v(k), \omega_r(k), \hat{\beta}(k))$.

6.4.2 Simulation Study

The performance of the FDI unit for the drive train system is illustrated by simulation in Figure 6-1. The fault is a 10 rad/s offset fault in the generator speed sensor applied from 30s to 40s. The threshold is set as $\varepsilon_r = 0.75$ and the sampling time is 0.25s.

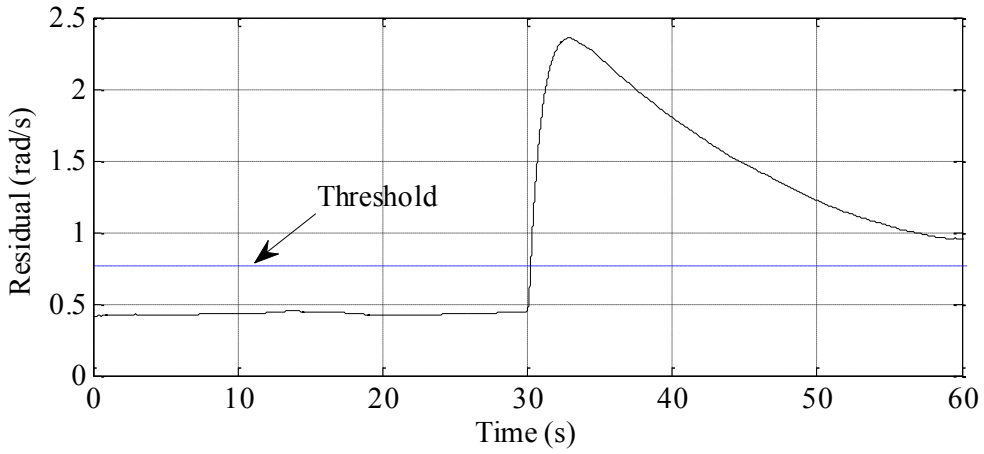

Figure 6-1 FDI for generator speed sensor fault

It is shown in simulation that the fault can be detected within 3 time instants.

6.5 AFTC for wind turbine sensor faults

Based on the FDI and FE unit in this Chapter, an AFTC scheme can be designed for wind turbine sensor faults. AFTC for generator speed sensor faults is achieved by switching to the healthy redundant sensor when the faulty sensor is isolated by the FDI unit. As for the pitch angle sensor and the generator torque sensor faults, the descriptor

observer proposed in Section 6.3.2 naturally decouples faults from the outputs of these two sensors.

The T-S fuzzy MPC for wind turbine systems proposed in Section 5.4.2 is used in this AFTC scheme and serves as the baseline controller. Therefore, the wind turbine system constraints and the nonlinearity effect are still considered in this AFTC scheme. Furthermore, both cases of single and multiple sensor faults can be dealt with in this scheme.

6.5.1 Design of AFTC system for wind turbine sensor faults

The proposed AFTC scheme is shown in Figure 6-2.

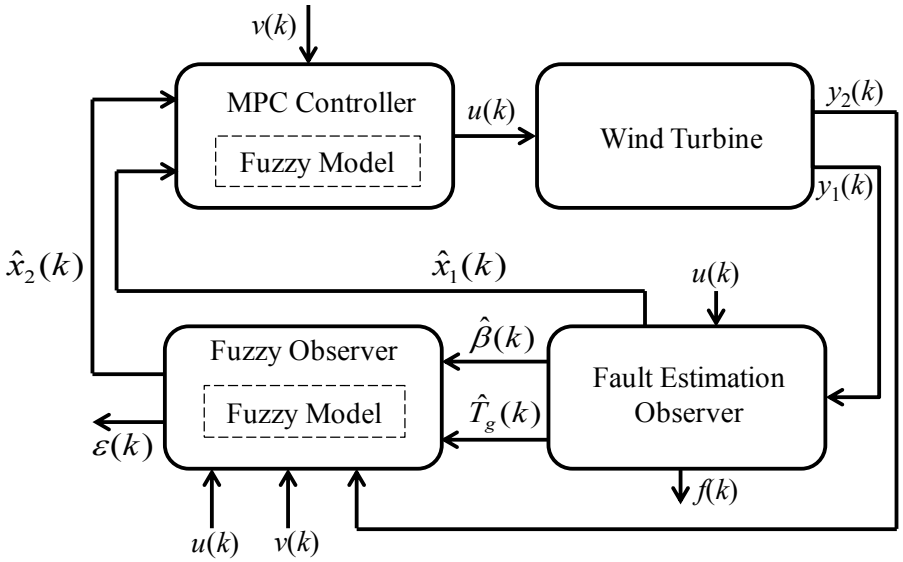

Figure 6-2 AFTC scheme

The wind turbine outputs are divided into two sets: (1) outputs from the pitch angle and generator torque sensors (i.e. $y_1(k)$) and (2) output from the generator speed sensor (i.e. $y_2(k)$). Theses two sets of outputs are used by different observers for either FDI or FE. The estimated $\hat{\beta}(k)$ and $\hat{T}_g(k)$ from the descriptor observer is used by the fuzzy observer for building the membership function η_k and the known disturbance term $d_2(k)$ in (6-11).

Once again, it is assumed that the wind speed is known, which can be obtained using the estimation method presented in Section 4.3.1 or the measurement from the wind speed sensor.

It should be noted that the fuzzy model in the fuzzy observer is based on the submodel of the drivetrain system presented in (6-11). On the other hand, the fuzzy model used by the T-S fuzzy predictive controller is the overall T-S fuzzy wind turbine in (5-22).

6.5.2 Simulation study

The AFTC strategy proposed in Section 6.5.1 is simulated and tested on the nonlinear wind turbine model presented in (3-8). Both offset faults and gain factor error faults in the sensors are considered. The sensors outputs include random measurement noise. The noise level is presented in Table 5-2. The rated generator power and generator speed are $P_{gr} = 4.8 \times 10^6$ W and $\omega_{gr} = 162$ rad/s.

The baseline turbine T-S fuzzy predictive controller used in the simulation is the one proposed in Section 5.4.2 with the prediction horizon chosen as $N = 6$. Switching of the weighting matrix in (5-47) is based on the switching criteria presented at the end of Section 3.5.3.

The wind speed data used for simulation are shown in Figure 5-5. The pitch angle sensor fault estimation performance using the descriptor observer approach is shown in Figures 6-3 and the generator torque sensor fault estimation performance is shown in Figure 6-4. A 10 degree offset fault in the pitch angle sensor and a 10% gain factor error fault in the torque sensor are simulated. These two types of fault are applied to the sensor after 30 seconds. It is shown in Figure 6-3 and Figure 6-4 that the estimation performance for faults in both sensors is satisfactory.

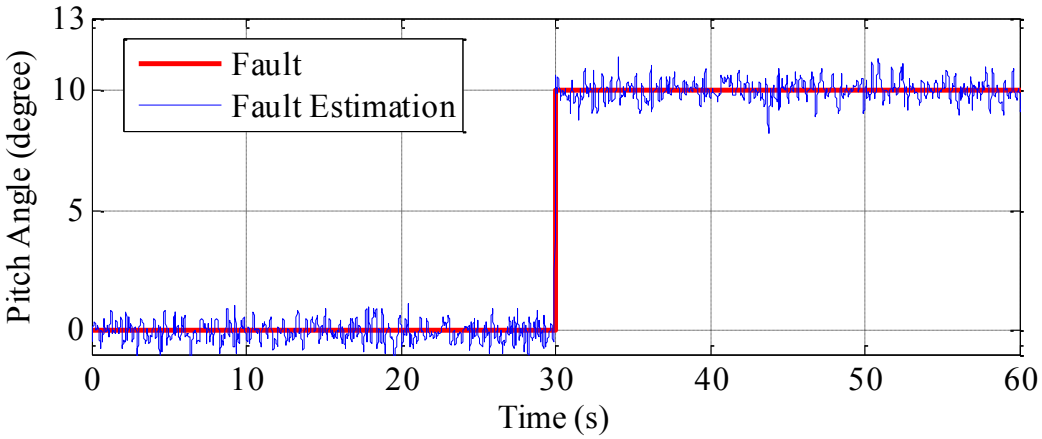

Figure 6-3 FE for pitch angle sensor fault

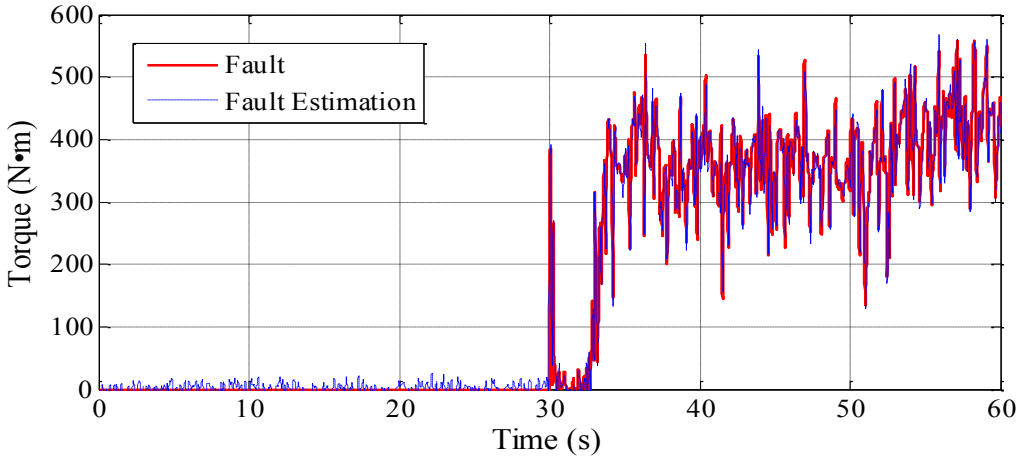

Figure 6-4 FE for generator torque sensor fault

The optimal rotor speed tracking performance for the fault-free case using the proposed AFTC scheme is shown in Figure 6-5. Once again, the reference to be tracked is the filtered optimal rotor speed to avoid heavy drive train torsion.

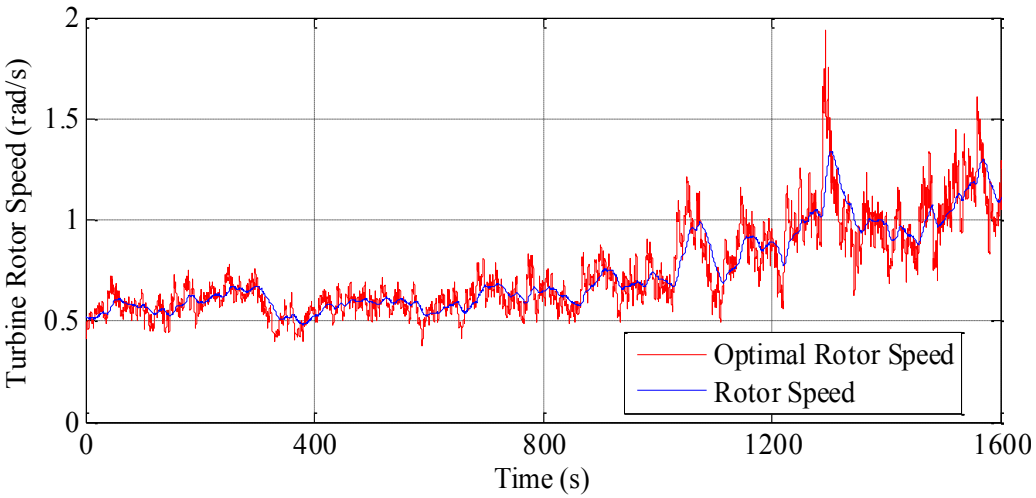

Figure 6-5 Optimal rotor speed tracking in fault-free case

The performance of the power generation for the fault-free case using the proposed AFTC scheme is shown in Figure 6-6. The power is clearly regulated around the rated value $P_{gr} = 4.8 \times 10^6$ MW when wind speed is high.

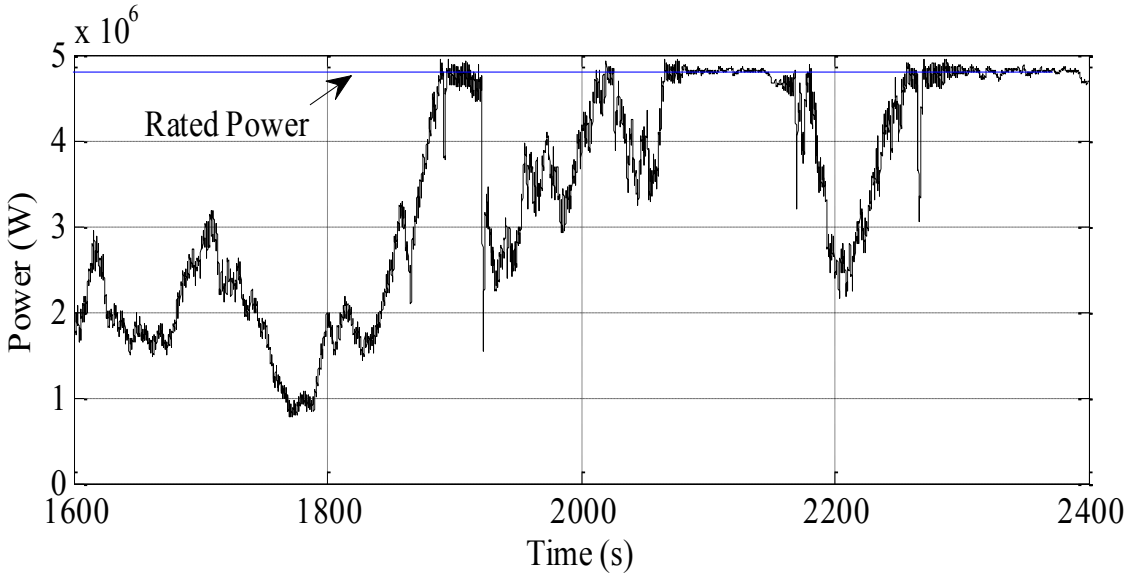

Figure 6-6 Power regulation in fault-free case

The performance of the regulated generator speed for the fault-free case using the proposed AFTC scheme is shown in Figure 6-7. The generator speed is regulated around the rated value $\omega_{gr} = 162$ rad/s when the wind speed is high. The small error in tracking the reference speed is probably due to the following two reasons: (1) There is model mismatch between the original nonlinear wind turbine model and its corresponding T-S fuzzy model. (2) The wind speed is highly fluctuating and thus the controller frequently switches between the two control goals. Therefore it is difficult to regulate the generator speed around the rated values perfectly.

The performance of this AFTC strategy for the wind turbine operating in the region below rated wind speed is shown in Figure 6-8. The most severe case of all sensors becoming faulty simultaneously is simulated. Simultaneous faults involved in this scenario are: (1) a 10% gain factor error in the generator torque sensor, and (2) a 10 degree offset fault in the pitch angle sensor, and (3) a 10 rad/s offset fault in the

generator speed sensor. For comparison purposes, the performance of the baseline controller without using the AFTC scheme is also presented. It is shown that the rotor speed loses the reference signal (i.e. optimal rotor speed) without the proposed AFTC.

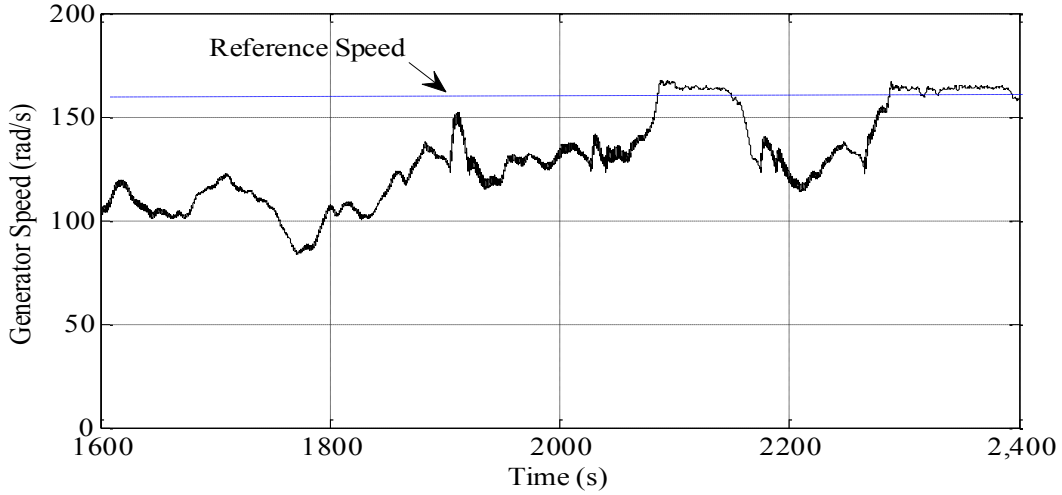

Figure 6-7 Generator speed regulation in fault-free case

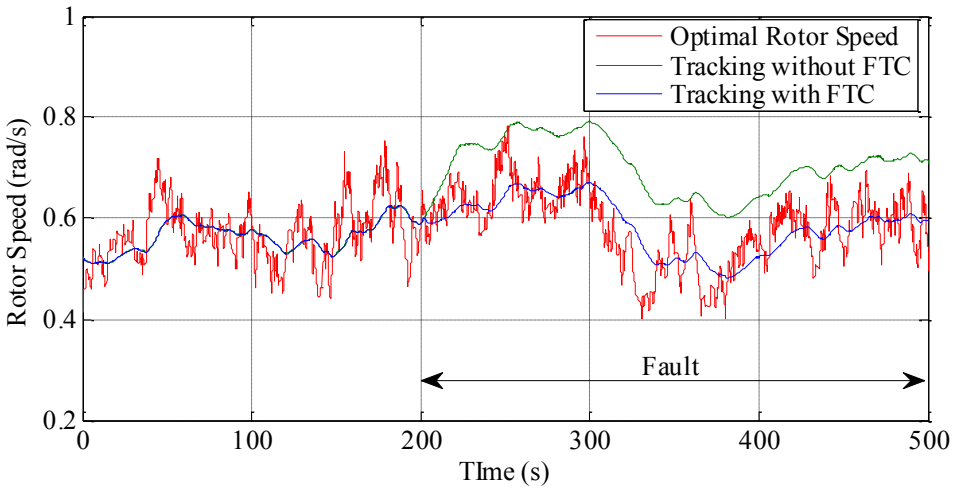

Figure 6-8 Optimal rotor speed tracking in the presence of sensor faults

The power regulation performance of the proposed AFTC strategy for wind turbine operating in the region above rated wind speed is shown in Figures 6-9. Once again, the worst case in which all sensors become faulty is considered. It is also shown that the generator power can still be kept around the rated power in such an extreme case with the proposed AFTC strategy. Hence, safe operation of the generator at high wind speed can be guaranteed by using this AFTC scheme. Without the AFTC scheme, the

generator power exceeds the rated power greatly and thus will either destroy the generator or result in an emergency shutdown.

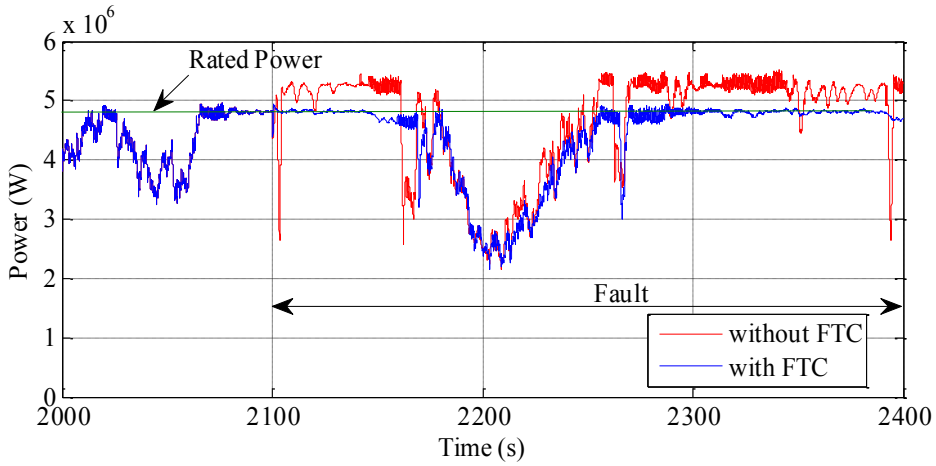

Figure 6-9 Power regulation in the presence of sensor faults

6.6 Conclusions

In this Chapter, the wind turbine system is separated into two subsystems such that an FE unit and an FDI unit can be designed for each subsystem separately. The FE unit is designed for the subsystem without enough redundant sensors while the FDI unit is designed for the subsystem with enough redundant sensors.

The proposed FE unit is based on a descriptor observer approach in which the faults and system states can be estimated simultaneously. An advantage of this approach is that the fault signal is naturally decoupled from the sensor measurement. The proposed FDI unit is based on the residual generation method using the T-S fuzzy observer proposed in Section 5.5.1.

Based on the FDI unit and FE unit, an AFTC scheme is proposed for wind turbine sensor faults. The performance of this AFTC in faulty and fault-free cases is tested through simulation with results showing the strong AFTC features of this system in terms of fault-tolerance and satisfactory control performance.

In Chapter 7, an AFTC approach using moving horizon estimation (MHE) based on T-S fuzzy modelling for wind turbine actuator faults is presented. The T-S fuzzy observer with online eigenvalue assignment proposed in Chapter 4 is utilized in this AFTC scheme. Another T-S fuzzy MPC method is also proposed in this scheme. This method

is different from the T-S fuzzy MPC approaches used in Chapter 5 and Chapter 6 since fault compensation can be achieved in this method while the fuzzy MPC in Chapter 5 and Chapter 6 are only used as the baseline controller in the AFTC schemes. Therefore, the new T-S fuzzy MPC with the ability of fault compensation is an extension to the standard T-S fuzzy MPC method used in Chapter 5 and 6.

Chapter 7: FTC for wind turbine actuator faults based on fuzzy MHE

7.1 Introduction

The actuator faults in a wind turbine can also severely affect the wind turbine system performance like sensor faults do. Therefore, several approaches have been proposed for wind turbine actuator faults (Sloth, Esbensen and Stoustrup, 2010; Soliman, Malik and Westwick, 2012; Badihi, Zhang and Hong, 2014). In the above approaches, wind turbine systems are modelled using the following techniques: (1) LPV modelling, (2) subspace identification based modelling and (3) T-S fuzzy modelling. Therefore, a key idea of dealing with wind turbine actuator faults is to transform the original nonlinear wind turbine model into other forms of model with simpler and regular structure. This is because it is difficult to deal with the actuator faults using the original highly nonlinear wind turbine model.

Based on the above ideas of model simplification, an AFTC scheme for wind turbine actuator faults is presented in this Chapter. This scheme comprises an FE unit and a fault tolerant controller. A novel approach of T-S fuzzy MHE is proposed as the FE unit for estimating actuator faults. T-S fuzzy modelling is used in this approach to transform the nonlinear wind turbine fault model into a simple LTV model to facilitate FE. Meanwhile, a fault tolerant controller based on T-S fuzzy MPC is proposed as the wind turbine controller. Fault tolerance is achieved by considering the estimated faults in the prediction model and compensating these faults with T-S fuzzy MPC.

This Chapter extends the T-S fuzzy MPC approach used in Chapters 5 and 6, which has been used only to design a baseline controller without considering faults. However, that approach is modified in this Chapter to propose another T-S fuzzy predictive controller, which is used as both a fault compensator and a wind turbine controller rather than just a baseline controller.

The remainder of this Chapter is organized as follows: The moving horizon estimation for FE of wind turbine actuator faults is proposed in Section 7.2. Actuator fault

compensation using the T-S fuzzy MPC is presented in Section 7.3. The AFTC scheme for wind turbine actuator faults and the simulation results are also described in Section 7.3. Conclusions are drawn in Section 7.4.

7.2 MHE for actuator fault estimation in wind turbine systems

MHE was proposed as a tool for estimating system states (Allgöwer et al., 1999; Rao and Rawlings, 2002; Rao, Rawlings and Mayne, 2003). It is considered as a dual problem of MPC since it involves the on-line solution of an optimization problem over a horizon in the past while MPC involves online solving a similar optimization problem over a horizon in the future.

MHE can be applied to fault estimation if the optimization problem is formulated to calculate the fault parameters rather than the system states. This idea has been noticed by some researchers and used by them for fault estimation. However, the research area of AFTC or FE based on MHE is still primitive since only a few research works in this area appeared after the year 2000 (Tyler, Asano and Morari, 2000; Samar, Gorinevsky and Boyd, 2006; Casavola and Garone, 2010; Izadi, Zhang and Gordon, 2011). In (Tyler, Asano and Morari, 2000), an MHE based approach was used for FE of a cold tandem steel mill with satisfactory simulation results. However, that approach is only applicable to linear systems. In (Samar, Gorinevsky and Boyd, 2006), an FE strategy based on MHE is proposed for an unmanned aircraft system.

To the best of the author's knowledge, the only research works of using MHE for AFTC appeared in (Casavola and Garone, 2010) and (Izadi, Zhang and Gordon, 2011). In (Casavola and Garone, 2010), a fault tolerant adaptive control allocation scheme is proposed for nonlinear discrete-time systems subject to loss of effectiveness in actuators. MHE is used in this scheme as an FE unit for estimating multiplicative actuator faults. Once the faults are estimated, an allocation unit scheme is used to redistribute the total control effort to actuators. In (Izadi, Zhang and Gordon, 2011), a fault tolerant MPC scheme is also proposed for nonlinear discrete-time systems subject to multiplicative actuator faults. MHE is also used in this scheme to estimate actuator faults. An assumption of these two approaches is that all the system states should be measurable.

A challenge of using MHE for FE of nonlinear systems is that the fault may be in a complex nonlinear form and thus the cost function for estimating a fault is not a regular quadratic programming problem. In this Section, a novel approach of fault estimation based on T-S fuzzy MHE is proposed for FE of actuator faults in the nonlinear wind turbine system. This approach utilizes T-S fuzzy modelling to deal with the nonlinearity in the model such that the faults of nonlinear form can be transformed into that of linear form. This FE unit will be combined with a fault tolerant controller based on T-S fuzzy MPC to form an AFTC scheme.

7.2.1 Moving horizon estimation

The principle of MHE for state estimation is to minimize a cost function defined over a horizon in the past (Rao and Rawlings, 2002; Alessandri, Baglietto, Battistelli and Zavala, 2010). The cost function is formulated to try to let the estimated past system states fit in the past system behaviour over the horizon, which is explained below.

Consider a discrete-time nonlinear system:

$$\begin{aligned} x(k+1) &= g(x(k), u(k)) \\ y &= h(x(k)) \end{aligned} \tag{7-1}$$

subject to:

$$u_{\min} \le u(k) \le u_{\max}$$

$$\Delta u_{\min} \le \Delta u(k) \le \Delta u_{\max} \tag{7-2}$$

$$y_{\min} \le y(k) \le y_{\max}$$

where $x(k) \in \mathbb{R}^{\mathrm{n}}$ and $u(k) \in \mathbb{R}^{l}$ are the state vector and input vector. $y(k) \in \mathbb{R}^{m}$ are the measured outputs. (7-2) represents system constraints.

State estimation using MHE is achieve by minimize a cost function formulated as a quadratic form as follows:

$$\min_{\hat{x}(k-N),\hat{x}(k-N+1),\ldots,\hat{x}(k)} J(\hat{x}(k-N),\hat{x}(k-N+1),\ldots,\hat{x}(k)) \tag{7-3}$$

in which

$$\begin{aligned} &J(\hat{x}(k-N),\hat{x}(k-N+1),\ldots,\hat{x}(k)) \\ &\quad = \Gamma(\hat{x}(k-N)) + \sum_{i=k-N}^{k-1} \left\| \hat{x}(i+1) - g(\hat{x}(i),u(i)) \right\|_Q^2 + \sum_{i=k-N}^{k} \left\| y(i) - h(\hat{x}(i)) \right\|_R^2 \end{aligned} \tag{7-4}$$

where Q and R are positive definite matrices and can be seen as design parameters. The past system inputs $u(i)$, $i = k-N, k-N+1, \ldots, k-1$ together with the past and present outputs $y(i)$, $i = k-N, k-N+1, \ldots, k$ are known information of system (7-1). $\Gamma(\hat{x}(k-N))$ is the so-called arrival cost, which summarize the past data not considered in the cost function (i.e. $\{y(0), y(1), \ldots, y(k-N-1)\}$ and $\{u(0), u(1), \ldots, u(k-N-1)\}$). Several forms of arrival cost are available in (Alessandri, Baglietto, Parisini and Zoppoli, 1999; Rao, Rawlings and Mayne, 2003; Alessandri, Baglietto, Battistelli and Zavala, 2010).

The estimated past and present system states (i.e. $\{\hat{x}(k-N), \hat{x}(k-N+1), \ldots, \hat{x}(k)\}$) can be obtained by minimizing (7-4). Minimization of the second and third terms on the right side of (7-4) means fitting the estimated system states into the dynamic behaviour of system (7-1) over the past horizon in order to obtain the most accurate state estimation. (7-3) is solved online at every time instant to calculate $\hat{x}(k)$.

Remark 7-1: Stability and feasibility of MHE is achieved if the optimization problem (7-3) satisfies the assumptions proposed in (Raff, Ebenbauer, Findeisen and Allgöwer, 2005; Alessandri, Baglietto, Battistelli and Zavala, 2010) and the nonlinear system (7-1) is observable.

7.2.2 Actuator fault estimation for linear systems using MHE

The parameter estimation ability of MHE can be used not only to estimate system states but other parameters in the system. For a system subject to actuator faults, MHE can be used to estimate these fault parameters in the system. This idea can be utilized to design FE methods based on MHE for linear systems.

In this Section, a method for FE of actuator faults based on MHE is proposed for linear systems. This approach is based on the FE method using MHE presented in (Izadi, Zhang and Gordon, 2011). An assumption of using the method in (Izadi, Zhang and Gordon, 2011) is that all system states should be measurable, which is not practical in many cases. That assumption is not required in the method presented here since only the measured outputs rather than all the system states is utilized. The method presented in this Section can be seen as the preliminary for FE using T-S fuzzy MHE presented in Section 7.2.3.

Consider the following linear system with actuator faults:

$$x(k+1) = Gx(k) + H(u(k) + f(k)) \tag{7-5}$$

$$y(k) = Cx(k) \tag{7-6}$$

in which $x(k) \in \mathbb{R}^n$ is the state vector, $u(k) \in \mathbb{R}^l$ is the input vector and $y(k) \in \mathbb{R}^m$ is the measured outputs. $f(k) \in \mathbb{R}^l$ is the actuator fault. G, H and C are system matrices with proper dimensions. The faults are bounded as $f_{\min} \le f(k) \le f_{\max}$.

The actuator fault $f(k)$ in (7-5) can be estimated using the idea of MHE together with an observer. If a standard Luenberger observer is designed for the system (7-5) to (7-6) without considering the actuator fault (i.e. the observer assumes $f(k) = 0$) and the estimation error dynamics are given as follows:

$$e(k) = x(k) - \hat{x}(k) \tag{7-7}$$

Then $\lim_{k\to\infty} e(k) = 0$ when $f(k) = 0$. However, $e(k)$ will not converge to zero in the presence of the actuator fault. Therefore, the fault information will be reflected by the value of $e(k)$.

The following equation can be derived from (7-7) as:

$$Ce(k) = Cx(k) - C\hat{x}(k) = y(k) - \hat{y}(k) \tag{7-8}$$

in which $\hat{y}(k)$ are the estimated outputs. It is shown in (7-8) that the fault information is further reflected in the difference between the measured and estimated system outputs. This characteristic can be used to design an actuator fault estimation unit using MHE, which is presented in the following optimization problem:

$$\min_{\hat{f}(k-N),\hat{f}(k-N+1),\ldots,\hat{f}(k-1)} \sum_{i=k-N+1}^{k} \left\| \hat{y}(i) - y(i) \right\|_Q^2 \tag{7-9}$$

subject to:

$$\hat{y}(i) = C\hat{x}(i) \tag{7-10}$$

$$\hat{x}(i) = G\hat{x}(i-1) + H(u(i-1) + \hat{f}(i-1)) \tag{7-11}$$

$$f_{\min} \le f(i-1) \le f_{\max} \tag{7-12}$$

$i = k-N+1, k-N, \ldots, k$

k denotes the current time instant, Q is a positive define matrix and N is the estimation horizon. $\hat{x}(k)$ is the state estimation from the observer without considering the actuator fault. $\hat{f}(i-1),\ i = k-N+1, k-N, \ldots, k$ are the estimates of the actuator fault. $y(i)$ and $u(i-1)$, $i = k-N+1, k-N, \ldots, k$ are the measured past and current output data and the measured past input data in the estimation horizon. $f_{\min}$ and $f_{\max}$ are the bounds of the actuator fault if a bounded fault is considered.

The optimization problem (7-9) is a constrained quadratic programming problem and thus can be solved efficiently with mature numerical methods. (7-9) is calculated online at every time instant for fault estimation.

Remark 7-2: It should be noted that the faults in the past can be estimated up to the time instant $\hat{f}(k-1)$ using this method. Therefore, the above method can only be used to estimate slow time-varying or constant faults.

Remark 7-3: This FE approach is able to estimate multiple actuator faults. This is because the estimated $\hat{f}(k-1) \in \mathbb{R}^l$ is a fault vector with l elements corresponding to the l actuators in the input vector $u(k) \in \mathbb{R}^l$.

7.2.3 Actuator fault estimation for nonlinear system using T-S fuzzy MHE

The method presented in Section 7.2.2 is designed for actuator FE in linear systems. However, the idea of this method can also be extended for actuator FE in nonlinear systems using T-S fuzzy modelling.

In this Section, a method of MHE based on T-S fuzzy modelling is proposed for actuator FE in nonlinear systems. The idea of the method presented in Section 7.2.2 is utilized in this method. In this T-S fuzzy MHE approach, a nonlinear system model is transformed into a T-S fuzzy model and used as the prediction model of MHE. This T-S fuzzy prediction model is a linear time-varying model and thus a linear model at every time instant. Therefore, a quadratic programming problem can be used to estimate actuator faults in nonlinear systems if this T-S fuzzy prediction model is used. The principle of this method is described below.

Consider the nonlinear discrete-time system (7-1) and its corresponding T-S fuzzy model given as:

$$\begin{aligned} x(k+1) &= G(\eta_k)x(k) + H(\eta_k)u(k) + a(\eta_k) \\ y(k) &= C(\eta_k)x(k) \end{aligned} \tag{7-13}$$

(7-13) can be obtained using the T-S fuzzy modelling method presented in Section 5.2.1.

Based on (7-13), a T-S fuzzy observer with online eigenvalue assignment can be designed for system (7-1) and given as:

$$\hat{x}(k+1) = G(\eta_k)\hat{x}(k) + H(\eta_k)u(k) + a(\eta_k) + F[\hat{y}(k) - y(k)] \tag{7-14}$$

$$\hat{y}(k) = C(\eta_k)\hat{x}(k) \tag{7-15}$$

(7-14) to (7-15) are based on the T-S fuzzy system (7-13) without considering actuator faults. The T-S fuzzy model in the presence of actuator faults is given as follows:

$$\begin{aligned} x(k+1) &= G(\eta_k)x(k) + H(\eta_k)(u(k) + f(k)) + a(\eta_k) \\ y(k) &= C(\eta_k)x(k) \end{aligned} \tag{7-16}$$

It can be seen from the observer (7-14) to (7-15) and the corresponding fuzzy system (7-16) that $e(k) = x(k) - \hat{x}(k)$ will not converge to zero in the presence of actuator faults. The information on faults will be reflected in $e(k)$ and further reflected in the difference between the measured outputs $y(k)$ and the estimation $\hat{y}(k)$ as explained in (7-8). Using this difference, the idea of actuator FE using MHE proposed in Section 7.2.2 can be utilized to design an actuator FE method for the nonlinear system (7-1), which is presented as follows:

$$\min_{\hat{f}(k-N),\hat{f}(k-N+1),\ldots,\hat{f}(k-1)} \sum_{i=k-N+1}^{k} \left\| \hat{y}(i) - y(i) \right\|_Q^2 \tag{7-17}$$

subject to:

$$\hat{y}(i) = C(\eta_i)\hat{x}(i) \tag{7-18}$$

$$\hat{x}(i) = G(\eta_{i-1})\hat{x}(i-1) + H(\eta_{i-1})(u(i-1) + \hat{f}(i-1)) + a(\eta_{i-1}) \tag{7-19}$$

$$f_{\min} \le f(i-1) \le f_{\max} \tag{7-20}$$

$$i = k-N+1, k-N, \ldots, k$$

in which k is the current time instant, N is the estimation horizon. Q is a positive definite matrix which is a design parameter. $\hat{x}(k)$ is the estimated state from the T-S fuzzy observer (7-14) to (7-15) without considering the actuator fault. $\hat{f}(i-1),\ i = k-N+1, k-N, \ldots, k$ are the estimated faults in the past. $y(i)$ and $u(i-1)$, $i = k-N+1, k-N, \ldots, k$ are the measured past and current output data and the measured past input data over the estimation horizon.

It is shown that the prediction models in (7-19) are LTV models due to T-S fuzzy modelling and thus are linear models at every time instant. Therefore, (7-17) is a constrained quadratic programming problem at every time instant and can be solved efficiently. (7-17) is solved online at every time instant to calculate $\hat{f}(k-1)$. Again, the method presented in this Section is designed to estimate either slow time-varying faults or constant faults.

A requirement of using the approach in this Section is that the premise variables of the membership function η_{i-1}, $i=k-N+1,k-N,...,k$ in (7-14) and (7-19) should be known (i.e. either measurable or can be estimated). This is because system matrices of the T-S fuzzy prediction model (7-19) and the T-S fuzzy observer (7-14) to (7-15) are calculated using the membership function and thus determined by these premise variables. It is shown in Section 7.2.4 that this requirement can be satisfied by the wind turbine system.

7.2.4 T-S fuzzy MHE for wind turbine actuator fault estimation

The actuator fault estimation approach using T-S fuzzy MHE presented in Section 7.2.3 is used in this Section to design an FE unit for nonlinear wind turbine systems. The causes of actuator faults are explained in Section 2.2.1. They can be formulated as two fault variables added to each of the two wind turbine system inputs (i.e. generator torque reference T_{gr} and pitch angle reference β_r) as shown in (3-10). These inputs are responsible for providing the appropriate actuation to the wind turbine system.

The proposed FE unit for the wind turbine system is formulated as the following optimization problem:

$$\min_{\hat{f}(k-N),\hat{f}(k-N+1),...,\hat{f}(k-1)} \sum_{i=k-N+1}^{k} \left\| \hat{y}(i)-y(i) \right\|_Q^2 \tag{7-21}$$

subject to

$$\hat{y}(k)=C\hat{x}(k) \tag{7-22}$$

$$\hat{x}(i) = G(\eta_{i-1})\hat{x}(i-1) + H(\eta_{i-1})(u(i-1) + \hat{f}(i-1)) + D(\eta_{i-1})v(i-1) + a(\eta_{i-1}) \tag{7-23}$$

$$f_{\min} \le f(i-1) \le f_{\max} \tag{7-24}$$

$i = k-N+1, k-N, ..., k$

where $\hat{x}(k) = [\hat{\omega}_r(k) \quad \hat{\omega}_g(k) \quad \hat{\theta}_\Delta(k) \quad \hat{\dot{\beta}}(k) \quad \hat{\beta}(k) \quad \hat{T}_g(k)]^{\mathrm{T}}$ are the estimated wind turbine system states obtained using the wind turbine T-S fuzzy observer (5-48) without considering the actuator fault. $u(k) = [T_{gr}(k) \quad \beta_r(k)]^{\mathrm{T}}$ and $v(k)$ is the EWS. η_k is the membership function of the T-S fuzzy wind turbine model (5-22) and can also be written as $\eta_k(v(k), \omega_r(k), \beta(k))$. The measured outputs of the wind turbine system are defined in $y(k) = [\omega_g(k) \quad \beta(k) \quad T_g(k)]^{\mathrm{T}}$. The system matrices in (7-22) and (7-23) are the same as those defined in (5-22). $\hat{f}(i-1), i = k-N+1, k-N, ..., k$ are the faults to be estimated. Once again, (7-21) is solved online at every time instant to estimate $\hat{f}(k-1)$.

Remark 7-4: The three variables in the membership function $\eta_k(v(k), \omega_r(k), \beta(k))$ can be either measured or estimated. $v(k)$ can be obtained from the wind speed sensor or the EWS estimation method proposed in Section 4.3.1. The wind turbine rotor speed $\omega_r(k)$ can be obtained from the filtered rotor speed sensor data. It should be noted that the noise in the rotor speed sensor is generally much larger than the noise in other sensors. In practice, the measurement from the rotor speed sensor is generally used as a condition monitoring signal and not for feedback control. In the FE approach of this Section, the filtered rotor speed sensor data are only used as one of the premise variables in the membership function. The pitch angle $\beta(k)$ in the premise variable can be obtained from the pitch angle sensor.

Remark 7-5: The stability and feasibility conditions proposed in (Raff, Ebenbauer, Findeisen and Allgöwer, 2005; Alessandri, Baglietto, Battistelli and Zavala, 2010) can not be applied to the T-S fuzzy MHE proposed in this Section. This is because the fuzzy MHE in this Section is a linear time varying system and thus the model parameters are

changing at every time instant. However, the standard stability and feasibility conditions are proposed for systems with fixed model parameters. Therefore, the stability and feasibility of the T-S fuzzy MHE need further investigation and can only be tested through simulation experiments so far. It is shown in the simulation results in Section 7.3.3 that the feasibility of the T-S fuzzy MHE for the wind turbine sytem can be achieved. Meanwhile, no problems due to instability occur during the simulation test.

7.3 AFTC for wind turbine actuator faults

In this Section, an AFTC scheme based on the FE unit in Section 7.2.4 and a T-S fuzzy predictive controller is proposed for the wind turbine actuator fault tolerant control. This T-S fuzzy predictive controller servers for two purpose: (1) to compensate the actuator fault estimate from the FE unit and (2) control the wind turbine.

7.3.1 Actuator fault compensation using T-S fuzzy MPC

Once the actuator fault is estimated, it can be considered and compensated in the prediction model of a T-S fuzzy predictive controller. This strategy can be used to develop a fault compensator based on T-S fuzzy MPC, which is described as follows:

Considering the T-S fuzzy model (7-13) designed for the nonlinear system (7-1), the fault compensator and baseline controller can be designed in the T-S fuzzy MPC framework and formulated as the following optimization problem:

$$\min_{u(k),u(k+1),,,u(k+N-1)} \sum_{i=1}^{N} \left\| x(k+i) - x_r(k) \right\|_R \tag{7-25}$$

subject to:

$$f = \hat{f}(k-1) \tag{7-26}$$

$$x(k) = G(\eta_{k-1})\hat{x}(k-1) + H(\eta_{k-1})(u(k-1) + f) + a(\eta_{k-1}) \tag{7-27}$$

$$x(k+i+1) = G(\eta_k)x(k+i) + H(\eta_k)[u(k+i) + f] + a(\eta_{k-1}) \tag{7-28}$$

$$u_{\min} \le u(k+i) \le u_{\max} \tag{7-29}$$

$$\Delta u_{\min} \le \Delta u(k+i) \le \Delta u_{\max} \tag{7-30}$$

$$y_{\min} \le y(k+i) \le y_{\max} \tag{7-31}$$

$i = 0,1,2,...N-1$

in which $u_{\min}$, $u_{\max}$, $\Delta u_{\min}$, $\Delta u_{\max}$, $y_{\min}$, $y_{\max}$ are the system constraints in (7-1). $x_r(k)$ is the reference signal to be tracked and N serves as both the prediction and control horizons. R is a positive definite matrix, which is a design parameter. $\hat{f}(k-1)$ is the actuator fault estimated from the FE approach presented in Section 7.2.3. $\hat{x}(k-1)$ is the estimated system states using the T-S fuzzy observer in (7-14) to (7-15), without considering the actuator fault. (7-27) means the current system states are obtained from the T-S fuzzy observer (7-14) to (7-15) taking into account actuator faults f. (7-25) is solved online at every time instant and $u(k)$ is calculated and used as the control input.

Remark 7-6: It is shown in (7-25) that the T-S fuzzy MPC in this AFTC scheme is not only a baseline controller without considering faults since the faults are externally considered in the prediction model (7-28). This is quite different from the AFTC schemes proposed in Chapter 5 and Chapter 6 in which T-S fuzzy MPC is only used to design a baseline controller without considering faults.

Remark 7-7: It is shown in (7-28) that faults over the prediction horizon is assumed to be the same as the fault f. Therefore this approach is valid only for constant or slowly time-varying actuator faults.

7.3.2 AFTC for wind turbine actuator faults

As shown in Section 7.3.1, a T-S fuzzy MPC approach can be used for both controlling a nonlinear system subject to constraints and compensating the actuator faults, provided that the actuator fault is estimated from a FE unit. Therefore, this approach can be combined with an FE unit to design an AFTC scheme for wind turbine actuator faults. The diagram of this scheme is shown in Figure 7-1.

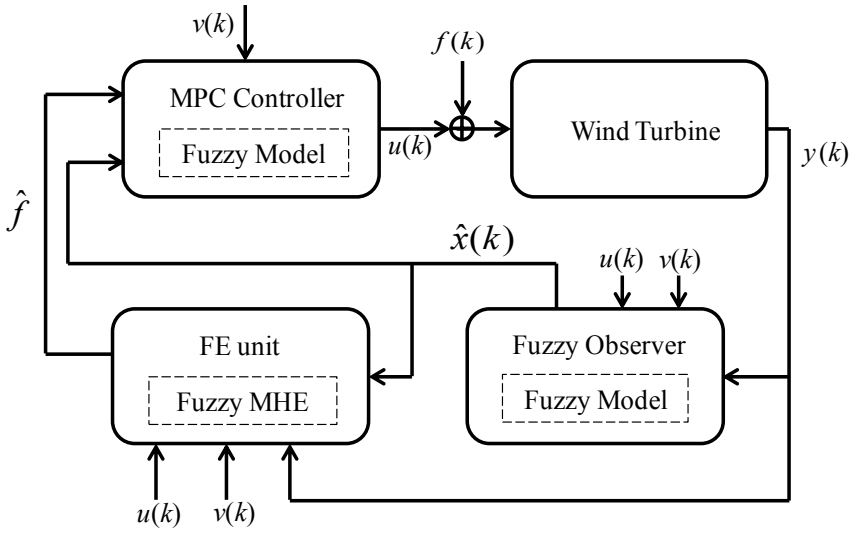

Figure 7-1 AFTC scheme for wind turbine system

The design of the FE unit is this scheme is presented in Section 7.2.4. The controller in this scheme is used to solve an online optimization problem which is reformulated from (7-25) as follows:

$$\min_{u(k),u(k+1),,u(k+N-1)} \sum_{i=1}^{N} \left\| x(k+i) - x_r(k) \right\|_R \tag{7-32}$$

subject to:

$$f = \hat{f}(k-1) \tag{7-33}$$

$$x(k) = G(\eta_{k-1})\hat{x}(k-1) + H(\eta_{k-1})[u(k-1) + f] + D(\eta_{k-1})v(k-1) + a(\eta_{k-1}) \tag{7-34}$$

$$x(k+i+1) = G(\eta_k)x(k+i) + H(\eta_k)[u(k+i) + f] + D(\eta_k)v(k) + a(\eta_k) \tag{7-35}$$

$$\begin{aligned} &\beta_{\min}(k+i) \le \beta_r(k+i) \le \beta_{\max}(k+i) \\ &\Delta\beta_{\min}(k+i) \le \beta_r(k+i) - \beta_r(k+i-1) \le \Delta\beta_{\max}(k+i) \\ &T_{\min}(k+i) \le T_{gr}(k+i) \le T_{\max}(k+i) \\ &\Delta T_{\min}(k+i) \le T_{gr}(k+i) - T_{gr}(k+i-1) \le \Delta T_{\max}(k+i) \end{aligned} \tag{7-36}$$

$i = 0,1,2,...N-1$

in which $\hat{f}(k-1)$ is the estimated wind turbine actuator fault obtained from the solution of the optimization problem (7-21). Other parameters in (7-34) to (7-36) are all the same as those defined in the optimization problem (5-43). (7-32) is solved online at every time instant and the calculated $u(k)$ is used as the control input.

7.3.3 Simulation Study

The AFTC scheme is tested on the nonlinear wind turbine model presented in Section 3.2. The wind speed data used in simulation are given in Figure 5-5. The simulation results and discussions of this scheme are presented below.

The FE performance corresponding to the pitch actuator and generator torque faults is shown in Figures 7-2 and Figure 7-3. A 10 degree offset fault is added to the pitch reference and a 2000 N·m offset fault is added to the generator torque. These two offsets are used to simulate the realistic wind turbine actuator faults described in Section 2.2.1.

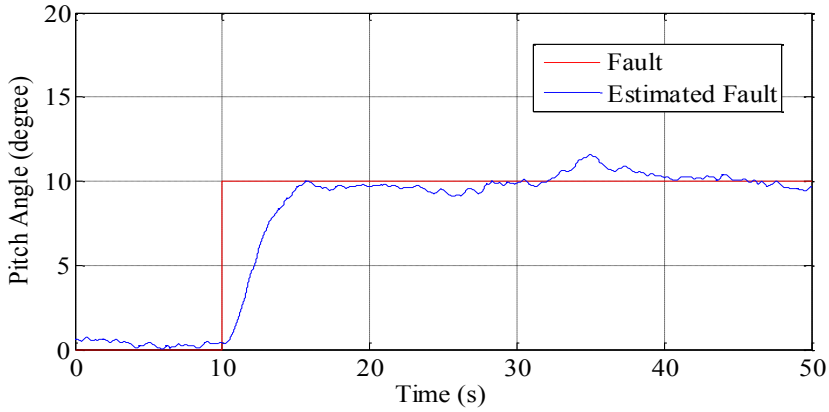

Figure 7-2 FE for pitch actuator fault

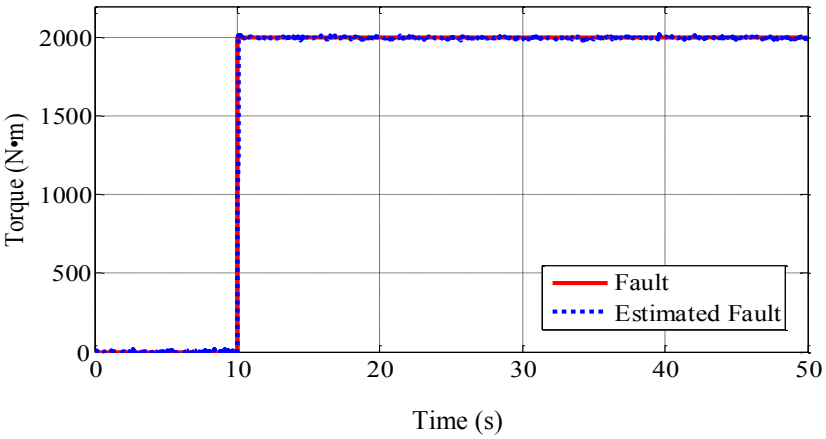

Figure 7-3 FE for generator torque sensor fault

It is shown in Figures 7-2 and 7-3 that the FE performance for the generator actuator fault is much better than that for the pitch actuator fault. This is due to the very high signal to noise ratio of the generator torque sensor.

The performance of the proposed AFTC scheme for the fault-free case is shown in Figures 7-4 to 7-6. Figure 7-4 shows the tracking performance for the wind turbine operating in the region below rated wind speed. Once again, the filtered optimal rotor speed is tracked to avoid heavy drive train torsion, as explained in Section 4.5.3. The performance of the generator power and speed regulation is shown in Figures 7-5 and Figure 7-6. Both the generator speed and power are regulated within their safety limits.

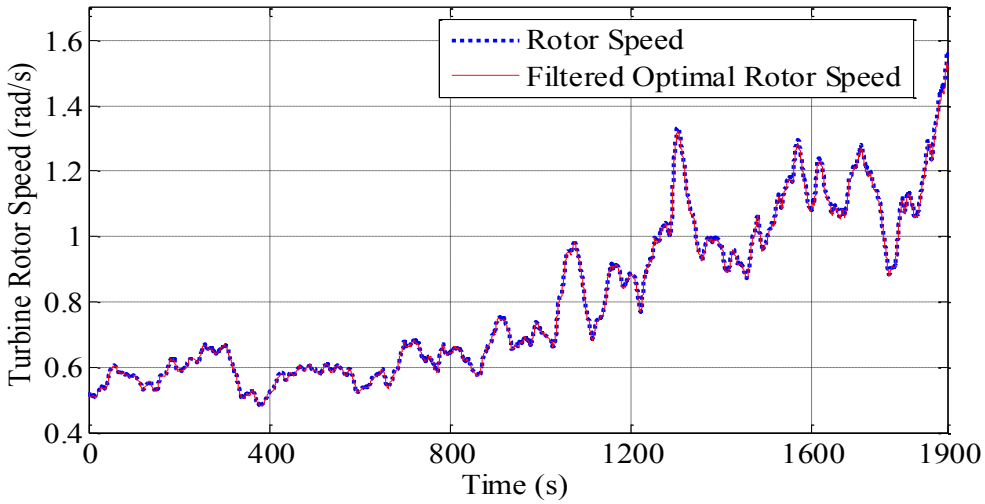

Figure 7-4 optimal rotor speed tracking in fault-free case

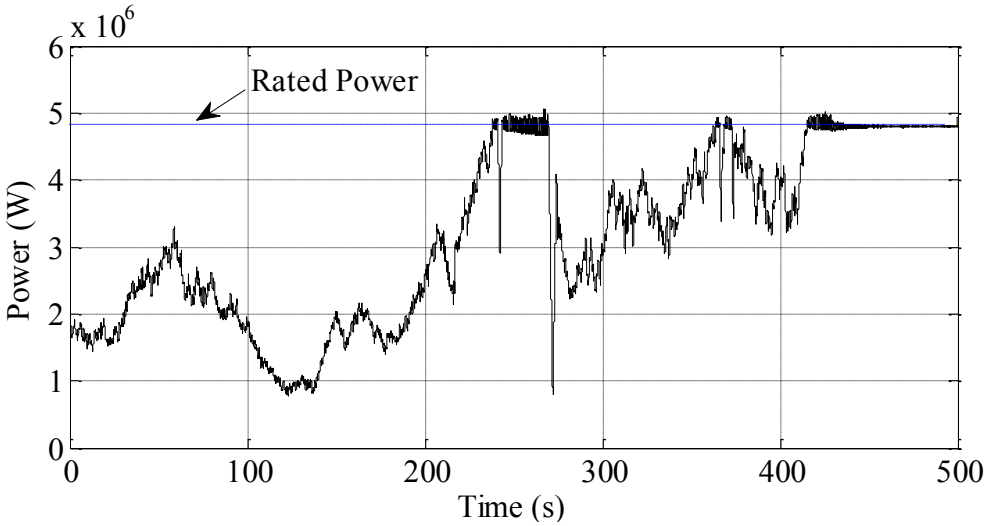

Figure 7-5 Power regulation in fault-free case

The performance of the AFTC scheme considering a pitch actuator fault is shown in Figure 7-7. A 10 degree offset actuator fault is added to the pitch actuator for 100 seconds in this scenario. It is shown that the degradation for the optimal rotor speed tracking performance is acceptable using the AFTC scheme, whilst the tracking performance degradation without AFTC is much greater.

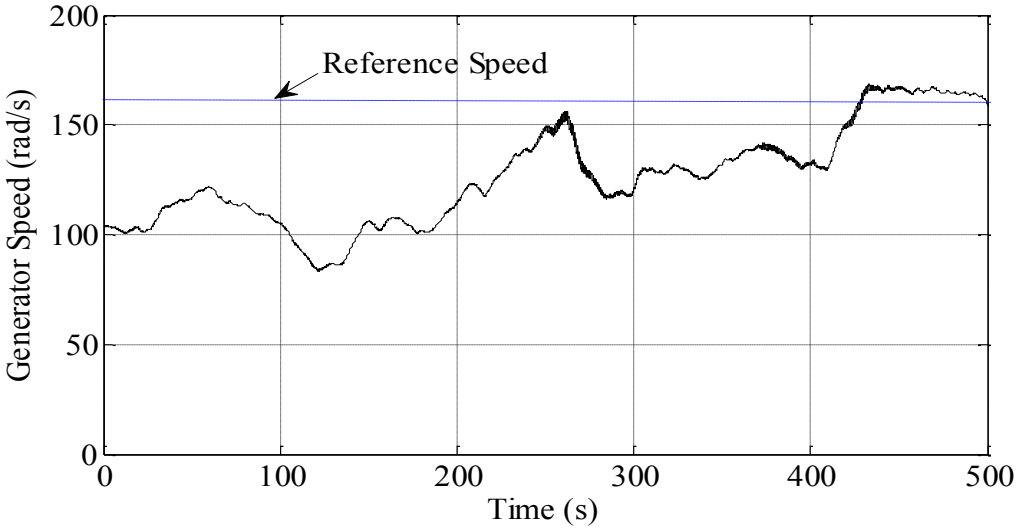

Figure 7-6 Generator speed regulation in fault-free case

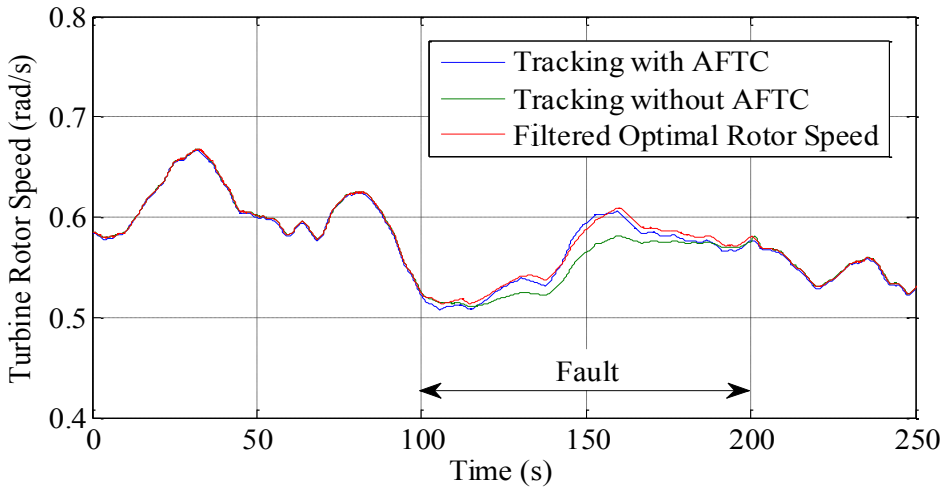

Figure 7-7 Tracking performance in the presence of pitch actuator fault

The performance of the AFTC scheme for the generator torque actuator fault is shown in Figure 7-8. A 2000N·m torque offset fault is added to the generator torque in this scenario. It is shown at 50s and at 220s that the generator power exceeds the rated value when the control goal switches from tracking the optimal rotor speed to tracking the power regulation or vice-versa even when FTC is used. However, it is shown that when the control goal does not change and becomes stable after 200s the power can be regulated at the value of rated power using FTC.

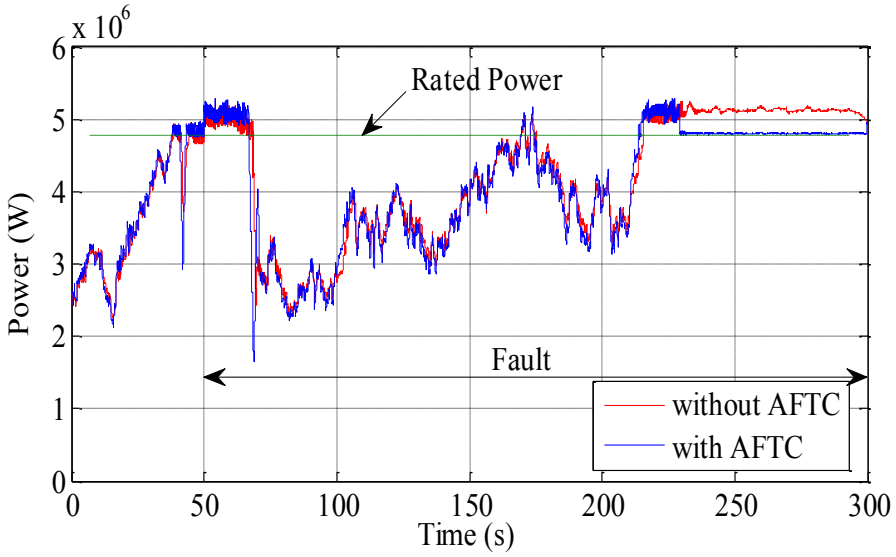

Figure 7-8 Power regulation in the presence of torque actuator fault

On the other hand, it is shown in Figure 7-8 that the generator power always exceeds the rated value when the control goal is power regulation and FTC is not used.

7.4 Conclusions

In this Chapter, an FE approach for actuator faults using MHE is proposed. For linear systems, faults can be estimated by the MHE strategy using the measured and estimated outputs from an observer. For nonlinear systems, the actuator faults can be estimated via a T-S fuzzy MHE using the measured and estimated outputs from a T-S fuzzy observer.

Based on the use of the FE unit, a controller using T-S fuzzy MPC is proposed and used as both a standard controller and an actuator fault compensator. Therefore, system

nonlinearity and constraints can still be handled since this controller is designed based on the T-S fuzzy MPC framework introduced in Chapter 5.

An AFTC scheme for wind turbine actuator faults is then proposed by combining the FE unit and the T-S fuzzy controller. The performance of this scheme is demonstrated by simulation.

Chapter 8: Summary and future work

8.1 Summary

FTC of wind turbine systems is a relatively new research subject with most of the research work in this area appearing since the late 2000s. This is therefore a relatively under-developed application subject compared with the subject of general wind turbine control without considering fault tolerance. However, it has become a fast developing research area due to some practical concerns about wind turbine operation and maintenance, such as fault tolerant ability, sustainable operation and reliability. This thesis is motivated by these practical concerns and has proposed some AFTC strategies as potential solutions. These strategies deal with faults acting in different locations of the wind turbine. Some practical issues such as inadequate or redundant sensors are considered in the design of these AFTC schemes.

The wind turbine AFTC strategies in this thesis are proposed and described in Chapters 4, 5, 6 & 7. The presentation of each strategy comprises three steps. Firstly, a detailed description of the mathematical methods used in each strategy is given. Secondly, the design of the wind turbine AFTC scheme based on these mathematical methods is described. Thirdly, the performance of the AFTC scheme is tested with simulation, using a wind turbine model derived from a realistic modern large wind turbine benchmark model.

As an Introduction to this thesis, Chapter 1 provides some general information about the research area of FTC, including definitions and some literature review. The general ideas of FTC are explained in this Chapter as well as reasons why FTC is an important research subject. This provides the reader with an opportunity to gain familiarity with the basic research concepts within the research area considered, especially for the subject of AFTC. Furthermore, the reason why AFTC approaches are used in this thesis is also explained by comparing PFTC and AFTC approaches in Section 1.3.

The thesis goes further to introduce the specific subject of AFTC of wind turbines in Chapter 2. First of all, the research motivation of AFTC for wind turbine systems is

presented. It is shown in Section 2.1 that this research subject is driven by practical concerns arising from the industry. After the description of the motivation, the complete scenario of typical wind turbine faults is outlined in order to illustrate the challenges and problems being tackled in this research subject. A review of the main research progress in this subject is also described in this Chapter.

Chapter 3 outlines typical modelling of wind turbine subsystems and faults with reference to an industry standard nonlinear wind turbine benchmark model. This benchmark system contains the main elements of wind turbine control, excluding the more complex loading effects arising from blade flapping, wind shear and tower bending which are considered outside the scope of this thesis. The benchmark system is used in simulation to test the AFTC strategies in this thesis. A requirement for AFTC approaches is that the basic functions of a process should be realized in the fault-free case and the control performance in this case should be as close as possible to the desired control performance. Therefore, the basic principle of wind turbine operation and control is introduced in Chapter 3 following the modelling of wind turbine subsystems and faults, in order to show the basic functions of the various wind turbine control systems and the control challenges (e.g. the concept of the dual control goal in different operating regions). These functions and challenges should be addressed in the design of wind turbine AFTC systems.

The main contributions of this thesis are in Chapters 4, 5, 6 & 7, although the preliminary knowledge and the literature review in earlier Chapters are also considered as important and relevant contributions (i.e. Chapters 1, 2 & 3). Chapter 4 proposes an AFTC scheme for the wind turbine operating in the region below rated wind speed in order to deal with speed sensor faults. This scheme comprises an FDI unit and a baseline controller. The FDI unit is based on the method of LSSVM (outlined early in the Chapter). Since a controller is always required in an AFTC scheme, a baseline controller based on a 1-norm robust MPC is proposed. Before introducing the concept of robust MPC, the basic principles of MPC are presented in Section 4.4.1. Finally, in Section 4.5 the design of an MPC-based AFTC scheme is given for handling wind speed sensor faults, based on the linearized wind turbine benchmark model.

Apart from wind speed sensor faults, faults also occur in other important wind turbine sensors that are typically used to provide feedback to the wind turbine control system. Hence, Chapter 5 continues to develop the AFTC scheme based on MPC, focussing on the wind turbine operation in the presence of faults in generator speed, generator torque and pitch angle sensors. Chapter 5 extends the ability of the AFTC scheme in Chapter 4 to encompass fault tolerance in both regions below and above rated wind speed. The linearized model approach in Chapter 4 cannot be used for designing AFTC system for wind turbines if two operating regions are considered since the nonlinearity is more obvious in this case. Therefore, T-S fuzzy modelling of wind turbine systems is used in Chapter 5 to approximate the original nonlinear wind turbine system for the purpose of designing an AFTC scheme for the two wind turbine operating regions. A residual based FDI unit is designed to identify and isolate sensor faults. The baseline controller is based on T-S fuzzy MPC in order to deal with the nonlinear wind turbine model and system constraints. Fault tolerance is achieved by switching to healthy sensors when the faulty sensor is identified by the FDI unit.

The fault tolerance mechanism of the AFTC approach in Chapter 5 requires that there should be enough redundant output sensors. However, this is not always the case and in some cases there are not enough redundant sensors. Therefore, an AFTC scheme utilizing analytical redundancy and limited hardware redundancy in the wind turbine system is proposed for output sensor faults and presented in Chapter 6. This scheme comprises three units. The first unit is an FDI unit which is a T-S fuzzy observer using online eigenvalue assignment. This FDI unit is for detecting and isolating generator speed sensor faults. The second unit is an FE unit using a descriptor observer approach. This unit is for estimating and decoupling the faults from the pitch angle sensor and the generator torque sensor. The third unit is the baseline controller using T-S fuzzy MPC. Fault tolerance for generator speed sensor faults is achieved by switching to a healthy generator speed sensor when the faulty one is identified by the FDI unit. Meanwhile, Fault tolerance for pitch angle and generator torque sensors is achieved by decoupling faults from the outputs of these two sensors using the FE unit.

The T-S fuzzy MPC is used in Chapter 5 and Chapter 6 as the baseline controller without considering faults. The faults are considered by an FE unit and/or the switching mechanism based on an FDI unit. In Chapter 7, another T-S fuzzy MPC with the ability

to compensate actuator faults is proposed, which can be seen as an extension of the baseline controller designed in Chapter 5 and Chapter 6. The AFTC scheme in Chapter 7 comprises an FE unit and a controller. An approach of actuator fault estimation via T-S fuzzy MHE is proposed and used as the FE unit. Meanwhile, a T-S fuzzy predictive controller is used in this scheme to compensate the estimated faults and control the wind turbine.

The following conclusions can be drawn from the research work in this thesis. First of all, it is shown in this thesis that MPC is an effective method to deal with the wind turbine control problem and has the potential to be applied in real wind turbines. Secondly, it is shown in Chapters 5, 6 and 7 that a T-S fuzzy model is able to approximate the nonlinear wind turbine model and facilitate design of the wind turbine controller. Thirdly, it is shown in simulation results that the proposed FE and FDI methods in this thesis can be combined with MPC to form AFTC schemes with satisfactory fault tolerant performance.

8.2 Future work

Although some new approaches for AFTC of wind turbines have been proposed in this thesis, there are still some future work which could be done following this work. These potential future works are presented as follows.

The simulation results show that the T-S fuzzy MPC proposed in this thesis is effective for controlling a nonlinear wind turbine system. However, this method is still in a primitive stage which needs further development. At the time of finishing this thesis, the stability of this method is still being investigated in our laboratory. This stability condition is complicated by the dual control goal problem in the wind turbine. This is because the weighting matrix in (5-47) becomes time-varying in the case of the dual control goals. A potential solution for the stability issue of this method is to refer to an idea of robust stability presented in (Casavola, Giannelli and Mosca, 2000) which is proposed for input-constrained linear uncertain system. The system to be controlled in that approach and the T-S fuzzy wind turbine system in this thesis are both polytopic dynamic systems in essence and are both controlled using MPC.

The FDI unit using residual generation proposed in Section 5.5.1 and Section 6.4.1 takes into account modelling error and sensor noise by setting a proper threshold for residual signals. This is an implicit way of considering uncertainties. However, it could be valuable to investigate using robust approaches to consider these uncertainties externally.

During the construction of the T-S Fuzzy wind turbine model, the high order terms in the Taylor series expansion are ignored. Although simulation results in this thesis show that the wind turbine system is insensitive to this small uncertainty effects, it is still theoretically valuable to consider this effect in the design of the wind turbine AFTC scheme.

Most of the research works on AFTC of wind turbines have focused on either actuator faults or sensor faults so far. However, component faults in the wind turbine are seldom considered in the literature. Therefore, AFTC for wind turbine component faults is still a primitive research area that worth investigating. One possible method to deal with component faults is the online model identification approach, in which the model is updated online to consider the change of model due to component faults.

This thesis considers AFTC of wind turbines only from the power control aspect. Therefore, the performance of the AFTC schemes in this thesis is judged by whether maximum power production and generator power regulation can still be achieved by the control system in the presence of faults. However, there is another aspect of wind turbine control which is the control of structure load in wind turbines. Although this aspect is beyond the scope of this thesis, it is valuable to investigate how to design wind turbine AFTC schemes such that the control performance of both power production and structure load can be acceptable in the presence of various faults.

REFERENCES

Abad, G. L., J.; Rodríguez, M.; Marroyo, L.; Iwanski, G. 2011. *Doubly Fed Induction Machine: Modeling and Control for Wind Energy Generation Applications*, Wiley-IEEE Press.

Abo-Khalil, A. G. & Lee, D.-C. 2008. MPPT control of wind generation systems based on estimated wind speed using SVR. *Industrial Electronics, IEEE Transactions on,* 55**,** 1489-1490.

Alessandri, A., Baglietto, M., Battistelli, G. & Zavala, V. Advances in moving horizon estimation for nonlinear systems. Decision and Control (CDC), 2010 49th IEEE Conference on, 2010. IEEE, 5681-5688.

Alessandri, A., Baglietto, M., Parisini, T. & Zoppoli, R. 1999. A neural state estimator with bounded errors for nonlinear systems. *Automatic Control, IEEE Transactions on,* 44**,** 2028-2042.

Allgöwer, F., Badgwell, T. A., Qin, J. S., Rawlings, J. B. & Wright, S. J. 1999. Nonlinear predictive control and moving horizon estimation—an introductory overview. *Advances in control.* Springer.

Alwi, H. & Edwards, C. 2008. Fault tolerant control using sliding modes with on-line control allocation. *Automatica,* 44**,** 1859-1866.

Amirat, Y., Benbouzid, M. E. H., Al-Ahmar, E., Bensaker, B. & Turri, S. 2009. A brief status on condition monitoring and fault diagnosis in wind energy conversion systems. *Renewable and Sustainable Energy Reviews,* 13**,** 2629-2636.

Anonymous. 2011a. *Gear tooth damage* [Online]. Available: http://powerelectronics.com/alternative-energy/heading-gearbox-failure [Accessed 1st August 2014].

Anonymous. 2011b. *Icing on wind turbine blades* [Online]. Available: http://www.windpowerengineering.com/maintenance/detecting-ice-on-wind-turbine-blades/ [Accessed 1st August 2014].

Anonymous. 2013a. *Wind turbine accidents summary* [Online]. Available: http://www.caithnesswindfarms.co.uk/accidents.pdf [Accessed 1st August.

Anonymous. 2013b. *Wind Turbine Maintenance* [Online]. Available: http://genievert.com/maintenance/ [Accessed 1st August 2014].

Babuska, R. 1998. *Fuzzy modeling for control*, Kluwer Academic Publishers.

Badihi, H., Zhang, Y. & Hong, H. A review on application of monitoring, diagnosis, and fault-tolerant control to wind turbines. Control and Fault-Tolerant Systems (SysTol), 2013 Conference on, 2013. IEEE, 365-370.

Badihi, H., Zhang, Y. & Hong, H. 2014. Fuzzy gain-scheduled active fault-tolerant control of a wind turbine. *Journal of the Franklin Institute,* 351**,** 3677-3706.

Bao, J., Zhang, W. Z. & Lee, P. L. 2003. Decentralized fault-tolerant control system design for unstable processes. *Chemical Engineering Science,* 58**,** 5045-5054.

Baranyi, P., Tikk, D., Yam, Y. & Patton, R. J. 2003. From differential equations to PDC controller design via numerical transformation. *Computers in Industry,* 51**,** 281-297.

Bemporad, A. & Morari, M. 1999. Robust model predictive control: A survey. *Robustness in identification and control.* Springer.

Bemporad, A., Oliveri, A., Poggi, T. & Storace, M. 2011. Ultra-fast stabilizing model predictive control via canonical piecewise affine approximations. *Automatic Control, IEEE Transactions on,* 56**,** 2883-2897.

Benosman, M. & Lum, K.-Y. 2009. Application of absolute stability theory to robust control against loss of actuator effectiveness. *IET Control Theory & Applications,* 3**,** 772-788.
Benosman, M. & Lum, K. Y. 2010. Application of passivity and cascade structure to robust control against loss of actuator effectiveness. *International Journal of Robust and Nonlinear Control,* 20**,** 673-693.
Bertsimas, D. & Tsitsiklis, J. N. 1997. *Introduction to linear optimization*, Athena Scientific Belmont, MA.
Blanke, M., Izadi-Zamanabadi, R., Bøgh, S. A. & Lunau, C. P. 1997. Fault-tolerant control systems—a holistic view. *Control Engineering Practice,* 5**,** 693-702.
Blanke, M. & Schröder, J. 2003. *Diagnosis and fault-tolerant control*, Springer.
Bonivento, C., Gentili, L. & Paoli, A. Internal model based fault tolerant control of a robot manipulator. Decision and Control, 2004. CDC. 43rd IEEE Conference on, 2004. IEEE, 5260-5265.
Bonivento, C., Isidori, A., Marconi, L. & Paoli, A. 2004. Implicit fault-tolerant control: application to induction motors. *Automatica,* 40**,** 355-371.
Bonivento, C., Paoli, A. & Marconi, L. 2003. Fault-tolerant control of the ship propulsion system benchmark. *Control engineering practice,* 11**,** 483-492.
Boskovic, J. & Mehra, R. An adaptive retrofit reconfigurable flight controller. Decision and Control, 2002, Proceedings of the 41st IEEE Conference on, 2002. IEEE, 1257-1262.
Boskovic, J. D. & Mehra, R. K. Stable multiple model adaptive flight control for accommodation of a large class of control effector failures. American Control Conference, 1999. Proceedings of the 1999, 1999. IEEE, 1920-1924.
Bossanyi, E. 2003. Wind turbine control for load reduction. *Wind Energy,* 6**,** 229-244.
Bukley, A. P. 1995. Hubble Space Telescope pointing control system design improvement study results. *Journal of Guidance, Control, and Dynamics,* 18**,** 194-199.
Bumroongsri, P. & Kheawhom, S. 2012. An off-line robust MPC algorithm for uncertain polytopic discrete-time systems using polyhedral invariant sets. *Journal of Process Control,* 22**,** 975-983.
Burton, T., Jenkins, N., Sharpe, D. & Bossanyi, E. 2011. *Wind energy handbook*, John Wiley & Sons.
Caglayan, A., Allen, S. & Wehmuller, K. Evaluation of a second generation reconfiguration strategy for aircraft flight control systems subjected to actuator failure/surface damage. Aerospace and Electronics Conference, 1988. NAECON 1988., Proceedings of the IEEE 1988 National, 1988. IEEE, 520-529.
Cai, W., Liao, X. & Song, D. Y. 2008. Indirect robust adaptive fault-tolerant control for attitude tracking of spacecraft. *Journal of Guidance, Control, and Dynamics,* 31**,** 1456-1463.
Camacho, E. F. & Bordons, C. 2004. *Model predictive control*, Springer Berlin.
Campo, P. J. & Morari, M. Robust model predictive control. American Control Conference, 1987, 1987. IEEE, 1021-1026.
Casavola, A. & Garone, E. 2010. Fault‐tolerant adaptive control allocation schemes for overactuated systems. *International journal of robust and nonlinear control,* 20**,** 1958-1980.
Casavola, A., Giannelli, M. & Mosca, E. 2000. Min–max predictive control strategies for input-saturated polytopic uncertain systems. *Automatica,* 36**,** 125-133.
Chandler, P. R. Self-repairing flight control system reliability and maintainability program executive overview. Proc. Nat. Aero. & Electr. Conf, 1984. 586-590.

Changzheng, C., Changcheng, S., Yu, Z. & Nan, W. Fault diagnosis for large-scale wind turbine rolling bearing using stress wave and wavelet analysis. Electrical Machines and Systems, 2005. ICEMS 2005. Proceedings of the Eighth International Conference on, 2005. IEEE, 2239-2244.

Chen, J., Lopez-Toribio, C. & Patton, R. 1999. Non-linear dynamic systems fault detection and isolation using fuzzy observers. *Proceedings of the Institution of Mechanical Engineers, Part I: Journal of Systems and Control Engineering,* 213**,** 467-476.

Chen, J. & Patton, R. J. 1999. *Robust model-based fault diagnosis for dynamic systems*, Springer Publishing Company, Incorporated.

Chen, L., Shi, F. & Patton, R. Active FTC for hydraulic pitch system for an off-shore wind turbine. Control and Fault-Tolerant Systems (SysTol), 2013 Conference on, 2013. IEEE, 510-515.

Cortes, C. & Vapnik, V. 1995. Support-vector networks. *Machine learning,* 20**,** 273-297.

Dang, D., Wu, S., Wang, Y. & Cai, W. Model predictive control for maximum power capture of variable speed wind turbines. IPEC, 2010 Conference Proceedings, 2010. IEEE, 274-279.

De Oca, S. M., Puig, V., Theillio, D. & Tornil-Sin, S. Fault-Tolerant Control design using LPV Admissible Model Matching: Application to a two-degree of freedom helicopter. Control and Automation, 2009. MED'09. 17th Mediterranean Conference on, 2009. IEEE, 522-527.

Ding, S. X. 2008. *Model-based fault diagnosis techniques*, Springer.

Ding, Y., Byon, E., Park, C., Tang, J., Lu, Y. & Wang, X. 2007. Dynamic data-driven fault diagnosis of wind turbine systems. *Computational Science–ICCS 2007.* Springer.

Donders, S., Verdult, V. & Verhaegen, M. 2002. Fault detection and identification for wind turbine systems: a closed-loop analysis. *Master's thesis, University of Twente*.

Edwards, C., Lombaerts, T. & Smaili, H. 2010. *Fault tolerant flight control: a benchmark challenge*, Springer.

Edwards, C. & Tan, C. P. 2006. Sensor fault tolerant control using sliding mode observers. *Control Engineering Practice,* 14**,** 897-908.

El-Farra, N. H. 2006. Integrated fault detection and fault-tolerant control architectures for distributed processes. *Industrial & engineering chemistry research,* 45**,** 8338-8351.

Eterno, J. S., Weiss, J. L., Looze, D. P. & Willsky, A. Design issues for fault tolerant-restructurable aircraft control. Decision and Control, 1985 24th IEEE Conference on, 1985. IEEE, 900-905.

Farina, M. & Scattolini, R. 2012. Tube-based robust sampled-data MPC for linear continuous-time systems. *Automatica,* 48**,** 1473-1476.

Feng, G. 2010. *Analysis and Synthesis of Fuzzy Control Systems: a model-based approach*, CRC Press.

Frank, P. M. 1996. Analytical and qualitative model-based fault diagnosis–a survey and some new results. *European Journal of control,* 2**,** 6-28.

Frank, P. M. & Ding, X. 1997. Survey of robust residual generation and evaluation methods in observer-based fault detection systems. *Journal of process control,* 7**,** 403-424.

Gao, M. M., Liu, J. Z., Zhang, X., Lei, X. J., Tang, J. & Zhong, J. W. 2013. Research Self-Adjusting TS Fuzzy Control System Based on LS-SVM Online Prediction on CFBB. *Applied Mechanics and Materials,* 241**,** 1109-1112.

Gao, Z. & Antsaklis, P. J. 1991. Stability of the pseudo-inverse method for reconfigurable control systems. *International Journal of Control,* 53**,** 717-729.
Gao, Z. & Ho, D. 2004. Proportional multiple-integral observer design for descriptor systems with measurement output disturbances. *IEE Proceedings-Control Theory and Applications,* 151**,** 279-288.
Gao, Z. & Wang, H. 2006. Descriptor observer approaches for multivariable systems with measurement noises and application in fault detection and diagnosis. *Systems & Control Letters,* 55**,** 304-313.
Garcia, H. E., Ray, A. & Edwards, R. M. 1991. Reconfigurable control of power plants using learning automata. *Control Systems, IEEE,* 11**,** 85-922.
Gelderloos, H. & Young, D. Redundancy management of shuttle flight control rate gyroscopes and accelerometers. American Control Conference, 1982, 1982. IEEE, 808-811.
Gertler, J. 1998. *Fault detection and diagnosis in engineering systems*, CRC press.
Global-Wind-Energy-Council. 2014. *Global Wind Statistics 2013* [Online]. Available: http://www.gwec.net/wp-content/uploads/2014/02/GWEC-PRstats-2013_EN.pdf [Accessed 1st August 2014].
Godwin, J. L., Matthews, P. & Watson, C. 2013. Classification and detection of electrical control system faults through SCADA data analysis. *Chemical Engineering Transactions*.
Golub, G. H. & Van Loan, C. F. 2012. *Matrix computations*, JHU Press.
Gopinathan, M., Mehra, R. K. & Runkle, J. C. A model predictive fault-tolerant temperature control scheme for hot isostatic pressing furnaces. American Control Conference, 1999. Proceedings of the 1999, 1999 1999. 637-641 vol.1.
Grüne, L. & Pannek, J. 2011. *Nonlinear model predictive control*, Springer.
Guérin, F., Druaux, F. & Lefebvre, D. 2005. Reliability analysis and FDI methods for wind turbines: a state of the art and some perspectives, 3ème French-German Scientific conference «. *Renewable and Alternative Energies*.
Haghani Abandan Sari, A. 2014. Data-driven design of fault diagnosis systems.
Hameed, Z., Hong, Y., Cho, Y., Ahn, S. & Song, C. 2009. Condition monitoring and fault detection of wind turbines and related algorithms: A review. *Renewable and Sustainable energy reviews,* 13**,** 1-39.
Himmelblau, D. M. 1978. *Fault detection and diagnosis in chemical and petrochemical processes*, Elsevier Science Ltd.
Hu, L. Robust fault-tolerant control of systems with time-varying structured uncertainties. Natural Computation (ICNC), 2013 Ninth International Conference on, 2013. IEEE, 1681-1685.
Hu, Q. & Xiao, B. 2013. Adaptive fault tolerant control using integral sliding mode strategy with application to flexible spacecraft. *International Journal of Systems Science,* 44**,** 2273-2286.
Huzmezan, M. & Maciejowski, J. 1998. Reconfigurable flight control of a high incidence research model using predictive control.
Hyers, R., Mcgowan, J., Sullivan, K., Manwell, J. & Syrett, B. 2006. Condition monitoring and prognosis of utility scale wind turbines. *Energy Materials,* 1**,** 187-203.
Ichtev, A., Hellendoom, J., Babuska, R. & Mollov, S. Fault-tolerant model-based predictive control using multiple takagi-sugeno fuzzy models. Fuzzy Systems, 2002. FUZZ-IEEE'02. Proceedings of the 2002 IEEE International Conference on, 2002. IEEE, 346-351.

Ifip. Proc. of the IFIP 9th World Computer Congress, September 1983 Paris, France. Elsevier.
Isermann, R. 2005. Model-based fault-detection and diagnosis–status and applications. *Annual Reviews in control,* 29**,** 71-85.
Isermann, R. 2006. *Fault-diagnosis systems*, Springer.
Isermann, R. 2011. *Fault-diagnosis applications: model-based condition monitoring: actuators, drives, machinery, plants, sensors, and fault-tolerant systems*, Springer.
Isermann, R. & Ballé, P. 1997. Trends in the application of model-based fault detection and diagnosis of technical processes. *Control engineering practice,* 5**,** 709-719.
Izadi-Zamanabadi, R. & Blanke, M. 1999. A ship propulsion system as a benchmark for fault-tolerant control. *Control Engineering Practice,* 7**,** 227-239.
Izadi, H. A., Zhang, Y. & Gordon, B. W. Fault tolerant model predictive control of quad-rotor helicopters with actuator fault estimation. World Congress, 2011. 6343-6348.
Jayaswal, P., Verma, S. & Wadhwani, A. 2011. Development of EBP-Artificial neural network expert system for rolling element bearing fault diagnosis. *Journal of Vibration and Control,* 17**,** 1131-1148.
Jeong, Y.-S., Sul, S.-K., Schulz, S. E. & Patel, N. R. 2005. Fault detection and fault-tolerant control of interior permanent-magnet motor drive system for electric vehicle. *Industry Applications, IEEE Transactions on,* 41**,** 46-51.
Jiang, B., Gao, Z., Shi, P. & Xu, Y. 2010. Adaptive fault-tolerant tracking control of near-space vehicle using Takagi–Sugeno fuzzy models. *Fuzzy Systems, IEEE Transactions on,* 18**,** 1000-1007.
Jiang, J. & Yu, X. 2012. Fault-tolerant control systems: A comparative study between active and passive approaches. *Annual Reviews in control,* 36**,** 60-72.
Jin, X. & Du, Z. 2006. Fault tolerant control of outdoor air and AHU supply air temperature in VAV air conditioning systems using PCA method. *Applied Thermal Engineering,* 26**,** 1226-1237.
Jonkman, J. M. & Buhl Jr, M. L. 2005. FAST user's guide. *Golden, CO: National Renewable Energy Laboratory*.
Kalinin, V., Leigh, A., Stopps, A. & Artigao, E. Resonant SAW torque sensor for wind turbines. European Frequency and Time Forum & International Frequency Control Symposium (EFTF/IFC), 2013 Joint, 2013. IEEE, 462-465.
Kamal, E., Aitouche, A., Ghorbani, R. & Bayart, M. 2012. Robust fuzzy fault-tolerant control of wind energy conversion systems subject to sensor faults. *Sustainable Energy, IEEE Transactions on,* 3**,** 231-241.
Kasabov, N. K. 1996. *Foundations of neural networks, fuzzy systems, and knowledge engineering*, Marcel Alencar.
Khong, T. H. & Shin, J. Robustness analysis of integrated LPV-FDI filters and LTI-FTC system for a transport aircraft. AIAA Guidance, Navigation and Control Conference and Exhibit, 2007.
Kk-Electronic. 2011. *http://www.kk-electronic.com/wind-turbine-control/competition-on-fault-detection/wind-turbine-benchmark-model.aspx* [Online].
Koh, M., Norton, M. & Khoo, S. 2012. Robust fault-tolerant leader-follower control of four-wheelsteering mobile robots using terminal sliding mode. *Australian Journal of Electrical & Electronic Engineering,* 9.
Kong, C., Bang, J. & Sugiyama, Y. 2005. Structural investigation of composite wind turbine blade considering various load cases and fatigue life. *Energy,* 30**,** 2101-2114.

Kwon, W. H. & Han, S. H. 2006. *Receding horizon control: model predictive control for state models*, Springer.
Lao, L., Ellis, M. & Christofides, P. D. 2013. Proactive fault‐tolerant model predictive control. *AIChE Journal,* 59**,** 2810-2820.
Lee, J. H. 2011. Model predictive control: review of the three decades of development. *International Journal of Control, Automation and Systems,* 9**,** 415-424.
Li, D.-Y., Song, Y.-D., Huang, D. & Chen, H.-N. 2013. Model-independent adaptive fault-tolerant output tracking control of 4WS4WD road vehicles. *Intelligent Transportation Systems, IEEE Transactions on,* 14**,** 169-179.
Li, D., Xi, Y. & Zheng, P. 2009. Constrained robust feedback model predictive control for uncertain systems with polytopic description. *International Journal of control,* 82**,** 1267-1274.
Li, Z., Yan, X., Yuan, C., Zhao, J. & Peng, Z. 2011. Fault detection and diagnosis of a gearbox in marine propulsion systems using bispectrum analysis and artificial neural networks. *Journal of Marine Science and Application,* 10**,** 17-24.
Liao, F., Wang, J. L. & Yang, G.-H. 2002. Reliable robust flight tracking control: an LMI approach. *Control Systems Technology, IEEE Transactions on,* 10**,** 76-89.
Lin, C.-M. & Chen, C.-H. 2007. Robust fault-tolerant control for a biped robot using a recurrent cerebellar model articulation controller. *Systems, Man, and Cybernetics, Part B: Cybernetics, IEEE Transactions on,* 37**,** 110-123.
Liu, J., Xu, D. & Yang, X. Sensor fault detection in variable speed wind turbine system using H_/H∞ method. Intelligent Control and Automation, 2008. WCICA 2008. 7th World Congress on, 2008. IEEE, 4265-4269.
Looze, D. P., Weiss, J. L., Eterno, J. S. & Barrett, N. M. 1985. An Automatic Redesign Approach for Restructurable Control Systems. *IEEE Control Systems Magazine*.
Lu, B., Li, Y., Wu, X. & Yang, Z. A review of recent advances in wind turbine condition monitoring and fault diagnosis. Power Electronics and Machines in Wind Applications, 2009. PEMWA 2009. IEEE, 2009. IEEE, 1-7.
Ma, X.-J., Sun, Z.-Q. & He, Y.-Y. 1998. Analysis and design of fuzzy controller and fuzzy observer. *Fuzzy Systems, IEEE Transactions on,* 6**,** 41-51.
Maciejowski, J. M. 1999. Predictive control with constraints.
Maciejowski, J. M. & Jones, C. N. MPC fault-tolerant flight control case study: Flight 1862. IFAC safeprocess conference, 2003. 121-126.
Magni, L., Raimondo, D. M. & Allgöwer, F. 2009. *Nonlinear model predictive control: towards new challenging applications*, Springer.
Mahmoud, M. S. & Xia, Y. 2013. *Analysis and Synthesis of Fault-tolerant Control Systems*, John Wiley & Sons.
Mathworks 2011. Matlab/Simulink.
Mayne, D. Q., Kerrigan, E. C. & Falugi, P. Robust model predictive control: advantages and disadvantages of tube-based methods. Proc. of the 18th IFAC World Congress Milano, 2011. 191-196.
Mayne, D. Q., Rawlings, J. B., Rao, C. V. & Scokaert, P. O. 2000. Constrained model predictive control: Stability and optimality. *Automatica,* 36**,** 789-814.
Mcmahan, J. 1978. Flight 1080. *Air Line Pilot*.
Mercer, J. 1909. Functions of positive and negative type, and their connection with the theory of integral equations. *Philosophical transactions of the royal society of London. Series A, containing papers of a mathematical or physical character***,** 415-446.
Merritt, H. E. 1967. *Hydraulic control systems*, John Wiley & Sons.

Mirzaee, A. & Salahshoor, K. 2012. Fault diagnosis and accommodation of nonlinear systems based on multiple-model adaptive unscented Kalman filter and switched MPC and H-infinity loop-shaping controller. *Journal of Process Control,* 22**,** 626-634.

Moerder, D. D., Halyo, N., Broussard, J. R. & Caglayan, A. K. 1989. Application of precomputed control laws in a reconfigurable aircraftflight control system. *Journal of Guidance, Control, and Dynamics,* 12**,** 325-333.

Monaco, J., Ward, D., Barron, R. & Bird, R. Implementation and flight test assessment of an adaptive, reconfigurable flight control system. Proceedings of the 1997 AIAA Guidance Navigation and Control Conference, AIAA Paper, 1997. 3738.

Montoya, R. J., Howell, W., Bundick, W., Ostroff, A., Hueschen, R. & Belcastro, C. M. 1983. *Restructurable controls*, Citeseer.

Morari, M. & Lee, J. 1999. Model predictive control: past, present and future. *Computers & Chemical Engineering,* 23**,** 667-682.

Niemann, H. & Stoustrup, J. Reliable control using the primary and dual Youla parameterizations. Decision and Control, 2002, Proceedings of the 41st IEEE Conference on, 2002. IEEE, 4353-4358.

Niemann, H. & Stoustrup, J. 2005. Passive fault tolerant control of a double inverted pendulum—a case study. *Control engineering practice,* 13**,** 1047-1059.

Nieto-Wire, C. & Sobel, K. 2014. Delta Operator Eigenstructure Assignment for Reconfigurable Control of a Tailless Aircraft. *Journal of Guidance, Control, and Dynamics***,** 1-16.

Nordex. 2013. *http://www.nordex-online.com/microsites/efficiency-class/downloads/Nordex_Gamma_en.pdf* [Online]. [Accessed July 27th 2014 2014].

Ochi, Y. & Kanai, K. 1991. Design of restructurable flight control systems using feedback linearization. *Journal of Guidance, Control, and Dynamics,* 14**,** 903-911.

Odgaard, P. F. & Johnson, K. E. Wind turbine fault detection and fault tolerant control-a second challenge. 8th IFAC Symposium on Fault Detection, Supervision and Safety of Technical Processes, 2012. 127.

Odgaard, P. F. & Stoustrup, J. Fault tolerant control of wind turbines using unknown input observers. 8th IFAC Symposium on Fault Detection, Supervision and Safety of Technical Processes, 2012. 313-318.

Odgaard, P. F., Stoustrup, J. & Kinnaert, M. 2009. Fault tolerant control of wind turbines: a benchmark model.

Odgaard, P. F., Stoustrup, J. & Kinnaert, M. 2013. Fault-Tolerant Control of Wind Turbines: A Benchmark Model. *Control Systems Technology, IEEE Transactions on,* 21**,** 1168-1182.

Omdahl, T. P. 1988. *Reliability, availability, and maintainability (RAM) dictionary*, ASQC Quality press Milwaukee, Wisconsin.

Østergaard, K. Z., Brath, P. & Stoustrup, J. Estimation of effective wind speed. Journal of Physics: Conference Series, 2007. IOP Publishing, 012082.

Ostroff, A. J. Techniques for accommodating control effector failures on a mildly statically unstable airplane. American Control Conference, 1985, 1985. IEEE, 906-913.

Oubellil, R. & Boukhnifer, M. Passive fault tolerant control design of energy management system for electric vehicle. Industrial Electronics (ISIE), 2014 IEEE 23rd International Symposium on, 2014. IEEE, 1402-1408.

Oudghiri, M., Chadli, M. & El Hajjaji, A. 2008. Robust observer-based fault-tolerant control for vehicle lateral dynamics. *International journal of vehicle design,* 48**,** 173-189.

Panagi, P. & Polycarpou, M. M. 2011. Decentralized fault tolerant control of a class of interconnected nonlinear systems. *Automatic Control, IEEE Transactions on,* 56**,** 178-184.

Patton, R., Kambhampati, C., Casavola, A. & Franze, G. Fault-tolerance as a key requirement for the control of modern systems. Fault Detection, Supervision and Safety of Technical Processes, 2006. 13-23.

Patton, R. J. Fault-tolerant control systems: The 1997 situation. IFAC symposium on fault detection supervision and safety for technical processes, 1997. 1033-1054.

Patton, R. J., Clark, R. N. & Frank, P. M. 2000. *Issues of fault diagnosis for dynamic systems*, Springer.

Patton, R. J., Frank, P. M. & Clarke, R. N. 1989. *Fault diagnosis in dynamic systems: theory and application*, Prentice-Hall, Inc.

Patton, R. J., Kambhampati, C., Casavola, A., Zhang, P., Ding, S. & Sauter, D. 2007. A generic strategy for fault-tolerance in control systems distributed over a network. *European journal of control,* 13**,** 280-296.

Piegat, A. 2001. *Fuzzy modeling and control*, Springer.

Pourmohammad, S. & Fekih, A. Fault-Tolerant control of wind turbine systems-A Review. Green Technologies Conference (IEEE-Green), 2011 IEEE, 2011. IEEE, 1-6.

Prakash, J., Narasimhan, S. & Patwardhan, S. C. 2005. Integrating model based fault diagnosis with model predictive control. *Industrial & engineering chemistry research,* 44**,** 4344-4360.

Qi, R., Zhu, L. & Jiang, B. 2013. Fault-tolerant reconfigurable control for MIMO systems using online fuzzy identification. *International Journal of Innovative Computing, Information and Control,* 9**,** 3915-3928.

Qin, S. J. & Badgwell, T. A. 2000. An overview of nonlinear model predictive control applications. *Nonlinear model predictive control.* Springer.

Qin, S. J. & Badgwell, T. A. 2003. A survey of industrial model predictive control technology. *Control engineering practice,* 11**,** 733-764.

Raff, T., Ebenbauer, C., Findeisen, R. & Allgöwer, F. 2005. Remarks on moving horizon state estimation with guaranteed convergence. *Control and Observer Design for Nonlinear Finite and Infinite Dimensional Systems.* Springer.

Rago, C., Prasanth, R., Mehra, R. & Fortenbaugh, R. Failure detection and identification and fault tolerant control using the IMM-KF with applications to the Eagle-Eye UAV. Decision and Control, 1998. Proceedings of the 37th IEEE Conference on, 1998. IEEE, 4208-4213.

Rao, C. V. & Rawlings, J. B. 2002. Constrained process monitoring: Moving‐horizon approach. *AIChE journal,* 48**,** 97-109.

Rao, C. V., Rawlings, J. B. & Mayne, D. Q. 2003. Constrained state estimation for nonlinear discrete-time systems: Stability and moving horizon approximations. *Automatic Control, IEEE Transactions on,* 48**,** 246-258.

Rauch, H. E. 1995. Autonomous control reconfiguration. *Control Systems, IEEE,* 15**,** 37-48.

Rawlings, J. B. & Mayne, D. Q. 2009. *Model predictive control: Theory and design*, Nob Hill Pub.

Ribrant, J. & Bertling, L. M. 2007. Survey of Failures in Wind Power Systems With Focus on Swedish Wind Power Plants During 1997–2005. *Energy Conversion, IEEE Transactions on,* 22**,** 167-173.

Rotondo, D., Puig, V., Acevedo Valle, J. M. & Nejjari, F. FTC of LPV systems using a bank of virtual sensors: Aapplication to wind turbines. Control and Fault-Tolerant Systems (SysTol), 2013 Conference on, 2013. IEEE, 492-497.

Samar, S., Gorinevsky, D. & Boyd, S. P. Embedded estimation of fault parameters in an unmanned aerial vehicle. Computer Aided Control System Design, 2006 IEEE International Conference on Control Applications, 2006 IEEE International Symposium on Intelligent Control, 2006 IEEE, 2006. IEEE, 3265-3270.

Sami, M. & Patton, R. J. An FTC approach to wind turbine power maximisation via TS fuzzy modelling and control. Fault Detection, Supervision and Safety of Technical Processes, 2012a. 349-354.

Sami, M. & Patton, R. J. Global wind turbine FTC via TS fuzzy modelling and control. Fault Detection, Supervision and Safety of Technical Processes, 2012b. 325-330.

Sami, M. & Patton, R. J. A multiple-model approach to fault tolerant tracking control for non-linear systems. Control & Automation (MED), 2012 20th Mediterranean Conference on, 2012c. IEEE, 498-503.

Sami, M. & Patton, R. J. Wind turbine power maximisation based on adaptive sensor fault tolerant sliding mode control. Control & Automation (MED), 2012 20th Mediterranean Conference on, 2012d. IEEE, 1183-1188.

Schulte, H. Fault-Tolerant Control of Wind Turbines using a Takagi-Sugeno Sliding Mode Observer. Journal of Physics: Conference Series, 2014. IOP Publishing, 012053.

Shaker, M. S. & Patton, R. J. 2014. Active sensor fault tolerant output feedback tracking control for wind turbine systems via T–S model. *Engineering Applications of Artificial Intelligence,* 34**,** 1-12.

Shen, H., Song, X. & Wang, Z. 2013. Robust fault-tolerant control of uncertain fractional-order systems against actuator faults. *Control Theory & Applications, IET,* 7.

Simani, S., Castaldi, P. & Tilli, A. Data-driven approach for wind turbine actuator and sensor fault detection and isolation. Proceedings of IFAC World Congress, 2011. 8301-8306.

Sloth, C., Esbensen, T. & Stoustrup, J. Active and passive fault-tolerant LPV control of wind turbines. American Control Conference (ACC), 2010, 2010. IEEE, 4640-4646.

Sloth, C., Esbensen, T. & Stoustrup, J. 2011. Robust and fault-tolerant linear parameter-varying control of wind turbines. *Mechatronics,* 21**,** 645-659.

Soliman, M., Malik, O. & Westwick, D. Fault Tolerant Control of Variable-Speed Variable-Pitch Wind Turbines: A Subspace Predictive Control Approach. System Identification, 2012. 1683-1688.

Soltani, M., Wisniewski, R., Brath, P. & Boyd, S. Load reduction of wind turbines using receding horizon control. Control Applications (CCA), 2011 IEEE International Conference on, 2011. IEEE, 852-857.

Steinwart, I. & Christmann, A. 2008. *Support vector machines*, Springer.

Stengel, R. F. 1991. Intelligent failure-tolerant control. *Control Systems, IEEE,* 11**,** 14-23.

Sun, S., Dong, L., Li, L. & Gu, S. 2008. Fault tolerant control for constrained linear systems based on mpc and fdi. *International Journal of Information and Systems Scienses,* 4**,** 512-523.

Suykens, J. & Vandewalle, J. 2000. Recurrent least squares support vector machines. *Circuits and Systems I: Fundamental Theory and Applications, IEEE Transactions on,* 47**,** 1109-1114.

Suykens, J. A. Nonlinear modelling and support vector machines. Instrumentation and Measurement Technology Conference, 2001. IMTC 2001. Proceedings of the 18th IEEE, 2001. IEEE, 287-294.

Suykens, J. A., De Brabanter, J., Lukas, L. & Vandewalle, J. 2002. Weighted least squares support vector machines: robustness and sparse approximation. *Neurocomputing,* 48**,** 85-105.

Suykens, J. A., Van Gestel, T., De Brabanter, J., De Moor, B., Vandewalle, J. & Van Gestel, T. 2002. *Least squares support vector machines*, World Scientific.

Suykens, J. A., Vandewalle, J. & De Moor, B. 2001. Optimal control by least squares support vector machines. *Neural Networks,* 14**,** 23-35.

Takagi, T. & Sugeno, M. 1985. Fuzzy identification of systems and its applications to modeling and control. *Systems, Man and Cybernetics, IEEE Transactions on***,** 116-132.

Tanaka, K., Ikeda, T. & Wang, H. O. 1998. Fuzzy regulators and fuzzy observers: relaxed stability conditions and LMI-based designs. *Fuzzy Systems, IEEE Transactions on,* 6**,** 250-265.

Tao, G., Joshi, S. M. & Ma, X. 2001. Adaptive state feedback and tracking control of systems with actuator failures. *Automatic Control, IEEE Transactions on,* 46**,** 78-95.

Tarbouriech, S. & Garcia, G. 1997. *Control of uncertain systems with bounded inputs*, Springer-Verlag New York, Inc.

Tayarani-Bathaie, S. S., Vanini, Z. N. S. & Khorasani, K. 2014. Dynamic neural network-based fault diagnosis of gas turbine engines. *Neurocomputing,* 125**,** 153-165.

Tyler, M. L., Asano, K. & Morari, M. 2000. Application of moving horizon estimation based fault detection to cold tandem steel mill. *International Journal of Control,* 73**,** 427-438.

Vanek, B., Péni, T., Szabó, Z. & Bokor, J. 2014. Fault Tolerant LPV Control of the GTM UAV with Dynamic Control Allocation.

Vapnik, V. 1995. *The nature of statistical learning theory*, springer.

Vapnik, V., Golowich, S. E. & Smola, A. 1997. Support vector method for function approximation, regression estimation, and signal processing. *Advances in neural information processing systems***,** 281-287.

Varrier, S., Koenig, D. & Martinez Molina, J. J. Integrated Fault Estimation and Fault Tolerant Control Design for LPV Systems. System, Structure and Control, 2013. 689-694.

Veillette, R. J., Medanic, J. & Perkins, W. R. 1992. Design of reliable control systems. *Automatic Control, IEEE Transactions on,* 37**,** 290-304.

Venkatasubramanian, V., Rengaswamy, R. & Kavuri, S. N. 2003. A review of process fault detection and diagnosis: Part II: Qualitative models and search strategies. *Computers & Chemical Engineering,* 27**,** 313-326.

Wang, H., Chai, T., Ding, J. & Brown, M. 2009. Data driven fault diagnosis and fault tolerant control: some advances and possible new directions. *Acta Automatica Sinica,* 35**,** 739-747.

Wang, H. & Hu, D. Comparison of SVM and LS-SVM for regression. Neural Networks and Brain, 2005. ICNN&B'05. International Conference on, 2005. IEEE, 279-283.

Wang, J. & Shen, H. 2014. Passivity-based fault-tolerant synchronization control of chaotic neural networks against actuator faults using the semi-Markov jump model approach. *Neurocomputing,* 143**,** 51-56.
Wang, L. 2005. *Support Vector Machines: theory and applications*, Springer.
Wang, L. 2009. *Model predictive control system design and implementation using MATLAB®*, springer.
Wang, W., Men, C. & Lu, W. 2008. Online prediction model based on support vector machine. *Neurocomputing,* 71**,** 550-558.
Wang, Z., Zhang, Z. & Mao, J. Adaptive tracking control based on online LS-SVM identifier for unknown nonlinear system. Information Science and Technology (ICIST), 2012 International Conference on, 2012. IEEE, 112-117.
Wilkinson, M. R., Spinato, F. & Tavner, P. J. Condition monitoring of generators & other subassemblies in wind turbine drive trains. Diagnostics for Electric Machines, Power Electronics and Drives, 2007. SDEMPED 2007. IEEE International Symposium on, 2007. IEEE, 388-392.
Wu, B., Lang, Y., Zargari, N. & Kouro, S. 2011. *Power Conversion and Control of Wind Energy Systems*, Wiley-IEEE Press.
Wu, S.-F., Grimble, M. J. & Wei, W. QFT based robust/fault tolerant flight control design for a remote pilotless vehicle. Control Applications, 1999. Proceedings of the 1999 IEEE International Conference on, 1999. IEEE, 57-62.
Xin-Fang, Z., Da-Ping, X. & Yi-Bing, L. Adaptive optimal fuzzy control for variable speed fixed pitch wind turbines. Intelligent Control and Automation, 2004. WCICA 2004. Fifth World Congress on, 2004. IEEE, 2481-2485.
Xu, Z., Hu, Q. & Ehsani, M. 2012. Estimation of effective wind speed for fixed-speed wind turbines based on frequency domain data fusion. *Sustainable Energy, IEEE Transactions on,* 3**,** 57-64.
Yang, X. & Maciejowski, J. Fault-tolerant model predictive control of a wind turbine benchmark. Proc. IFAC Safeprocess, 2012. 337-342.
Ye, D. & Yang, G.-H. 2006. Adaptive fault-tolerant tracking control against actuator faults with application to flight control. *Control Systems Technology, IEEE Transactions on,* 14**,** 1088-1096.
Yin, S., Wang, G. & Karimi, H. R. 2013. Data-driven design of robust fault detection system for wind turbines. *Mechatronics*.
Yin, Z., Zheng, W., Chang, X. & Lun, S. H∞ robust fault-tolerant control for a class of uncertain nonlinear singular systems with time delay based on TS fuzzy models. Control and Decision Conference (CCDC), 2013 25th Chinese, 2013. IEEE, 1123-1127.
Yu, X. & Jiang, J. 2012. Hybrid fault-tolerant flight control system design against partial actuator failures. *Control Systems Technology, IEEE Transactions on,* 20**,** 871-886.
Zeilinger, M. N., Morari, M. & Jones, C. N. 2014. Soft Constrained Model Predictive Control With Robust Stability Guarantees. *Ieee Transactions On Automatic Control,* 59**,** 1190-1202.
Zhang, K., Jiang, B. & Shi, P. 2013. *Observer-based fault estimation and accomodation for dynamic systems*, Springer.
Zhang, R., Lu, R., Xue, A. & Gao, F. 2014. Predictive functional control for linear systems under partial actuator faults and application on an injection molding batch process. *Industrial & Engineering Chemistry Research,* 53**,** 723-731.

Zhang, Y. & Jiang, J. Design of integrated fault detection, diagnosis and reconfigurable control systems. Decision and Control, 1999. Proceedings of the 38th IEEE Conference on, 1999. IEEE, 3587-3592.

Zhang, Y. & Jiang, J. 2002. Active fault-tolerant control system against partial actuator failures. *IEE Proceedings-Control Theory and Applications,* 149**,** 95-104.

Zhang, Y. & Jiang, J. 2008. Bibliographical review on reconfigurable fault-tolerant control systems. *Annual reviews in control,* 32**,** 229-252.

Zhao, J., Jiang, B., Shi, P. & He, Z. 2014. Fault tolerant control for damaged aircraft based on sliding mode control scheme. *Int. J. Innov. Comput. Inf. Control,* 10**,** 293-302.

Zhihong, H. & Huajing, F. 2007. Research on robust fault-tolerant control for networked control system with packet dropout. *Systems Engineering and Electronics, Journal of,* 18**,** 76-82.